Aus dem Institut für Virologie
Direktor: Prof. Dr. Stephan Becker
Des Fachbereichs Medizin der Philipps-Universität Marburg

Philipps Universität Marburg

Polymerase mutations promoting adaptation of avian influenza virus of subtype H9N2 to mammals

Inaugural-Dissertation zur Erlangung des Doktorgrades der Naturwissenschaften (Dr.rer.nat.)

Dem Fachbereich Medizin der Philipps-Universität Marburg vorgelegt von

Hanna Sediri
aus Maisons-Laffitte, France

Marburg, 2015

Aus dem Institut für Virologie
Direktor: Prof. Dr. Stephan Becker
Des Fachbereichs Medizin der Philipps-Universität Marburg

Philipps Universität Marburg

Polymerase mutations promoting adaptation of avian influenza virus of subtype H9N2 to mammals

Inaugural-Dissertation zur Erlangung des Doktorgrades der Naturwissenschaften (Dr.rer.nat.)

Dem Fachbereich Medizin der Philipps-Universität Marburg vorgelegt von

Hanna Sediri
aus Maisons-Laffitte, France

Marburg, 2015

Angenommen vom Fachbereich Medizin der Philipps-Universität Marburg am:

Gedruckt mit Genehmigung des Fachbereichs.

Dekan: Prof. Dr. Helmut Schäfer

Referent: Prof. Dr. Hans-Dieter Klenk

Korreferent: Prof. Dr. Stefan Bauer

1 TABLE OF CONTENTS

2 ABBREVIATIONS

A

APS	Ammonium Persulphate

B

BSA	Bovine Serum Albumin
BSL	Biosafety Level

C

CARD	Caspase Recruitment Domains
CHX	Cycloheximide
CLSM	Confocal Laser Scanning Microscopy
CPSF	Cleavage and Polyadenylation Specificity Factor
cRNA	complementary RNA
cRNP	complementary Ribonucleoprotein
CTD	Carboxy-Terminal Domain
CTRL	Control

D

Da	Dalton
DANN	Deoxyribonucleic Acid
DAPI	4’,6-diamidino-2-phenylindole
DMEM	Dulbecco’s Modified Eagle’s Medium
DMSO	Dimethyl Sulfoxide
dNTP	Deoxyribonucleoside Triphosphate
dsRNA	double-stranded RNA

E

EDTA	Ethylenediaminetetraacetic Acid
eIF2a	eukaryotic translation Initiation Factor 2 alpha

F

FCS	Foetal Calf Serum
Fire	Firefly luciferase
FP	Fusion Peptide

H

h	Hour
HA	Hemagglutinin
HAT	Human airway trypsin-like protease
HBS	HEPES-Buffered-Saline
HF	High Fidelity
HPAI	Highly pathogenic avian Influenza
HRP	Horseradish peroxidase
Hsp40	Heat shock protein 40
Hz	Hertz

I

IFN	Interferon
IFNAR	Interferon-a receptor

IKK	IκB kinase
IL	Interleukine
IRF-3	Interferon Regulatory Factor 3
ISG	Interferon Stimulated Gene
J	
JAK	Janus Kinase
L	
LB	Luria Bertani
LMB	Leptomycine B
LPAI	Low pathogenic avian Influenza
M	
M	Matrix
mA	Milliampere
MAVS	Mitochondrial antiviral-signaling protein
MDA-5	Melanoma Differentiation-Associated protein 5
MDCK	Madin Darby Canine Kidney
MEM	Modified Eagle's Medium
min	Minute
MOI	Multiplicity of infection
N	
NA	Neuraminidase
NEP	Nuclear Export Protein
NES	Nuclear Export Signal
NFKB	Nuclear Factor 'kappa-light-chain-enhancer' of activated B-cells
NLS	Nuclear Localisation Signal
NP	Nucleoprotein
NS	Non-Structural
O	
OAS	2'-5' Oligoadenylate synthetase
ORF	Open Reading Frame
P	
p.i	post infection
PA	Polymerase acidic protein
PAGE	Polyacrylamide gel electrophoresis
PAMP	Pathogen-Associated Molecular Patterns
PB1	Polymerase basic protein 1
PB2	Polymerase basic protein 2
PBS^{def}	Phosphate Buffered Saline deficient
PCR	Polymerase-Chain-Reaction
PFA	Paraformaldehyde
PFU	Plaque Forming Unit
pH	potentia hydrogenii
PKR	Protein kinase RNA dependent
PRR	Pattern-Recognition Receptors
PVDF	Polyvinylidenfluorid

R

Ren	Renilla luciferase
RIG-I	Retinoic Acid Inducible Gene I
RING	Really Interesting New Gene
RNA	Ribonucleic acid
rpm	Round per minute
RT	Room Temperature
RT-PCR	Reverse-Transcription-Polymerase-Chain-Reaction

S

s	Second
SDS	Sodium DodecylSulfate
SOB	Super Optimal Broth
STAT	Signal Transducer and Activator of Transcription
SV40	Simian vacuolating virus 40

T

TAE	TRIS-acetate-EDTA
TBK1	TANK-binding kinase 1
TEMED	N,N,N',N'Tetramethylethylendiamine
TGN	Trans-Golgi-Network
TM	Transmembrane
TMPRSS	Transmembrane protease, serine S1 family member
TPCK	L-1-tosylamido-2-phenylethyl chloromethyl ketone
TRIM	Tripartite Motif
TRIS	Trishydroxymethyl-aminomethan

U

UAP56	56 kDa U2AF65-associated protein
URH49	UAP56-related helicase, 49 kDa

V

V	Volt
vRNA	Viral RNA
vRNP	Viral ribonucleoprotein

W

WHO	World Health Organization
WT	Wild Type

3 SUMMARY

Transmission of influenza viruses from aquatic birds to mammals is promoted by the adaptation of the viral proteins to the new host. This includes the PB2 subunit of the viral polymerase complex. This protein has been described as an important host range factor, able to modulate the virulence of influenza viruses. Several adaptive mutations in the PB2 subunit of various influenza-A subtypes have been described, such as D253N, Q591K, E627K, D701N, S714I and S714R. H9N2 influenza viruses are endemic in poultry in Asia and other parts of the world. Moreover these viruses have been occasionally transmitted to humans and are often involved in the generation of viruses causing zoonotic infections in humans by providing internal genes. H9N2 viruses have therefore the potential to cause a pandemic. This study was undertaken to analyse the role of the PB2 subunit in the adaptation of avian influenza virus of subtype H9N2 to mammals.

In the first part of the thesis, the results demonstrated that PB2 mutations D253N, E627K, D701N, S714I and S714R increase the H9N2 polymerase activity in mammalian cells. Furthermore, mutations E627K, D701N and S714I/R also enhance viral growth in mammalian cells. Pathogenicity studies indicated that combination of mutations E627K-D701N-S714R increase the lethality of H9N2 virus in mice. The effects of the adaptive mutations have then been compared in H9N2, H1N1pdm09 and H7N7 viruses. The results have shown that the enhancement of the polymerase activity by the adaptive mutations is higher in the phylogenetically related H9N2 and H7N9 than in the non-related H7N7 and H1N1pdm09 viruses. In addition, analysis of heterologous polymerase complexes composed of H9N2, H1N1pdm09, H7N7, and H7N9 subunits provides further evidence for the concept that this enhancing effect is a specific trait of H9N2-PB2 without significant contribution of PA and PB1. From these observations, it can be concluded that the PB2 subunit of the H9N2 viruses is characterised by a particularly high adaptability to mammalian cells.

In the second part of the thesis, the mechanisms by which E627K and D701N promote adaptation to a mammalian host were analysed. The results demonstrated that viruses bearing the avian signature 627E in PB2 are sensitive to RIG-I activation. This sensitivity is mediated by the destabilisation of the nucleocapsid by RIG-I, exposing thereby the double-stranded RNA required for RIG-I activation. In contrast viruses containing mutation E627K interfere with RIG-I activation, by stabilizing the association of the polymerase complex to the nucleocapsid. These observations indicate that PB2 mutation E627K modulates the inhibition of virus replication mediated by RIG-I. Furthermore, the data showed that mutation D701N promotes not only the nuclear import of newly synthesized PB2 protein, but also the nuclear import of PB2 bound to the incoming vRNPs.

4 ZUSAMMENFASSUNG

Influenza-A-Viren kommen in großer Vielzahl bei Vögeln vor. Wenn Viren aus diesem Reservoir auf den Menschen übertragen werden und sich an den neuen Wirt anpassen, kann es zu einer Pandemie kommen. Unter den aviären Viren verdienen hierbei Viren vom Subtyp H9N2 besondere Aufmerksamkeit. Diese Viren zeichnen sich durch weltweite Verbreitung, außergewöhnliche genetische Flexibilität, die Fähigkeit zu menschlicher Infektion und somit durch ein erhebliches pandemisches Potential aus. Bei ihrer Vermehrung gehen die Viren vielfältige Wechselwirkungen mit dem Wirt ein. Der Wirtswechsel vom Vogel auf den Menschen beruht deswegen wesentlich auf der Adaption der Virusproteine an menschliche Gewebe und Zellen. Eine wichtige Rolle spielt dabei das zum viralen Polymerasekomplex gehörende PB2-Protein. In der vorliegenden Arbeit wurde die funktionelle Bedeutung von 6 adaptiven Mutationen im PB2-Protein von H9N2 Viren untersucht.

Im ersten Teil dieser Arbeit konnte gezeigt werden, dass die Mutationen D253N, E627K, D701N, S714I und S714R in der PB2-Untereinheit die Polymeraseaktivität von H9N2-Viren in Säugerzellen erhöhen. Darüber hinaus führten die Mutationen E627K, D701N und S714I/R zu einem erhöhten Viruswachstum in Säugerzellen. Pathogenitätsstudien zeigten, dass die Kombination der Mutationen E627K-D701N-S714R die Letalität von H9N2-Viren in Mäusen erhöht. Um die Relevanz der adaptiven Mutationen, die im H9N2 Hintergrund beobachtet wurden, zu validieren, wurde der Einfluss dieser Mutationen in H9N2-, H7N9-, H1N1pdm09- und H7N7-Viren verglichen. Die Ergebnisse zeigen, dass die adaptiven Mutationen die Polymeraseaktivität in den phylogenetisch verwandten H9N2- und H7N9-Viren deutlich stärker erhöhten als in den nicht verwandten H7N7- und H1N1pdm09-Viren. Die Analyse von heterologen Polymerasekomplexen aus H9N2, H1N1pdm09, H7N7 und H7N9 Untereinheiten zeigte, dass die starke Aktivitätssteigerung der H9N2-Polymerase nur von den adaptiven PB2-Mutationen, jedoch nicht von PB1 und PA abhängt. Aus dieser Beobachtung kann geschlossen werden, dass sich die Polymerase der H9N2-Viren durch eine besonders hohe Anpassungsfähigkeit an Säugerzellen auszeichnet

Im zweiten Teil der Arbeit wurden die Mechanismen untersucht, aufgrund derer die E627K und D701N Mutationen die Adaptation an Säuger fördern. Es konnte gezeigt werden, dass die Nukleokapside aviärer Viren mit der PB2-Signatur 627E nach der Infektion einer Säugerzelle im Zytoplasma durch die Binding von RIG-I destabilisiert werden, so dass es zur Exposition der ds-RNA Domänen der viralen RNA kommt. Es konnte weiterhin gezeigt werden, dass die freiliegende ds-RNA nun in der Lage ist, die zytoplasmatische RNA-Helikase RIG-I zu binden und damit deren antivirale Eigenschaften zu aktivieren. Die Stabilität der Nukleokapside bleibt dagegen erhalten, wenn PB2 die Signatur 627K trägt, so dass die RIG-I-abhängige Hemmung der Virusvermehrung nun ausbleibt. Somit konnte nachgewiesen werden, dass die adaptive Mutation E627K die Hemmung der Virusvermehrung durch den Pathogensensor RIG-I moduliert. Darüber hinaus zeigten die Daten, dass die PB2-Mutation D701N nicht nur den nukleären Import von neu synthetisierten PB2-Proteinen steigert, sondern auch den Kernimport von Nukleokapsiden infizierender Viren.

5 INTRODUCTION

5.1 Influenza-A-viruses

Influenza-A-viruses are important human and animal pathogens with high impact on public health and animal livestock. They infect the respiratory and the gastrointestinal tract of the host. The available evidence indicates that all of these pathogens are from a large virus pool, indigenous to wild aquatic birds. Zoonotic infection of humans by avian influenza viruses has already been described and may play a role in the development of pandemic viruses.

5.2 Taxonomy

Influenza viruses are characterized by a segmented single-stranded RNA genome of negative polarity. They belong to the family *Orthomyxoviridae*, composed of five different genera: influenza-A, influenza-B and influenza-C viruses, as well as Thogotovirus, Isavirus and Quaranjavirus. The genomes of influenza-A and B viruses as well as Isavirus are composed of 8 segments, whereas influenza-C virus has 7 segments, and Thogoto and Quaranja viruses 6 segments.

Influenza-A-viruses are classified in different subtypes characterized by their surface glycoproteins: 18 different hemagglutinins (HA) and 10 neuraminidases (NA) [49, 166, 182]. Influenza-A-viruses are able to infect a broad spectrum of avian and mammalian species including humans, pigs, horses and seals. In contrast to influenza-A-viruses, influenza-B and C viruses are restricted to humans. Influenza-C infections are generally asymptomatic, whereas influenza-B virus causes respiratory diseases in humans, like influenza-A-virus. Thogotovirus and Quaranjavirus infect humans, and Isavirus infects fish.

The World Health Organization (WHO) standardized the nomenclature for influenza viruses [1]. It indicates: genus, host species (not mentioned for human isolate), place of isolation, isolate number and year of isolation. The subtype of the virus is usually indicated in parentheses. Here are two examples of avian and human isolates, respectively: A/Quail/Shantou/2061/2000 (H9N2) and A/Anhui/01/2013 (H7N9).

5.3 Morphology and structure of the genome

Influenza virus particles are usually spherical or ovoid with a diameter of 80 to 120 nm [14]. They are enveloped viruses with a membrane containing the two glycoproteins: HA and NA. The HA spike is a trimer consisting of three individual HA monomers, while the NA spike is a tetramer. 80 % of the glycoproteins present at the surface of the virion are HA, whereas NA represent only 20 %. The viral envelope contains as well the M2 protein, which forms a tetramer with ion channel activity [74, 94, 132]. On the inner side of the envelope is the matrix protein M1, surrounding and interacting with the viral genome organized into eight segments of single-stranded RNA [120] (**Figure 1**).

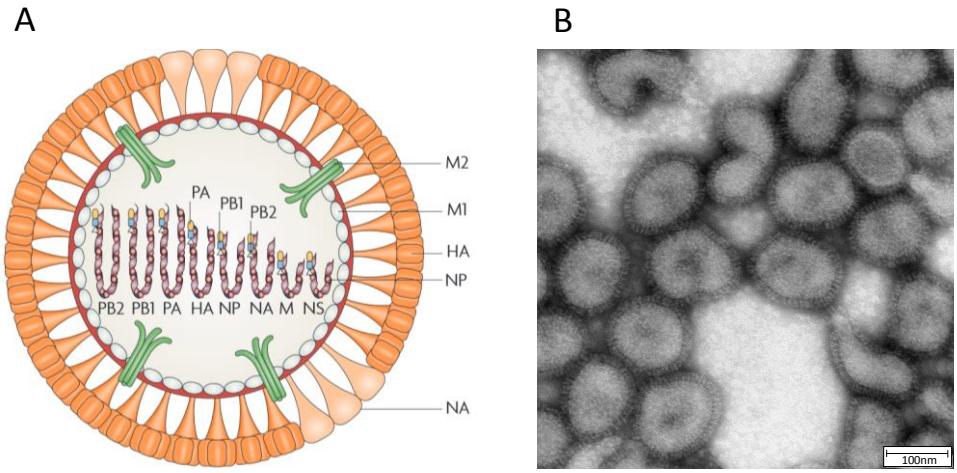

Figure 1 : Morphology of an influenza virus particle. *(A) Schematic representation of the virus particle structure (Subbarao et al 2007). (B) Electron microscopy picture of an influenza particle (image acquired by Dr. Larissa Kolesnikova, Institute of Virology, Marburg)*

The influenza-A-virus genome encodes for 10 major proteins: polymerase basic protein 2 (PB2), polymerase basic protein 1 (PB1), polymerase acidic protein (PA), nucleoprotein (NP), NA and HA, matrix proteins (M1 and M2) and non-structural proteins (NS1 and NS2) [168]. It has been demonstrated that auxiliary proteins were encoded from the segment 2 and 3 (**Table 1**). For example PB1-N40 is a truncated form corresponding to the N-terminal end of PB1, whereas PB1-F2 results from an alternative open reading frame (ORF) of PB1 [29]. Furthermore, the segment 3 encodes several additional proteins such as PA-X, PA-N55 and PA-N182. These are isoforms of PA resulting from the N-terminal truncated part of PA [117] or the fusion of the N-terminal region of PA and the C-terminal region of an additional ORF, called X-ORF [83]. For the segments 7 and 8, additional proteins have also been identified such as M42 and NS3. M42 is a variant of M2 translated from a second initiation codon [184] and NS3 is an isoform of NS1 with an internal deletion [149].

Segment	Protein	Number of amino acids	Function
1	PB2	759	Polymerase subunit responsible for the cap binding of cellular mRNA important for initiation of transcription. This protein affects host range and virulence
2	PB1	757	Polymerase subunit with the RNA dependent RNA polymerase activity required for transcription and replication
	PB1-F2	90	Protein responsible for mitochondria-associated apoptosis
	PB1-N40	718	Protein which maintains balanced expression of PB1 and PB1-F2
3	PA	716	Polymerase subunit with an endonuclease activity responsible for the cap snatching of cellular mRNA
	PA-X	252	Protein responsible for host cell shut-off to decrease the antiviral response
	PA-N155	568	Protein with a potential role in a replication step
	PA-N182	535	Protein with a potential role in a replication step

4	HA	550	Membrane protein responsible for the receptor binding and fusion of the endosomal and viral membrane
5	NP	498	Major protein of the vRNP, associated to the viral RNA. It is responsible for the translocation of the vRNP into the nucleus
6	NA	454	Membrane protein responsible for the release of progeny virus by removing the receptors present at the surface of the cell.
7	M1	252	Matrix protein involved in the export of vRNP from the nucleus to the assembling area
	M2	97	Protein with ion channel activity, responsible for the acidification of the inner core of the virus. Its function is important for genome release post entry
	M42	99	Protein with similar function as M2
8	NS1	230	Protein with interferon antagonist activity
	NS2/NEP	121	Protein responsible for the export of the vRNP in addition to M1 from the nucleus to the cytoplasm
	NS3	174	Protein with potential role in host adaptation

Table 1: Influenza-A-virus segments. *For each segment, the encoded proteins and their functions are listed.*

The viral RNA segments are associated with NP and one heterotrimeric polymerase complex composed of PB1, PB2 and PA [88]. This association of proteins and viral RNA (vRNA) forms a structure named viral ribonucleoprotein (vRNP), where NP plays an important role in the helical structure of the vRNP (**Figure 2**).

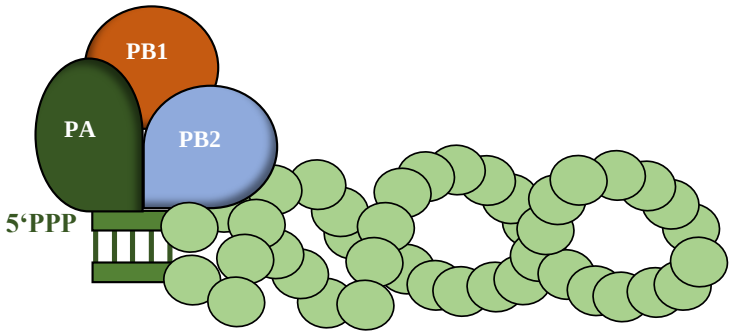

Figure 2 : Structure of an influenza-A-virus ribonucleoprotein*. The vRNPs are composed of a RNA of negative polarity associated with NP (light green). The partial complementarity of the RNA extremities leads to the formation of a double-stranded RNA structure with the exposure of a 5'-triphosphate(5'ppp) (dark green). The polymerase complex is associated to this structure (PB1, PB2 and PA) and is required for the initiation of transcription and replication.*

5.4 Ecology

The natural reservoir of influenza-A-viruses are aquatic birds, where replication usually does not cause signs of disease. Transmission to new species such as humans, pigs, horses, sea mammals and land birds is often observed [141, 171, 182] (**Figure 3**), and mammalian influenza viruses are suggested to emerge from the avian influenza reservoir.

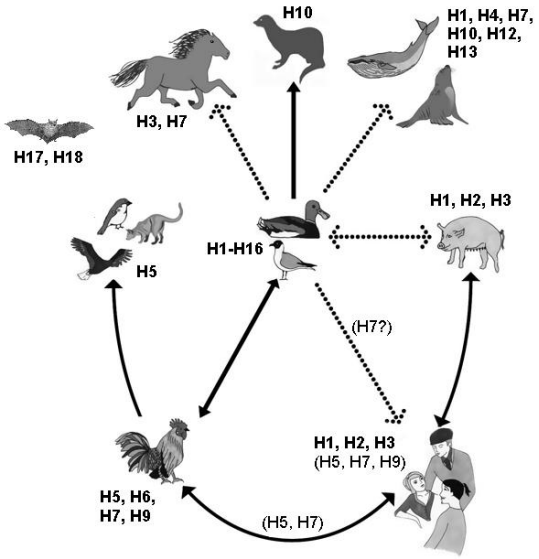

Figure 3 : Host range of influenza-A-viruses and interspecies transmission. *The arrows represent transmission routes between species. Wild waterfowl are the principal reservoirs for influenza-A-viruses which are occasionally transmitted to other host animals such as horses, pigs, and terrestrial birds. Transmissions to man can result in pandemics. (Adapted from Wahlgren et al 2011).*

The reservoir of influenza-A-viruses is found in aquatic birds of the orders *Anseriformes* and *Charadriiformes* [115, 116]. The different combinations of HA and NA subtypes have all been identified in wild birds [2]. Avian influenza-A-viruses are divided into two classes: low pathogenic avian influenza (LPAI) viruses and highly pathogenic avian influenza (HPAI) viruses. LPAI virus replication in birds is confined to the respiratory and intestinal tract resulting in mild disease or asymptomatic infection. The dissemination of the virus among aquatic birds occur via an oral-fecal route, caused by contaminated water [115]. They have HAs with monobasic cleavage site (-R-) that are activated by proteases present in respiratory or intestinal tissues such as TMPRSS2, TMPRSS4 and HAT [18, 24]. The HA glycoprotein needs to be processed to acquire its functional competence that is essential for virus infectivity [87].

HPAI viruses belong to serotype H5 or H7. They have a polybasic hemagglutinin cleavage site (-RXK/RR- or -RXXR-). They are supposed to arise by introduction of LPAI viruses into domestic poultry with subsequent mutations in HA [6]. Insertion of multiple basic amino acid residues in the HA cleavage site enable processing by ubiquitous cellular proteases, such as furin or PC5/6 [158], which do not cleave LPAI HAs. This property facilitates replication through a large spectrum of organs and is responsible of systemic infection, in contrast to LPAI viruses. Viruses that cause 75% or higher mortality during experimental infection of chickens are characterized as HPAI viruses. Those that do not fulfil these criteria are classified as LPAI viruses [58].

It has to be pointed out, that the virulence of an influenza virus is not only determined by the HA cleavage site but depends as well on other proteins such as NS1 and the polymerase complex.

5.5 Epidemiology

Most of the transmissions of avian viruses to mammals are transient and do not result in a new virus. On rare occasions, however, the virus may adapt to the new host and, thus, give rise to a new lineage. If such a new virus is introduced into man it may cause a pandemic.

Human influenza viruses cause seasonal epidemics and less frequent pandemics. Epidemic viruses are derived from pandemic viruses by antigenic drift resulting from the acquisition of point mutations on genes encoding HA and NA. These point mutations occur due to a high error rate of the viral polymerase and the lack of a proof reading function [186]. The antigenic drift generates viruses closely related to the preceding virus, which can still be partially recognized by the immune system. However, accumulation of point mutations eventually leads to immune escape.

The evolutionary mechanism leading to a pandemic virus is antigenic shift. It is based on reassortment events, which can occur during infection of a single cell by two different influenza-A subtypes and is

characterized by the acquisition of a different HA or HA and NA. Pigs may act as „mixing vessel" in this process. In fact, pigs are susceptible to both avian and human influenza viruses and may therefore promote reassortment. However, human infections with swine influenza virus are not observed frequently. This raises the hypothesis of another mixing vessel that may be an avian host. This concept is supported by the observation that quails, known to be susceptible to infection with avian H9N2 virus, contain cell receptors that allow also infection with human viruses [77, 172, 173].

Through the last decades, several pandemics have been observed in the human population (**Figure 4**). The most devastating pandemic occurred in 1918, named "Spanish influenza", which caused 20 million to 50 million deaths worldwide. The virus was reconstituted from RNA fragments preserved in lung tissue which belong to victims of this pandemic [164].Whether the H1N1 virus causing the 1918 pandemic was generated by reassortment or whether it was directly derived from a bird virus without reassortment is not clear [137].

Two other pandemics followed in 1957-1958 with an H2N2 isolate, first identified in China, and in 1968-1969 with a H3N2 isolate, first detected in Hong Kong. These two pandemic strains were generated by reassortant viruses with three or two genes of avian origin [85]. The most recent pandemic occurred in 2009 with an H1N1 isolate, derived from a triple reassortment with genes of human, swine and avian origin [122, 154].

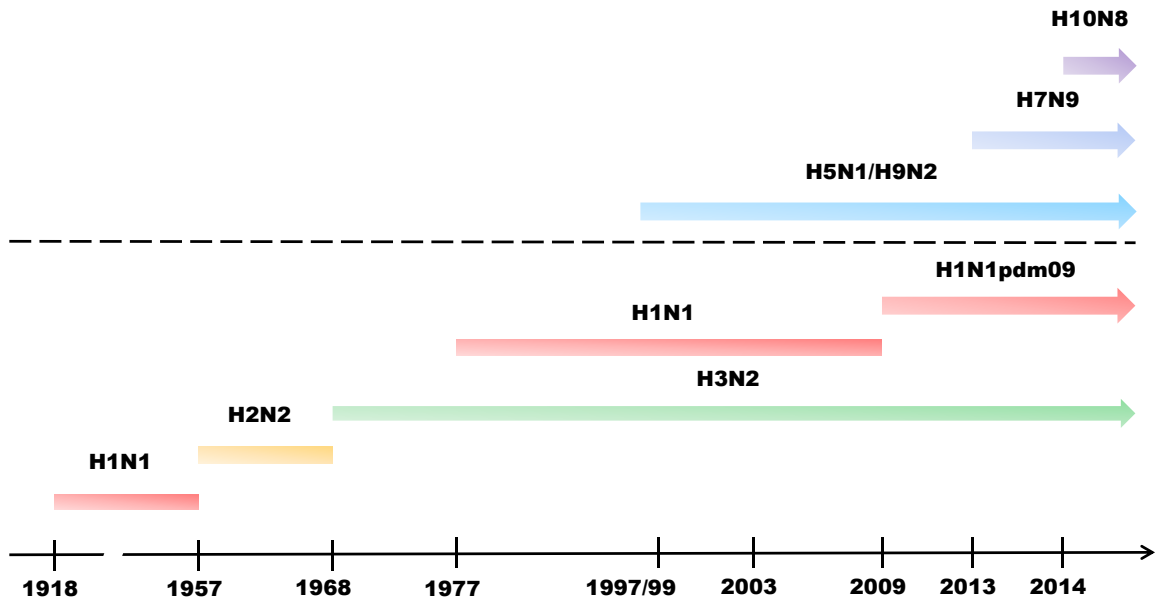

Figure 4 : Timeline of influenza pandemics and recent zoonotic infections in humans. *The pandemics infections are represented in red, yellow and green, and the zoonotic infections are represented in blue and purple (Adapted from NIH 2011)*

5.6 Transmission of avian influenza viruses to man

Human influenza viruses spread by airborne transmission from man-to-man. The transmission of human influenza viruses occurs (i) by direct contact with infected individuals; (ii) by contact with contaminated objects and (iii) by inhalation of virus aerosols.

On rare occasions, avian influenza may also infect man and cause a zoonotic infection without adaptation to the human host as it has been observed with H5N1, H9N2, H7N7, H7N9 or H10N8 subtypes. Transmission of an H5N1 virus in 1997 in Hong-Kong was the result of an epizootic event, where the virus was transmitted from infected chickens to humans with 18 confirmed cases. Since 2003, sporadic H5N1 outbreaks have been observed in many Asian countries with 658 confirmed human cases (including 388 deaths). Domestic ducks and land-based poultry probably played a critical role in the generation and maintenance of the H5N1 virus [76]. In 2003, during an H7N7 poultry outbreak in the Netherlands, a large number of human infections have been observed with suspected human-to-human transmission [48]. Most of the cases showed mild symptoms. Only one case showed an acute respiratory distress syndrome, resulting in the death of the patient.

On 31 March 2013, three cases of confirmed human infection with avian influenza A H7N9 virus were reported in China. Most patients initially developed an influenza-like illness that evolved to respiratory distress syndrome [56]. At the end of 2014, 470 cases (including at least 184 deaths) have been reported since the beginning of the outbreak. In December 2013, the first human case of H10N8 was also reported. These zoonotic outbreaks (H5N1-1997, H7N9 and H10N8) were the result of reassortment with H9N2-circulating viruses [26, 45, 64, 134].

5.7 H9N2 virus

Within the last 20 years, several H9N2 outbreaks have been documented throughout Europe, the Middle East and Asia. The viruses have become endemic in the last decade, and have been isolated from many different species of terrestrial poultry worldwide. In 1999 and 2003, zoonotic H9N2 outbreaks have been reported in China, with mild symptoms and no human-to-human transmission. Two distinct lineages of H9N2 viruses are now established in terrestrial poultry, A/Duck/Hong Kong/Y280/97 in chicken and A/Quail/Hong Kong/G1/97 in quail [64, 97]. The latter has already been isolated from humans and was involved in the generation of the highly pathogenic H5N1 virus in 1997 [64, 100]. Co-circulation and reassortment with other strains in terrestrial poultry generated the H7N9 virus [45, 56] and H10N8 virus causing outbreaks in human in 2013 and 2014 [26, 134]. H9N2 viruses also expanded their host range as indicated by the observation that a few strains isolated from land-based birds, efficiently replicate in and kill mice without prior adaptation. Quails are now considered to play an important role in the genesis of new influenza viruses, since their tissues have receptors for both avian

and human influenza viruses [77, 172, 191]. Furthermore, infections of pigs with H9N2 viruses have been observed since 1998 [32, 33]. Infected pigs presented typical illness signs, including fever, nasal and ocular discharge, coughing and dyspnoea, with a high mortality rate. In addition to the cases in 1999 and 2003, there have been more human H9N2 infections in the recent years causing respiratory disease, but without human-to-human transmission [23, 130]. The recurring presence of H9N2 infections in pigs and humans, as well as the establishment of the virus in poultry has raised concerns about the possibility that H9N2 viruses are capable of evolving into pandemic strains [129].

5.8 Disease in humans

Human influenza-A-viruses are the cause of contagious respiratory illness. The major symptoms of the disease are fever, cough, headaches and muscle aches. Acute symptoms and fever often persist for 7 to 10 days, but most of infected patients recover after a week. However severe complications are observed among children, elderly or immunocompromised patients. These complications include hemorrhagic bronchitis, pneumonia (often caused by bacterial co-infection), lung failure or death. In case of mild infection, the upper respiratory tract and trachea are predominantly infected, in contrast to severe influenza infections, usually associated with pneumonia [165].

Bacterial superinfection in the lungs of influenza infected patient promotes severe disease and mortality. This co-pathogenesis is characterized by the disruption of physical barriers and dysregulation of immune response [107]. In addition, some bacteria such as *S.aureus* secrete proteases capable of cleaving the HA protein and activate the virus [163], enhancing thereby its pathogenicity.

5.9 Prophylaxis and therapy

Vaccination is the most efficient measure against influenza infection, even if a constant adjustment is required to adapt to the evolving nature of the viruses. Vaccination is especially important for people at higher risk of serious influenza complications. The WHO recommends vaccination for pregnant women, young children, elderly and individuals with chronic medical conditions. The seasonal vaccine is trivalent and composed of two influenza-A-viruses (H1N1 and H3N2) and one influenza-B virus. For 2014/2015 influenza vaccines are composed of an A/California/7/2009 (H1N1) pdm09-like virus, an A/Texas/50/2012 (H3N2)-like virus and a B/Massachusetts/2/2012-like virus.

Two major types of influenza vaccines are available. First, there are inactivated vaccines, which are injected intramuscularly. There are three types of inactivated vaccines: whole virus vaccines, split virus vaccines (detergent-disrupted virus), and subunit vaccines (purified HA and NA without other viral components). Secondly, there are attenuated influenza vaccines, delivered intranasally. Attenuated vaccines are based on temperature-sensitive virus isolates that replicate well in the nasopharynx but poorly in the lower respiratory tract.

Antiviral therapy is also an option. There are two different types of inhibitors available, which need ideally to be administrated within 48 h after appearance of symptoms. First, there are inhibitors against the M2 ion channel protein, amantadine and rimantadine [70]. These inhibitors prevent the acidification of the inner core of the virion and therefore the release of the vRNP from the matrix protein 1 (M1) [183]. These molecules are active against influenza-A-viruses, but not influenza-B-viruses. Because of a high rate of resistance among influenza-A-viruses, these inhibitors are no longer recommended. Secondly, there are neuraminidase inhibitors, zanamivir, oseltamivir [70] and peramivir [145]. These molecules target the catalytic site of the enzyme [86, 169]. They are effective against influenza-A and B viruses. Zanamivir is used as an inhaled treatment, oseltamivir as an oral treatment and peramivir is administrated in the form of enteric capsules. However, influenza viruses develop also resistance to these compounds [145]. Thus, there is a need for the development of new molecules targeting other proteins, such as the polymerase complex.

5.10 Viral replication cycle

The virus cycle is initiated via the binding of sialic acid receptor present at the cell surface by the glycoprotein HA (**Figure 5, step 1**) [153]. Receptor binding leads to endocytosis of the virus and exposure to low pH (**Figure 5, step 2**). The ion channel M2 pumps protons into the inner core of the virion [132] leading to a conformational change of the matrix protein M1 [21]. Furthermore, acidification triggers a conformational change of HA, which allows the exposure of the fusion peptide [183]. The latter promotes the fusion of the viral and the endosomal membrane (**Figure 5, step 3**), and consequently the release of the viral RNP into the cytoplasm (**Figure 5, step 4**) [41, 78, 152]. They are then translocated into the nucleus where transcription and replication take place (**Figure 5, step 5**) [104, 125]. The primary transcription will lead to the synthesis of the early proteins, NP, PB1, PB2, PA, and NS1. These proteins are then imported into the nucleus (**Figure 5, step 6**) where NP monomers are bound to newly synthesized vRNA which in association with the polymerase complex will form new vRNP. The matrix protein M1, the nuclear export factor (NEP) and the glycoproteins HA and NA are synthesized at a late stage of infection. The M1 protein, which possesses a nuclear localisation signal (NLS), enters the nucleus and binds to the vRNPs. Because M1 does not present a nuclear export signal (NES), NEP is required. The protein is able to bind the NLS signal of M1 and mediates the export of both M1 and vRNP from the nucleus to the cytoplasm (**Figure 5, step 7**) [22, 175, 193]. The M1 protein interacts with the C-terminal domains of HA and NA forming high density patches at the cell plasma membrane [8, 61], where the eight segments of the influenza genome are assembled (**Figure 5, step 8**) [60]. After budding, the new virions are still attached to the cell surface through interaction of the HA with sialic acid residues (**Figure 5, step 9**). NA cleaves the remaining sialic acids, releasing consequently the virions from the host cell surface.

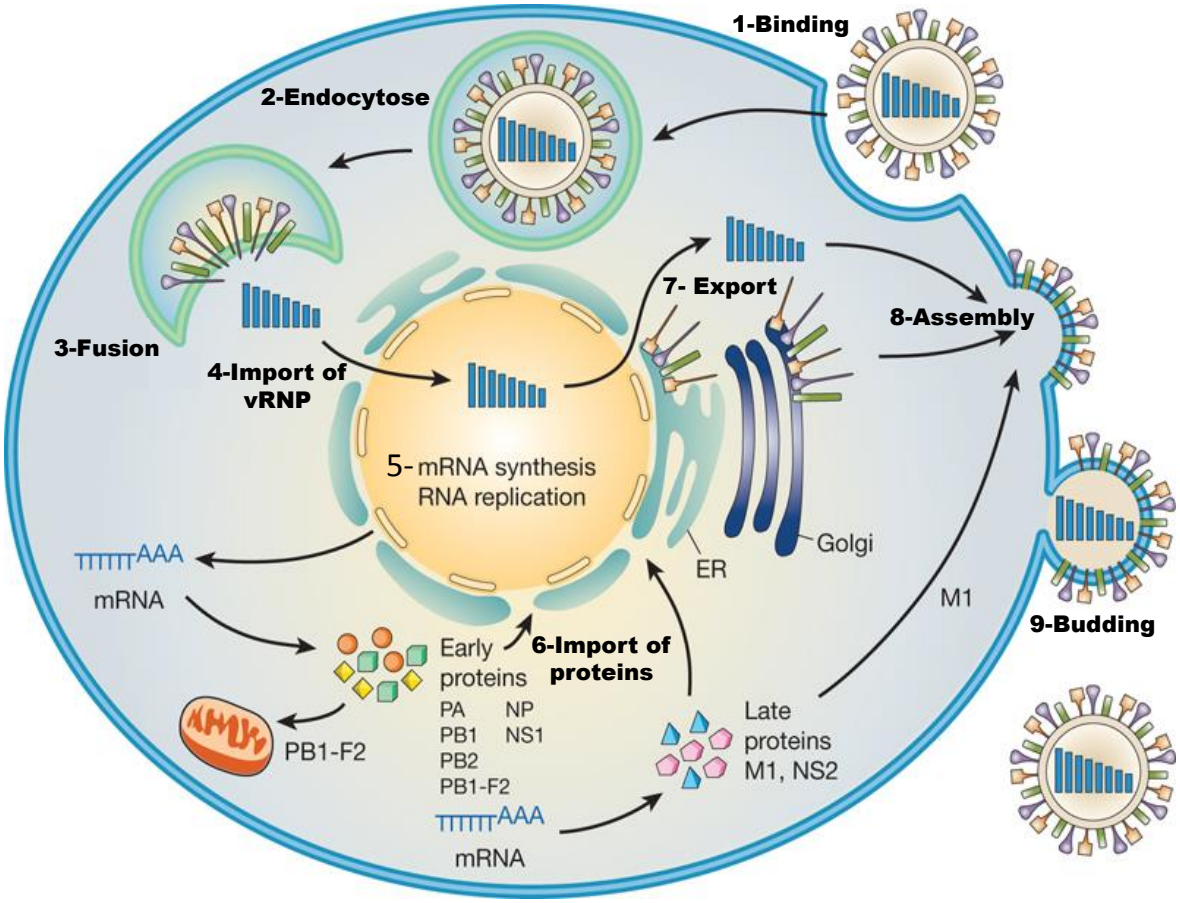

Figure 5 : Replication cycle of influenza-A-viruses*. (Modified from Neumann et al 2009)*

5.10.1 Transcription and replication

Initiation of the cap-dependent transcription starts with the binding of the 7-methylguanosine cap of the cellular pre-mRNA by PB2 (**Figure 6**). The endonuclease (localized in PA) cleaves this pre-mRNA 10-14 nucleotides downstream the cap. The capped primer is directed into the PB1 active site, where the viral sequence transcription occurs. The elongation of the transcription is supposed to lead to the release of the cap from the cap binding domain and the association with host cell factors [136]. The termination of the transcription results in the polyadenylation of the vRNA by stuttering of the polymerase [133, 140].

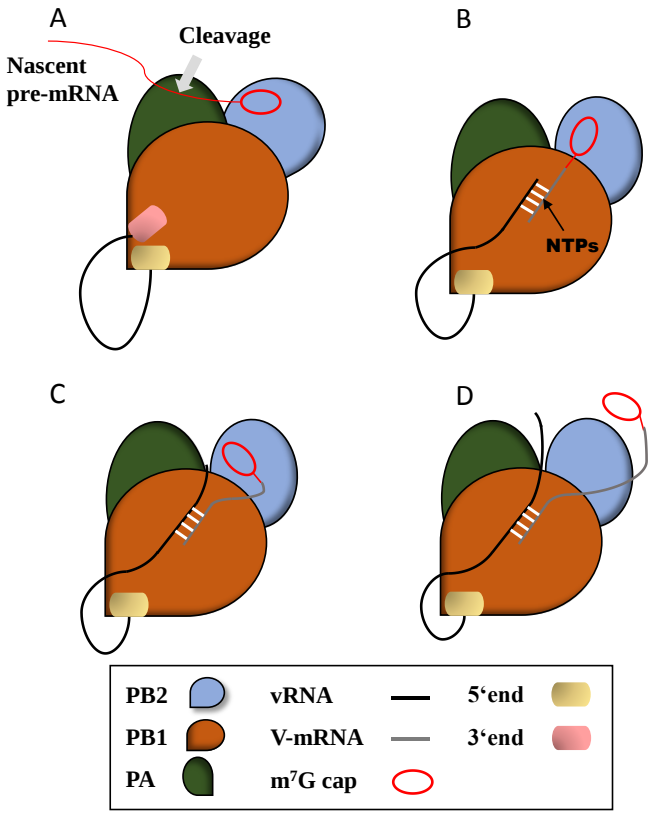

Figure 6 : Schematic representation of the transcription initiation step of influenza-A-virus. *(A) Binding of the pre-mRNA cap structure by the PB2 subunit. (B) Initiation of the transcription, PB2 rotates to enable the capped primer to enter the active site of PB1. (C) Elongation of the transcription. (D) Elongation of the transcript lead to the release of the cap from the cap-binding domain. (Modified from Reich et al 2014)*

In contrast to the transcription, the replication is cap independent. The replication process of influenza virus is driven by the synthesis of a complementary RNA (cRNA) of positive polarity, non-capped and not polyadenylated [69]. This cRNA is also associated with NP monomers and the polymerase complex and serves as template for the synthesis of vRNA. The switch from transcription to replication remains unclear, but two hypotheses have been proposed. It is first hypothesized that the cRNA transcripts are impaired in their elongation and prematurely degraded due to the absence of newly synthesized NP [75, 170]. The second hypothesis proposes a switch to replication via the binding of free NP to the polymerase complex [123].

5.10.2 Promoter structure

Influenza-A-virus vRNAs contain quasi-conserved and segment-specific sequences [73], which constitute the promoter for viral transcription and replication. Different structures of the vRNA promoter have been proposed such as a panhandle [176], a corkscrew [47] or a hook [131] (**Figure 7**).

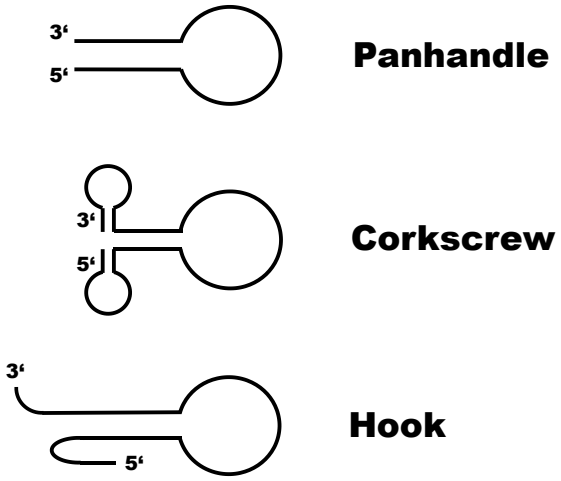

Figure 7 : Schematic representations of the viral promoter structure.

The 3' (characterized as the template) and 5' (characterized as the activator) extremities are partially complementary and form a double helix structure defined as panhandle [5, 11, 176]. However, these extremities are thought to bind the polymerase in a partially single-stranded conformation either as a corkscrew [46] or a hook [131]. A recent study has demonstrated that the influenza vRNA promoter has a hook structure. In fact, the 5' hook is localized in a pocket formed by PA and PB1 supposed to play an important role in the polymerase function [131]. The structure of the cRNA promoter is not known, but available data suggest that the structure is different from the vRNA promoter. This difference is thought crucial regarding the encapsidation process of vRNP.

5.11 Proteins of the nucleocapsid

As the genome of influenza viruses is of negative polarity, the virus encodes its own polymerase. The latter is a heterotrimeric complex composed of PB1, PB2, PA. The polymerase complex has an RNA-dependent RNA polymerase activity and in association with NP catalyses the transcription and replication of the virus [38, 79].

5.11.1 NP and vRNP

In contrast to other negative RNA viruses, the transcription and replication steps of influenza viruses occur into the nucleus. Therefore, the incoming polymerase, associated to the nucleocapsid, is directly imported into the nucleus. The vRNP import is driven by NP, which binds to the adaptor protein importin-α, and promotes the nuclear transport [125] (**Figure 8**).

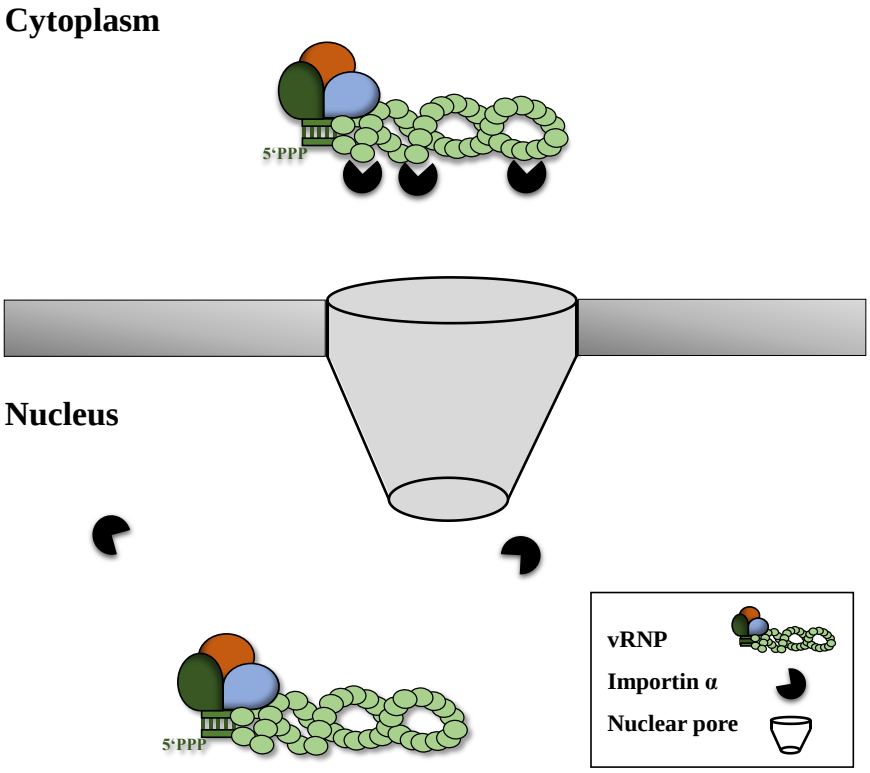

Figure 8 : Schematic representation of the vRNP transport into the nucleus of the infected cell. *vRNPs are imported via the classical import pathway, importin-α dependent. The binding of the importin-α to NP promotes this nuclear import. When presents into the nucleus, importin-α is released from the vRNPs.*

NP binds single-stranded RNA without sequence specificity and is essential for the RNA transcription and replication. It is required as a structural element in the RNP template, where interaction between two NP molecules is responsible for maintaining the double helical structures of vRNPs and cRNPs. This homo-oligomerisation occurs via the insertion of a NP tail loop into the cavity of an adjacent NP molecule [4, 31] (**Figure 9**).

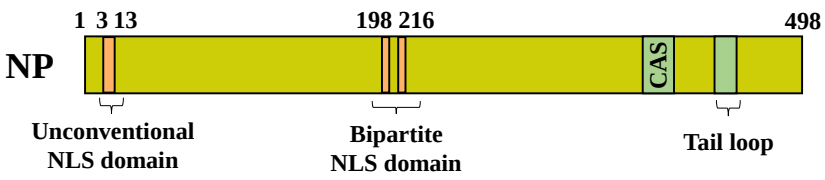

Figure 9 : Structure of NP. *Here are represented the cytoplasmic accumulation signal (CAS) and the tail loop domain important for the oligomerization. NP presents two NLS domains: the bipartite NLS and the unconventional NLS (dominant signal).*

5.11.2 PB1, PA and PB2

During the primary transcription step, newly synthesized proteins of the polymerase complex have to be imported into the nucleus for the subsequent steps of the infection. The subunit PA and PB1 are imported as a heterodimer via the non-classical nuclear import pathway, importin-α independent, by direct interaction with RanBP5 [39] (**Figure 10**).

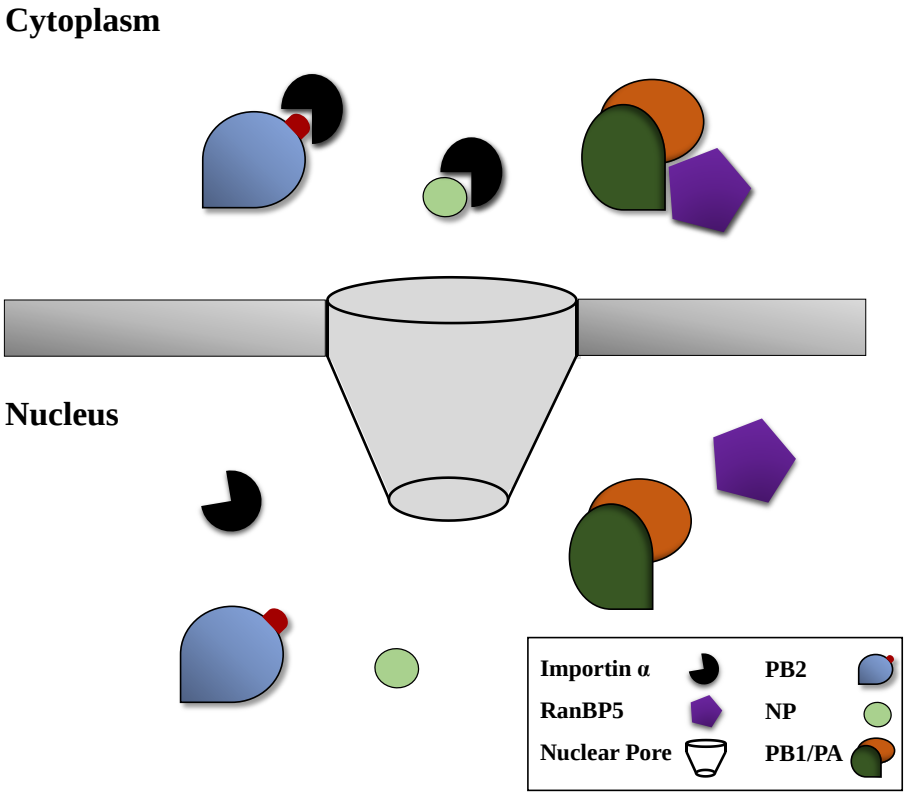

Figure 10: Schematic representation of the newly synthesized proteins essential for vRNP structure. *The entry of newly synthesized proteins is driven by two pathways: the classical and non-classical import pathway. The import of PB2 and NP is driven via the importin-α adaptors, as monomers. In contrast the entry of PB1 and PA is driven via the RanBP5 adaptors, as PB1/PA dimer.*

PB1 is the core of the polymerase trimer containing the RNA dependent RNA polymerase domain important for the transcription and the replication step [15, 20]. PB1 can specifically recognize the vRNP promoter sequence [62, 136]. Its close interaction with PA forms a pocket where the 5' hook of the genome is maintained. PB1 interacts with PA and PB2 [136] (**Figure 11**).

PA is composed of 2 major domains, the N-Terminal part containing the endonuclease domain [40] and the C-terminal part responsible for the interaction with PB1 [31]. The endonuclease domain binds to the rest of the polymerase through the C-terminal region of PB1 which also interacts with the PB2 N-terminal region. These two domains of PA are connected via the PA-linker, which wraps around PB1. The enzymatic activity carried by PA enables the cleavage of the cap from pre-cellular mRNA, which promotes the initiation of the transcription [40] (**Figure 11**).

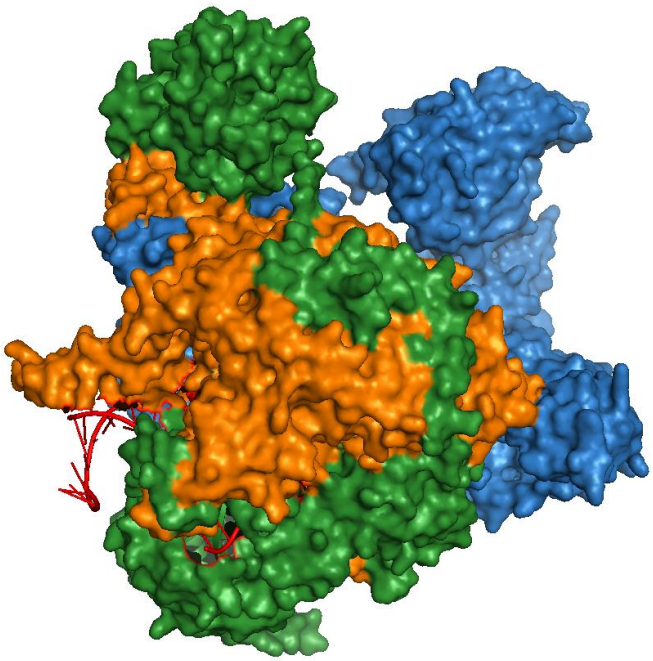

***Figure 11 : 3D structure of the polymerase complex**. Here is represented the interaction of the polymerase proteins. PB2 is coloured in blue, PB1 in orange and PA in green. (Adapted from Reich et al, 2014)*

In contrast to PB1/PA, PB2 is translocated to the nucleus as a monomer by the classical nuclear import pathway, using the importin-α/β adaptors [52, 162] (**Figure 10**).

PB2 is composed of 4 major domains: the region involved in PB1 binding, the domain responsible for the cap binding, the 627 domain and finally the NLS domain. It is involved as much in the replication as in the transcription process. Point mutations in this subunit, such as R142A or F130A, abolish RNA replication, but not transcription. In contrast, mutants defective in cap-recognition transcribe poorly but have an efficient replication [59, 65].

5.12 Polymerase complex: a host range determinant.

Viruses are obligatory intracellular pathogens and require the cell machinery for an efficient infection. As a result, viruses adapt to their host to subvert the host factors or counteract the immune defenses. The polymerase complex, as well as HA and NS1, play a central role in the host adaptation. As explained above, the polymerase complex of influenza virus is composed of three subunits: PB1, PA and PB2.

PB2 is responsible for the cap binding from cellular messenger RNA enabling viral transcription [16], and has been described as an important host range factor able to modulate the virulence of influenza viruses. Over the years, several mutations in the PB2 subunit have been identified that mediate adaptation of an avian virus to a mammalian host. Mutations at position 591, 627, 701 and 714 have been described to enhance polymerase activity as well as viral replication in mammalian cells, in addition to mice pathogenicity [36, 50, 159, 160, 194] (**Table 2**).

Virus	Host Range	Positions				Reference
		591	627	701	714	
H3N2	a-c		E-K			Subbarao et al., 1993
H5N1	a-m		E-K			Hatta et al.,2001
H5N1	a-h		E-K			Naffakh et al., 2002
SC35/M (H7N7)	a-m			D-N	S-R	Gabriel et al., 2005
H5N1	a-h		E-K	D-N	S-I	de Jong et al., 2006
H1N1	s-h	Q-R				Mehle et al, 2009
H5N1	a-m	Q-R				Yamada et al, 2010
H9N2	a-h			D-N		Baranovich,T et al, 2014
H7N9	a-h		E-K			Wong CK et al., 2013

Table 2 : Adaptive mutation characterized in PB2 subunit*. Mutations in PB2 have been described in several influenza-A subtypes. Here are listed for each virus subtype the host range, as well as the amino acid found in each species. Host range: a, avian; c, canine; m, murine and h, human.*

In 1993, the first mutation in the PB2 subunit was described to enhance the polymerase activity of an H3N2 virus [159]. In 1997, in Hong Kong, was reported the transmission of an H5N1 HPAI virus from infected poultry to humans with mutation in the PB2 subunit [160]. During the past years, it became more and more clear that the viral polymerase complex is linked to enhanced polymerase activity and pathogenicity, and is therefore a major determinant of mammalian adaptation.

In avian isolates the amino acid at position 627 is a glutamine, while it is a lysine in mammalian strains. This mutation E627K provokes an increased polymerase activity and viral replication, enhanced mice pathogenicity and temperature sensitivity [80, 93, 105, 159]. Furthermore, the NLS domain of PB2 contains position 701 which is also playing an important role in the host adaptation. Indeed, the amino acid present at this position is responsible for the open or close conformation of the NLS domain. The mutation from an aspartate present in avian isolates to asparagine present in mammalian strains induces a conformational change in the NLS of PB2 which favours its interaction with the importin-α [52, 162].

The other proteins of the polymerase complex PB1 and PA, as well as NP also play a role in host adaptation. Mutation N319K in the NP protein has been described to enhance binding to the importin-α factor, and therefore to increase the nuclear import [52]. In contrast to PB2, there are not many adaptive mutations described for PB1 or PA. Mutations L472V and L598P in the PB1 subunit

have been shown to compensate for the lack of mutation E627K in PB2 [190] and mutation K615N in the PA subunit has been shown to enhance the polymerase activity in mammalian cells [50]. The role in pathogenicity of these two subunits might be closely related to their auxiliary proteins PB1-F2 and PA-X [168].

5.13 Innate immunity

Innate immunity is based on pathogen recognition via cellular sensors known as "Pattern-Recognition Receptors" (PRRs). These sensors play a central role via their abilities to recognize "Pathogen-Associated Molecular Patterns" (PAMPs), and to promote the signaling pathways leading to the innate immune response. The two most characterized class of PRR are the "Toll-like" receptors and "RIG-like" receptors including Retinoic Acid Inducible Gene I (RIG-I) and Melanoma Differentiation-Associated protein 5 (MDA-5) [161]. These innate immunity sensors are present in the cytoplasm and detect cytoplasmic double-stranded RNA by size, secondary structure and nucleotide composition specificity. RIG-I is known as one of the major sensors of influenza viruses. RIG-I activation leads to the translocation of Interferon Regulatory Factor 3 (IRF-3) into the nucleus where the productions of type I interferon (IFN), including IFN-α and IFN-β, is induced. The recently discovered type III interferon, composed of IFN-λ1, IFN-λ2 and IFN-λ3, and type I IFN are essential factors preventing viral replication [3, 95].

The IFN production is one of the first lines of defence against viral infections. Secreted IFN-α and IFN-β bind the IFN receptor (IFNAR) which induces, via the JAK/STAT pathway, several IFN-stimulated genes (ISG). The best characterized ISG are: the protein kinase RNA dependent (PKR), the 2'-5' oligoadenylate synthetase (OAS), RIG-I, MDA-5 and Mx proteins [142].

Recognition of double-stranded RNA by PKR provokes its phosphorylation and therefore activation. Activated PKR phosphorylates the eukaryotic translation initiation factor 2 alpha (eIF2α), which leads to the inhibition of protein synthesis of cellular and viral mRNAs [112]. PKR also activates the transcription factor IRF-3, promoting IFN-β expression [57].

5.13.1.1 RIG-I signalling pathway

RIG-I is a member of the DExD/H box RNA helicase family and is therefore composed of a carboxy-terminal domain (CTD), a central DExD-H box RNA helicase domain and two caspase recruitment domains (CARDs) [90, 92] (**Figure 12**).

Figure 12: Schematic representation of RIG-I. *(Weber and Weber 2014)*

The ligand recognition is driven by the CTD and helicase domains, and the signal transduction is determined by the CARDs (**Figure 13**). RIG-I possess two conformations, an auto-repressed one where the RNA binding site is masked by the CARDs, and an active conformation where the CTD binds a specific ligand and exposes the RNA binding site [91]. The RIG-I active form will then oligomerize and be ubiquitinated by the Tripartite Motif 25 (TRIM25) [54]. RIG-I oligomers interact then with the adaptor protein mitochondrial antiviral-signaling protein (MAVS), which induces the TBK-1/IKK-ε kinases. This signaling pathway leads to the phosphorylation and nuclear translocation of IRF-3 transcription factor. Simultaneously, the NF-κB signaling pathway is induced, where NF-κB translocates as well into the nucleus. These two transcription factors promote the expression of type I IFN and pro-inflammatory cytokines [13] (**Figure 13**).

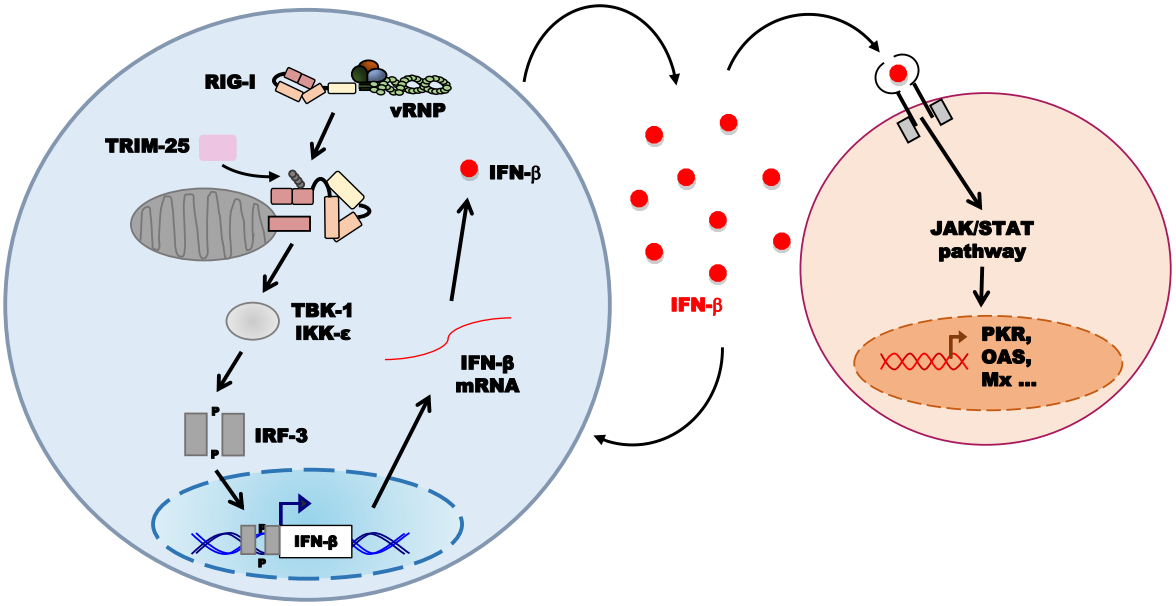

***Figure 13: IFN signaling pathway following RIG-I activation**. Presence of double-stranded RNA in the cytoplasm is sensed by RIG-I. The recognition of the 5'ppp lead to the conformational change of RIG-I, followed by its ubiquitination by TRIM25. RIG-I CARDs domains then interact with MAVS and induce the signaling pathway leading to the nuclear translocation of IRF-3. Expression and secretion of IFN-β induce the expression of Interferon Stimulated Genes (ISG) such as PKR, OAS and Mx.*

5.14 Innate immune system counteracting proteins

Influenza virus has developed several strategies to avoid sensing and signaling of the innate immune system. One of the major influenza proteins in immune counteraction is NS1 (**Figure 14**). It plays a central role in the inhibition of IFN production and IFN induced effectors [43]. The mechanism of IFN inhibition targeting RIG-I pathway, involves the degradation of the TRIM25 protein. TRIM proteins possess a common structure including an N-terminal RING domain, one or two B-box domains, a coiled-coil domain and a variable C-terminus [111]. The RING domain contains the E3 ubiquitin ligase activity, which in the case of TRIM25, regulates RIG-I K63-ubquitination, therefore activation. Upon influenza infection, the protein NS1 is able to bind TRIM25, inducing its K48-ubquitination and thus degradation. In the absence of the activating ubiquitination of RIG-I, the signaling pathway is abolished [55]. Additionally, NS1 is able to interfere with processing, nuclear export and translation of the host mRNA.

For example, NS1 inhibits type I IFN induction via interaction with the cleavage and polyadenylation specificity factor-30 (CPSF-30), which inhibits polyadenylation of cellular mRNAs [121]. NS1 inhibits also the maturation of pro-inflammatory cytokines such as interleukine-18 (IL-18) and IL-1β via the inhibition of the capase-1 [156]. NS1 has finally been described to bind dsRNA, preventing PKR recognition and therefore translation arrest [102].

Other proteins have demonstrated a role in innate immune response inhibition, such as NP which targets PKR activation (**Figure 14**). In the absence of infection, PKR is strongly regulated by cellular inhibitors such as protein $P58^{IPK}$. In uninfected cells, $P58^{IPK}$ forms a complex with the heat shock protein 40 (Hsp40). Upon influenza infection, NP promotes their dissociation. The release of $P58^{IPK}$ will provoke the inhibition of PKR, and thereby, the inhibition of the translation arrest [150]. Other viral proteins, such as the polymerase subunits PB1, PB2 and PA, are also able to impair MAVS signaling and consequently the IFN production [82].

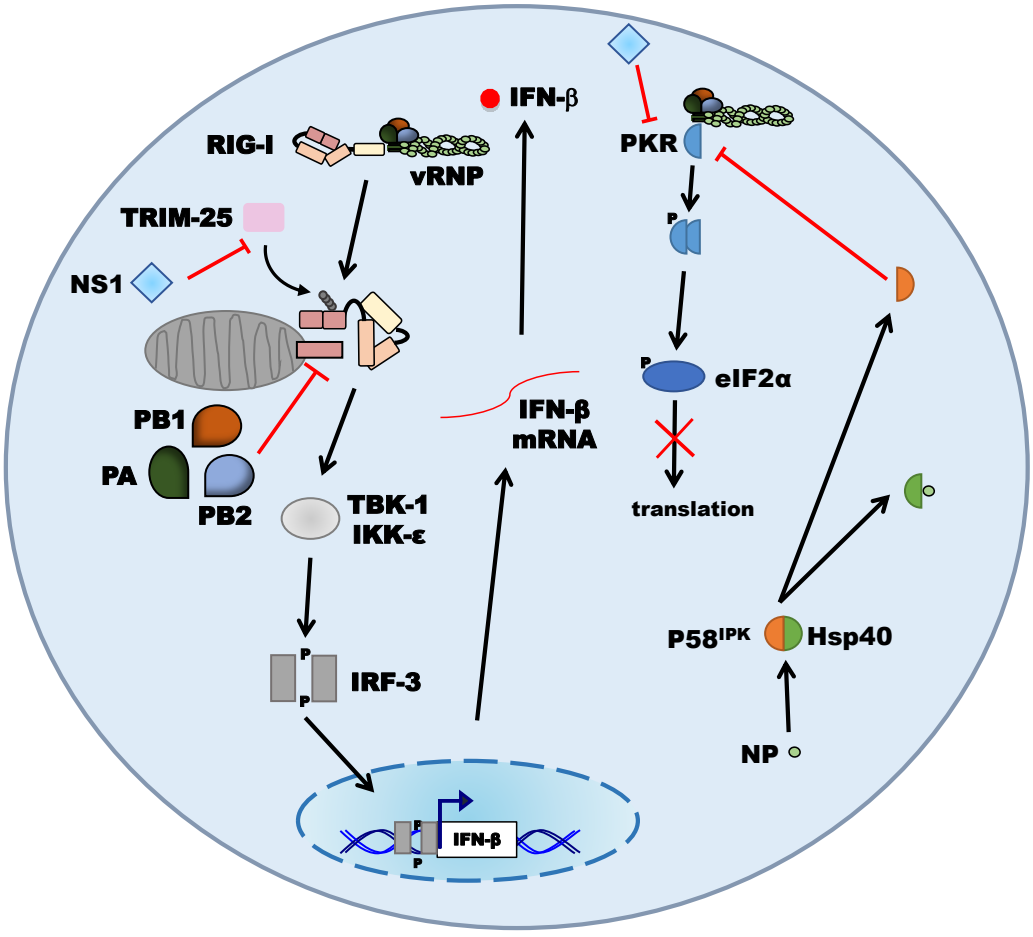

Figure 14: Viral inhibition of IFN production by influenza-A-virus proteins. *The NS1 protein targets TRIM25 and induces its degradation. The absence of TRIM25 prevents RIG-I full activation and consequently IFN-β expression. NS1 binds also to the double-stranded RNA structure of the genome and therefore counteracts PKR recognition. Furthermore, NP targets the protein Hsp40 and provokes the dissociation of the $P58^{IPK}$/Hsp40 complex. This cellular inhibitor interacts and inhibits PKR, which consequently restores the translation of cellular and viral proteins. In addition, the proteins of the polymerase complex interacts with MAVS and inhibits the downstream signaling pathway.*

5.15 Objectives of the thesis

Pandemic influenza-A-viruses are derived from avian influenza viruses from which they have acquired at least one gene segment. Avian influenza viruses of subtype H9N2 are circulating worldwide and are endemic in poultry in a large part of Asia. Furthermore, these viruses have been occasionally transmitted to man and have contributed genes to other avian viruses causing human infections. It is therefore of interest to find out if H9N2 viruses have the potential to fully adapt to man and to cause a pandemic. Increasing evidence has highlighted the role of the virus polymerase complex, and particularly the PB2 subunit, as critical determinants for host adaptation and virulence. The aim of this study is to determine if introduction of adaptive mutations in the PB2 subunit of the avian A/Quail/Shantou/2061/2000 and A/Quail/Shantou/782/2000 (H9N2) viruses promotes adaptation to mammals.

To answer this question, in the first part of the thesis the impact of the adaptive mutations on polymerase activity and viral growth will be investigated by performing minigenome assays and studies of growth kinetics, respectively. In order to evaluate the effect of the adaptive mutations on the virulence of H9N2 virus, mice pathogenicity studies will be conducted. The role of the adaptive mutations will also be compared in H9N2, H1N1pdm09, H7N7 and H7N9 viruses and the contribution of PB1 and PA will be analysed by generating heterologous polymerase complexes

To throw more light on the functional role of adaptive mutations E627K and D701N, their effects on the interaction of PB2 with host factors will be analysed in the second part of the thesis. The focus will be on the nuclear transport of the nucleocapsid and on PB2 interaction with the innate immune system.

6 MATERIALS

6.1 Chemicals

Acetic acid glacial, Acrylamide, Agarose, Ammonium persulphate (APS), Avicel, **B**acto agar, Bacto tryptone, Bromophenol blue, **D**API (4',6-diamidino-2-phenylindole), Dimethyl sulfoxide (DMSO), Disodium hydrogen phosphate (Na_2HPO_4), **E**thanol, Ethidium bromide, Ethylenediaminetetraacetic acid (EDTA), **F**luoroprep, **G**lutamine, Glycerol, Glycine, **I**sopropanol, **M**agnesium chloride ($MgCl_2$), Magnesium sulfate ($MgSO_4$), ß-Mercaptoethanol, Methanol, **P**araformaldehyde (PFA), Peptone, Potassium chloride (KCl), Potassium dihydrogen phosphate (KH_2PO_4), **S**kimmed milk powder, Sodium chloride (NaCl), Sodium dodecylsulfate (SDS), N,N,N',N'**T**etramethylethylendiamine (TEMED), Trishydroxymethyl-aminomethan (TRIS), Triton X-100, Tween20/80, **X**ylene cyanol, **Y**east extract

All the chemicals were purchased from the following companies:
BD Biosciences (USA), Biomérieux (Lyon), Biorad (Munich), Gibco BRL (Eggenstein), Life technology (Darmstadt), Lonza (USA), Merk (Darmstadt), PAA (Cölbe), Roth (Karlsruhe), Saliter (Obergünzburg), Serva (Heidelberg), Sigma-Aldrich (Steinheim).

6.2 Consumables

Combi-tips Ritips	Ritter GmbH, Schwabmünchen
Cryotubes	Corning, Niederlande
Slides	Menzel-Glaser, Braunschweig
Syringes	B Braun AG, Melsungen
Eppendorf-reaction tubes	Eppendorf AG, Hamburg
HybondTM-P Polyvinylidenfluorid **(**PVDF)-Membrane (0.45µm)	GE Healthcare, UK
Needles (20 to 26 G)	BD GmbH, Heidelberg
Milk powder	Topfer, Dietmannsried
Cover slips	Menzel-Glaser, Braunschweig
Parafilm	Structure Probe Inc., München
PCR-Tubes	Biozym, Hess. Oldendorf
Petri dishes	Greiner, Frickenhausen
TipOne-Pipette tips	Starlab GmbH, Ahrensburg
Whatman 3MM-Filter paper	Schleicher & Schuell, Dassel
Cell culture flasks (25 and 75 cm^2)	Greiner, Frickenhausen
Cell culture plates with multiwells	Greiner, Frickenhausen

Cell culture tubes	Greiner, Frickenhausen
Cell scrapers	Sarstedt, Newton, USA
Falcon polypropylene round-bottom tubes	BD GmbH, Heidelberg

6.3 Kit

Plasmid DNA mini kit I	Omega, USA
QIAfilter Plasmid Maxi kit	Qiagen, Hilden
QiaAmp Viral RNA Minikit	Qiagen, Hilden
QIAquick PCR purification kit	Qiagen, Hilden
QuickChange™ Site-directed Mutagenesis Kit	Agilent, Frankfurt am Main
QuickChange™ Multi-directed Mutagenesis Kit	Agilent, Frankfurt am Main
RNeasy Mini Kit	Qiagen, Hilden
Profection Mammalian Transfection System	
Calcium phosphate	Promega, Mannheim
Dual-Luciferase® Reporter Assay System	Promega, Mannheim
SuperSignal West Femto Luminol/Enhancer Solution	Thermo Scientific, St. Leon-Rot
True Blue Peroxidase Substrate	KPL, USA
Transcriptor One-step RT-PCR kit	Roche, Mannheim
Z-Competent E.Coli Transformation Buffer set	Zymo Research, USA

6.4 DNA and Protein Markers

1 kb DNA Ladder	NEB, Schwalbach
PageRuler Plus Prestained Protein Ladder	Thermo Scientific, St. Leon-Rot

6.5 Enzyme

TPCK-trypsin	Sigma-Aldrich, Steinheim

6.6 Antibodies

6.6.1 Primary antibodies

Rabbit α -H9N2 (serum)	Institute of Virology, Marburg
Mouse α-NP (monoclonal)	Abcam, Cambridge
Rabbit α- A/chicken/Rostock/34 (H7N1) (serum)	Institute of Virology, Marburg
Mouse α- ß-actin	Sigma Aldrich, Steinheim
Mouse α-RIG-I (monoclonal) ALME-1	Enzo life science

6.6.2 Secondary antibodies

Goat α-mouse IgG FITC coupled	Jackson Immuno Research Laboratories
Rabbit α-mouse IgG, HRP coupled	Dako, Denmark
Swine α-rabbit, HRP coupled	Dako, Denmark

6.7 Plasmids

pHW2000

Eukaryotic expression vector, Institute of Virology, Marburg

pHW2000-HA/-PB2/-PB1/-PA/-NA/-NP/-M-/-NS of A/Quail/Shantou/2061/2000 (H9N2)

Eukaryotic expression vector encoding protein of the isolate A/Quail/Shantou/2061/2000. It contains the promoter of human RNA-polymerase-I and RNA-polymerase-II of cytomegalovirus, Institute of Virology, Marburg (These plasmids were kindly provided by F. Schwalm and J. Baron)

pHW2000-HA/-PB2/-PB1/-PA/-NA/-NP/-M-/-NS of A/Quail/Shantou/782/2000 (H9N2)

Eukaryotic expression vector encoding protein of the isolate A/Quail/Shantou/782/2000 It contains the promoter of human RNA-polymerase-I and RNA-polymerase-II of cytomegalovirus, Institute of Virology, Marburg (These plasmids were kindly provided by F. Schwalm and J. Baron)

pHW2000-HA/-PB2/-PB1/-PA/-NA/-NP/-M-/-NS of A/Hamburg/05/2009 (H1N1)

Eukaryotic expression vector encoding protein of the isolate A/Hamburg/05/2009. It contains the promoter of human RNA-polymerase-I and RNA-polymerase-II of cytomegalovirus, Institute of Virology, Marburg (These plasmids were kindly provided by F. Schwalm)

pHW2000-HA/-PB2/-PB1/-PA/-NA/-NP/-M-/-NS of A/Seal/Massachusetts/1/1980 (H7N7)

Eukaryotic expression vector encoding protein of the isolate A/Seal/Massachusetts/1/1980 H7N7. It contains the promoter of human RNA-polymerase-I and RNA-polymerase-II of cytomegalovirus, Institute of Virology, Marburg (These plasmids were kindly provided by G.Gabriel)

pHW2000-HA/-PB2/-PB1/-PA/-NA/-NP/-M-/-NS of A/Anhui/1/2013 (H7N9)

Eukaryotic expression vector encoding protein of the isolate A/Anhui/1/2013. It contains the promoter of human RNA-polymerase-I and RNA-polymerase-II of cytomegalovirus, Institute of Virology, Marburg (These plasmids were kindly provided by F. Schwalm)

pPolI-NP-Luc

Eukaryotic expression vector encoding the Firefly luciferase gene flanked by the non-coding region of the NP segment of influenza A WSN 33. The reporter gene is under the control of human RNA polymerase I (Accession number AF053462). This plasmid was kindly provided by Dr. Thorsten Wolff.

pRen (pGL4.73)

Eukaryotic expression vector encoding the Renilla luciferase expression plasmid. The reporter gene is under the control of SV40 promoter. (Promega)

6.8 Viruses

A/Quail/Shantou/2061/2000	H9N2, avian	provided by Y. Guan, Hong-Kong
A/Turkey/Wisconsin/1/1966	H9N2, avian	provided by I. Capua, Italy
A/Aichi/1/1968	H3N2, human	Institute of Virology, Marburg
A/Quail/Hong-Kong/G1/1997	H9N2, avian	Institute of Virology, Marburg
A/Seal/Massachusetts/1/1980	H7N7, avian	Institute of Virology, Marburg
A/Thailand/Kan-1/2004	H5N1, human	provided by M. Schwemmle, Freiburg
A/Hamburg/05/2009	H1N1, human	Institute of Virology, Marburg
A/Anhui/1/2013	H7N9, human	provided by J. McCauley, London
A/Puerto-Rico/8/1934	H1N1, human	Institute of Virology, Marburg

6.9 Eukaryotic cells

A549	Human lung adenocarcinoma epithelial cells
Calu-3	Human airway epithelial cells
DF1	Chicken embryonic fibroblast cells
HEK 293T	Human embryonic kidney cells
HEK 293T del-RIG-I	Human embryonic kidney cells, RIG-I deficient
MDCK H/II	Canine kidney epithelial cells (Madin Darby Canine Kidney)

All cell stocks are from the Institute of Virology (Marburg), except HEK 293T del-RIG-I, kindly provided by Veit Hornung, Bonn.

6.9.1 Media and additives for cell culture

Autoclaved Avicel solution [2.5% (w/v) in dH_2O]	Instituted of Virology, Marburg
30% Bovine Serum Albumin (BSA)	PAA, Cölbe
Dulbecco's modified Eagle's medium (DMEM)	Gibco BRL, Eggenstein
Foetal Calf Serum (FCS)	Gibco BRL, Eggenstein
L-Glutamine (200MM, 100x)	Gibco BRL, Eggenstein
Lipofectamine2000®	Invitrogen, Karlsruhe
Modified Eagle's medium (2x MEM)	Gibco BRL, Eggenstein
OptiMEM®	Gibco BRL, Eggenstein
Penicillin/Streptomycin (5000 U/ml)	Gibco BRL, Eggenstein
Trypsin/EDTA-solution 0.05% 1X	Gibco BRL, Eggenstein

Culture Medium	Composition	Quantity
Growth Medium	1X DMEM	500 ml
	L-Glutamine	1%
	Penicillin/Streptomycin	1%
	Foetal Calf Serum	10%

Serum Free Medium/ Infection Medium (IFN-DMEM)	1X DMEM	500 ml
	L-Glutamine	1%
	Penicillin/Streptomycin	1%
	30%BSA	0.30%

Growth Medium (Calu-3cells)	1X DMEM F12	500 ml
	L-Glutamine	1%
	Penicillin/Streptomycin	1%
	Foetal Calf Serum	10%

Overlay Medium	2X MEM-infectious Medium mixed with Avicel-Solution	1:1

6.10 Peptide inhibitors

$PB1_{1\text{-}15}$-TY6-Tat (used 10 ng/ml)	Provided by Martin Schlee [189]
Borna-X-Tat (used 10 ng/ml)	Provided by Martin Schlee [189]

6.11 Bacteria

Z competent XL1 blue *E.coli*	Institute of Virology, Marburg

6.11.1 Media and additives for bacteria culture

Luria Bertani (LB) Medium	peptone	10 g
	Yeast extract	5 g
	NaCl	10 g
	dH_2O	add 1 L
LB Agar	peptone	10 g
	Yeast extract	5 g
	NaCl	10 g
	Bacto Agar	15 g
	dH_2O	add 1 L
LB-Medium / Ampicillin	LB-Medium + Ampicillin	100 µg/ml
LB-Agar / Ampicillin	LB-Agar + Ampicillin	100 µg/ml

Super Optimal Broth (SOB) Medium (pH 6-7)	Bacto-tryptone	20 g
	Yeast extract	5 g
	NaCl	0.6 g
	KCl	0.2 g
	1M $MgCl_2$	10 ml
	1M $MgSO_4$	10 ml
	dH_2O	ad 1 L

6.12 Antibiotics

Ampicillin (1 g)	Ratiopharm, Ulm
Cycloheximide (CHX) (Stock: 50 mg/ml, solved in DMSO, used at 50µg/ml)	Sigma-Aldrich, Steinheim
Leptomycine B (LMB) (Stock: 16 mM, solved 7:3 methanol/ water, used 16nM)	Sigma-Aldrich, Steinheim
Anisomycin (Stock: 250 µg/ml, solved in DMSO, used at 250ng/ml)	Sigma-Aldrich, Steinheim

6.13 Buffer

Phosphate Buffered Saline deficient (PBS^{def})	NaCl	8 g
	KCl	0.2 g
	Na2HPO4	1.15g
	KH2PO4	0.2g
	dH_2O	ad 1 L

Plaque Test washing buffer	NaCl	12 g
	Na2HPO4 x 2H2O	3.4 g
	KH2PO4	0.3 g
	Tween 20	0.10%
	dH_2O	ad 1 L

Antibody Solution for Plaque Test	BSA powder diluted in Plaque Test Washing Buffer	1%

4×Sample Buffer	dH_2O	3.75 ml
	0,5 M Tris-HCl, pH 6,8	2.5 ml
	Glycerol	2.5 ml
	10 % (w/V) SDS	0.5 g
	Bromophenol Blue	25 mg
	b-Mercaptoethanol	2.5 ml

SDS- Running Buffer (2X)	SDS	5 g
	TRIS	15 g
	Glycerol	72 g
	dH_2O	ad 1 L

Transfer Buffer	Glycerol	2.5 g
	TRIS	5.8 g
	Ethanol absolute mixed with methyl ethyl ketone	200 ml
	dH_2O	ad 1 L

Western Blot Washing Buffer	PBS	ad 1 L
	Tween 80	0.10%

Blocking Buffer Western Blot	Skimmed-milk powder	7%
	PBS^{def}/0.1% Tween80	ad User defined volume

Antibody Solution for Western Blot	Skimmed-milk powder diluted in Western Blot Washing Buffer	1% or 7%

Blocking Buffer Immunofluorescence	BSA	2%
	Glycerol	5%
	Tween 20	0.20%

Antibody Solution for Immunofluorescence	FCS diluted in PBS^{def}	1%

50X TAE-Buffer	TRIS	242 g
	0,5M EDTA (pH 8)	100 ml
	Glacial acetic acid	51.1 ml
	dH_2O	ad 1 L

Ethidium Bromide Incubation Buffer	TAE- buffer	1X
	Ethidium Bromide	10 µg/ml

6X DNA-Sample Buffer	Glycerol	30% (w/v)
	Bromophenol Blue	0.25% (w/v)
	Xylene cyanol	0.25% (w/v)
	Solved in dH_2O	adjusted volume

6.14 Oligonucleotides

6.14.1 Oligonucleotides for sequencing

Name	Sequence
pHW2000 50 fo	5’-ctcactatagggagaccc-3‘
pHW2000 50 re	5’-gaggtatatctttcgctcc-3‘
H9N2 PB2 800 fo	5'-caggagagcaacagtatcag-3'
H7N9 PB2 918 re	5'-ctgttcttctgttgggttttgtc-3'
H7N9 PB2 1596 fo	5'-atcgtccatgatgtgggagatcaat-3'
H7N9 PB2 800 fo	5'-ttagaagagcaacagtatcagcag-3'

6.14.2 Oligonucleotides for PB2 amplification from viral RNA.

Name	Sequence
BA-PB2 fo	5'-tattggtctcagggagcgaaagcaggtc-3'
BA-PB2 re	5'-atatggtctcgtattagtagaaacaaggtcgttt-3'
H9N2 1694 fo	5'-cccaagaacccaccatgctatacaat-3'

6.14.3 Oligonucleotides for correction of H7N9 PB2

Name	Sequence
correction K62R fo	5'-ccaattacggcagacaaaaggataatggagatgatcccg-3'
correction K62R re	5'-cgggatcatctccattatccttttgtctgccgtaattgg-3'

6.14.4 Oligonucleotides for mutagenesis of PB2 H9N2

Name	Sequence
Q591K fo	5'-ccagaagcaagtacagtggatttgtgagaacgc-3'
Q591K re	5'-gcgttctcacaaatccactgtacttgcttcttctgg-3'
E627K fo	5'-atttgcagcagccccacctaagcagagtaggatgcaatttt-3'
E627K re	5'-aaaattgcatcctactctgcttaggtggggctgctgcaaat-3'
D701N	5'-tcggcaaagaaaataaaagatatggaccagc-3'
D701N	5'-gctggtccatatcttttattttctttgccga-3'
S714I fo	5'-gcattaagcatcaatgaactgattaatcttacgaaggggagaaag-3'
S714I re	5'-ctttctccccccttcgtaagattaatcagttcattgatgcttaatgc-3'
S714R fo	5'-cattaagcatcaatgaactgcggaatcttacgaaggggagaa-3'
S714R re	5'-ttctccccccttcgtaagattccgcagttcattgatgcttaatg-3'

D253N fo	5'-ggggaggtaagaaataacgatgttgaccaa-3'
D253N re	5'-cccctccattctttattgctacaactggtt-3'

6.14.5 Oligonucleotides for mutagenesis of PB2 H7N9

Name	Sequence
K627E fo	5'-cagcagccccgccggaacagagtaggatgcag-3'
K627E re	5'-ctgcatcctactctgttccggcggggctgctg-3'
S714R fo	5'- cattgagcatcaacgaattgcggaatcttgcgaaaggagagaa -3'
S714R re	5'- ttctctcctttcgcaagattccgcaattcgttgatgctcaatg -3'

6.15 Other materials

Avian erythrocytes — Hutches of the University Marburg

Embryonated chicken eggs — Lohmann GmbH, Cuxhaven

7 METHODS

7.1 Cellular Methods

7.1.1 Cell culture

Confluent cells are passaged every three days. Cells are cultivated in growth medium, where they are washed two times with PBS^{def} to discard dead cells and remove residual Foetal Calf Serum (FCS) (trypsin inhibitor). Trypsin/EDTA (1 ml in 25 cm² flask and 2 ml in 75 cm² flask) is added to detach cells. The trypsin-treated cells are incubated (37°C and 5% CO_2) until complete detachment of the cells (5 to 20 min). Cells are resuspended in growth medium, seeded in a new flask/ plaque and incubated at 37°C and 5% CO_2.

7.1.2 Cryopreservation and thawing of eukaryotic cells

Confluent cells (in 75 cm² flask) are treated as for cell passaging. After complete detachment, cells are resuspended in 2 ml of cold FCS and centrifuged at 800 rpm for 5 min. Supernatant is removed and cells are gently resuspended in 1 ml of culture medium containing 20% FCS in addition of 1 ml of culture medium containing 20% DMSO. Resuspended cells are aliquoted in cryotubes and stored in an isopropanol isolation box at -80°C overnight. Cells aliquots are then transferred in nitrogen tank for conservation.

Cells are thawed at 37°C, to allow a fast defrosting, then transferred in a 12 ml cell culture tube, where 10 ml of PBS^{def} are added to remove DMSO present in the mix. Cells are centrifuged at 1500 rpm for 5 min and the supernatant discarded. Cells are then gently resuspended in 5 ml of adequate pre-warmed medium and seeded in a 25 cm² flasks.

7.1.3 Transfection of eukaryotic cells

7.1.3.1 Lipofectamine

Transfection is based on introduction of free DNA (here plasmid DNA) into eukaryotic cells. For this purpose, a cationic liposomal agent (Lipofectamine 2000®) is used. The mix of this agent with DNA will lead to the formation of liposome/nucleic acid complex, which will allow fusion of this complex and the cell membrane. The plasmid DNA will then enter the nucleus, where the transcription will occur.

Amount per well (6well plate)	
Solution 1	1 µg/plasmid + 250 µl optiMEM
Solution 2	15 µl Lipofectamine + 235 µl optiMEM

Solution one, containing the DNA for transfection and optiMEM, and solution two, containing lipofectamine and optiMEM, are prepared separately in cell culture tubes and incubated for 5 min at room temperature (RT). Solution one is added to solution two and incubated for 25 min at RT to allow DNA-lipofectamine complex formation. Subconfluent HEK 293T cells (80%) seeded one day pre-transfection are gently washed with PBS^{def} and 1.5 ml of optiMEM is added to each well. Transfection mix is added to the cells and incubated at 37°C and 5% CO_2. After six hours, transfection medium is replaced with serum-free medium and transfected cells incubated for 48 h at 37°C and 5% CO_2.

7.1.3.2 Calcium phosphate

Another method of transfection using carrier molecules is the calcium phosphate transfection. Here we used "*Profection Mammalian Transfection System Calcium Phosphate kit*". Medium of subconfluent cells is replaced by fresh growth medium 3h pre-transfection and incubated at 37°C, 5% CO_2. Solution one containing a mix of DNA and calcium chloride is added drop-by-drop in solution two containing HEPES-Buffered-Saline (HBS) solution with phosphate ions, while vortexing. A fine precipitate of positively charged calcium and negatively charged phosphate is formed with attached DNA on its surface. After incubation for 30 min at RT, the DNA mix is added dropwise on the cells and incubated at 37°C, 5% CO_2. After 24 h incubation, medium is replaced by fresh growth medium and cells are incubated for additional 24 h at 37°C, 5% CO_2 until measurement of luciferase activity.

Amount per well (12well plate)	
Solution 1	Solution 2
200 ng per plasmid (PB2, PB1, PA, NP)	150 µl HBS 2X
200 ng Firefly Luciferase plasmid + 75 ng Renilla Luciferase plasmid	
1.8 µl $CaCl_2$	
adjust to 150 µl H_2O	

7.2 Bacterial Methods

7.2.1 Bacteria

Escherichia coli (*E.coli*) bacteria are cultured on agar plates containing a selective antibiotic (Ampicillin, final concentration 100 µg/ml). This antibiotic enables the selection of plasmids of interest. Colonies present on the plate are picked and cultured in 5 ml Luria Bertani Medium (LB) medium containing Ampicillin (final concentration 100 µg/ml). The culture is incubated overnight at 37°C on a shaker (200 rpm).

7.2.2 Preparation and transformation of Z-competent cells

For preparation of Z-competent bacteria, the "*Z-Competent™ E.coli transformation kit & buffer set*" is used. *E.coli* bacteria are cultivated overnight in 5 ml LB medium 37°C, on shaker 200 rpm. The next day, 800 µl of the bacteria culture are added to 50 ml Super Optimal Broth (SOB) medium and incubated on a shaker at 30°C, 200 rpm, for 3 h. During incubation, wash buffer 1X and competent buffer 1X are prepared and stored on ice, according to manufacturer protocol. After 3 h incubation, bacteria culture is stored on ice for 10 min and pelleted at 3000 rpm, 4°C for 10 min. Supernatant is removed and cells are gently resuspended in 5 ml ice cold wash buffer. Bacteria are once more pelleted at 3000 rpm and 4°C for 10 min. Supernatant is discarded and bacteria are resuspended in 5 ml ice cold competent buffer. Competent bacteria are aliquoted into sterile Eppendorf tubes and stored at -80°C. This protocol eliminates heat-shock treatment for bacteria transformation.

Transformation is based on introduction of free DNA (plasmid) into bacteria. Z-competent bacteria are thawed and 500 ng of DNA is added to the mix. After incubation on ice for 30 min, bacteria mix is added to 200 ml culture of LB medium containing ampicillin (final concentration of 100 µg/ml) and incubated overnight on a shaker at 37°C.

7.2.3 Preparation of plasmid DNA from bacteria

For the isolation of plasmid-DNA, the Qiagen-kit "*QIAfilter plasmid maxi kit*" or Omega-kit "*Plasmid DNA mini kit*" are used. The protocols provided by manufacturers are followed. Briefly, after centrifugation of the cultured bacteria, the pellet is resuspended in buffer containing RNAse. After bacteria lysis and neutralization of the lysate, the chromosomal DNA and proteins are precipitated and separated from the plasmid DNA. The filtrate is then poured on a column containing plasmid DNA linked to an anion-exchanger under low salt conditions. After washing, DNA is eluted in water for minipreparation with "*plasmid DNA mini kit*" and eluted in high salt conditions for maxipreparation with "*QIAfilter plasmid maxi kit*". For maxipreparation, DNA is precipitated with 10.5 ml isopropanol and centrifuged 1 h at 6000 rpm 4°C. The pellet is then cleaned and centrifuged in 5 ml of 70% ethanol for 30 min 6000 rpm at 4°C. DNA is then resuspended in water and stored at -20°C.

Concentration and purity of DNA is measured with Nanodrop device.

7.3 Molecular Methods

7.3.1 Site directed mutagenesis

PB2 mutations are generated by using the "*QuickChange™ site-directed Mutagenesis kit*" or the "*QuickChange™ multisite-directed Mutagenesis kit*" from Agilent. Mutations are introduced via use of designed primer added in the polymerase reaction mix. To eliminate parental DNA (not mutated) the reaction is then submitted to digestion with *Dpn*I for 1 h at 37°C. The *Dpn*I endonuclease recognizes methylated or hemimethylated DNA and is used to digest the parental DNA template (DNA isolated from almost all *E.coli* is methylated). The final product is transformed in provided XL-1 Blue or XL-10 Gold bacteria and plated on LB agar containing ampicillin (100 µl/ml).

Standard Reaction

QuickChange® II Site-directed Mutagenesis kit

Component	Volume/Quantity
10X reaction buffer	5 µl
DNA template	5-50 ng
Primer fo	10 pmol
Primer re	10 pmol
dNTP mix	1 µl
PfuUltra HF DNA polymerase (2.5 U/µl)	1 µl
ddH2O	adjust to 50 µl

Cycle Parameters

QuickChange® II Site-Directed Mutagenesis

Step	Temperature	Time	Cycles
Initial Denaturation	95°C	30 s	1
Denaturation	95°C	30 s	16
Annealing	55°C	1 min	
Elongation	68°C	6 min*	

*1 minute/kb of plasmid length

Standard reaction

QuickChange® II Multisite-directed Mutagenesis kit

Component	Volume/Quantity for > 5 kb plasmid
10X reaction buffer	2.5 µl
DNA template	100 ng
Primer fo	10 pmol
Primer re	10 pmol
dNTP mix	1 µl
QuickChange® II Multi enzyme blend	1 µl
ddH2O	adjust to 25 µl

Cycle parameter

QuickChange® II Multisite-directed Mutagenesis

Step	Temperature	Time	Cycles
Initial Denaturation	95°C	1 min	1
Denaturation	95°C	1 min	30
Annealing	55°C	1 min	
Elongation	65°C	12 min*	

*2 minute/kb of plasmid length

7.3.2 DNA sequencing

To verify the proper sequence of the isolated plasmid, sequencing based on the chain termination method is performed. The reaction-mixture contains 1.5 µg DNA and 30 pmol of a specific primer in a final volume of 15 µl resuspension buffer. The preparation is then sequenced by the Seqlab Company and analysis is conducted using the BioEdit Sequence Alignment Editor.

7.3.3 Minigenome Assay (measurement of viral polymerase activity)

This assay enables the measurement of the activity of the viral polymerase (composed of PB1, PA, PB2) by quantification of reporter genes.

Subconfluent (70%) HEK 293T cells are transfected using the "*Profection Mammalian Transfection System Calcium Phosphate kit*" (as described above) with plasmid (pHW2000) encoding for the polymerase subunits (PB1, PB2, PA), NP and the reporter genes Firefly and Renilla luciferase. The Firefly luciferase gene is flanked by non-coding regions of the influenza virus NP segment under the control of the Pol I promoter (accession no. AF053462). When plasmid is transfected and diffuses to the nucleus, the transcription of the Firefly plasmid leads to the synthesis of viral RNA of negative polarity. This RNA is recognized by the viral polymerase (PB2/PB1/PA/NP) and mRNA is produced. Quantification of Firefly luciferase allows determination of the polymerase efficiency. To normalize this quantification, an additional plasmid encoding Renilla luciferase is transfected. The Renilla gene is constitutively expressed, under the control of a SV40 promoter (**Figure 15** and **Figure 16**).

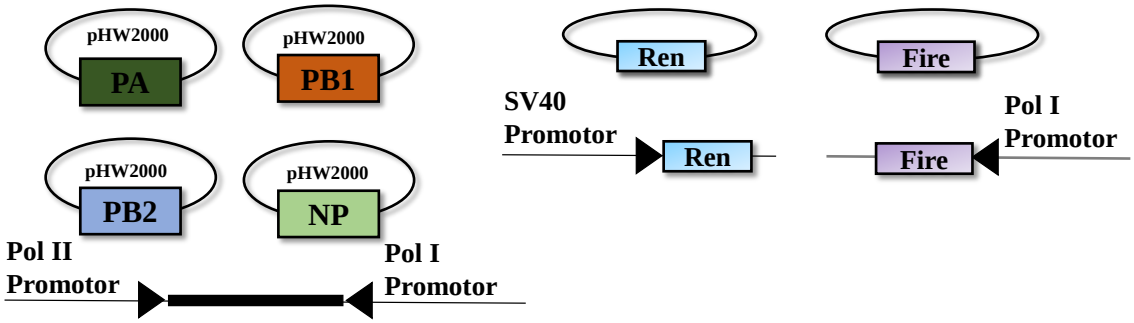

Figure 15: Schematic representation of expression plasmids for the minigenome assay. *The plasmid encoding the Renilla luciferase (Ren) is under the control of the SV40 promoter and is constitutively expressed. The plasmids encoding the Firefly luciferase (Fire) is under the control of the Pol I promoter and leads to the synthesis of RNA of negative polarity.*

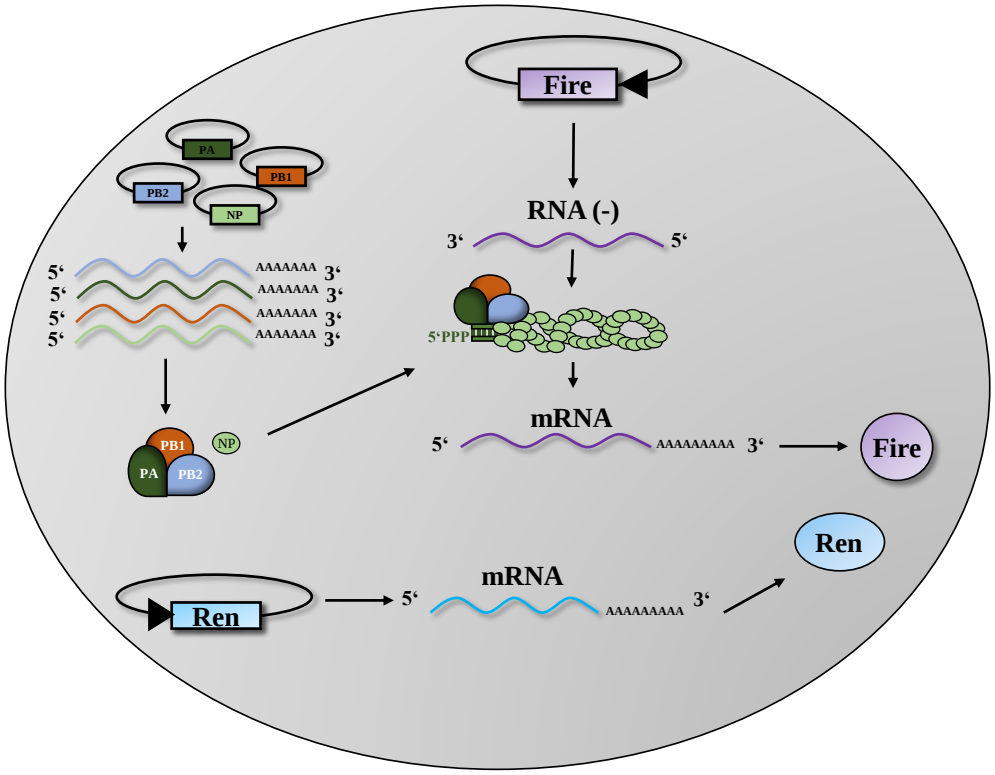

Figure 16: Schematic representation of the minigenome assay*. Six expression plasmids encoding for the viral polymerase complex (PB2, PB1, PA), NP and the reporter genes Firefly (Fire) and Renilla (Ren) luciferase are transfected into HEK 293T cells. The transcription by Pol I of the Firefly luciferase plasmid leads to the synthesis of a RNA (-) recognized by the viral polymerase complex. The mRNA resulting from the viral transcription leads to the synthesis of the Firefly luciferase protein. Renilla luciferase is under the control of a SV40 promoter and results in the constitutive expression of the plasmid. The quantification of the Firefly luciferase normalized by the Renilla luciferase enables the quantification of the polymerase activity. Fire: Firefly luciferase, Ren: Renilla luciferase.*

7.4 Biochemical methods

7.4.1 Conformational switch of RIG-I: Trypsin digestion

The infected A549 cells are harvested at 1 h post infection. Cells are washed with PBS^{def} and centrifuged at 3500 g for 5 min at RT. Supernatant is discarded and cells are resuspended in 25 µl of 0.5% Triton 100-X, followed by an incubation for 10 min at 4°C. Cells are centrifuged at 10000 g for 10 min at 4°C. From the supernatant, 10 µl are used for input control, and 10 µl used for the trypsin treatment. The

untreated samples are mixed with 3.5 µl of 4X sample buffer and boiled for 10 min at 100°C. The trypsin treated samples are mixed with 1.1 µl of trypsin TPCK (2 µg/µl) and incubated for 25 min at 37°C . The reaction is stopped by addition of 3.5 µl of 4X sample buffer, and boiled for 10 min at 100°C. Analysis of the samples is performed by sodium dodecylsulfate- polyacrylamide gel electrophoresis (SDS-PAGE) and Western Blot using anti-RIG-I antibody (diluted 1:1000).

7.4.2 Cell lysis and preparation of samples for SDS- polyacrylamide gel electrophoresis (SDS-PAGE)

The infected cells (A549 or DF-1 cells) are harvested at different time point post infection. Cells are washed with PBS^{def}, and 50 µl of SDS sample buffer (2X, diluted in PBS) are added into the well. Sample buffer is swirled into the well to resuspend and lyse the cells. Mix of cell and sample buffer is transferred in a sterile Eppendorf vial and boiled (2 times when these are BSL-3 samples) for 10 min at 100°C. After cooling, the samples were stored at -20°C or directly used for SDS-PAGE followed by Western Blot.

7.4.3 Protein separation by SDS-PAGE

SDS-polyacrylamide gel electrophoresis is a common method to separate proteins electrophoretically according to their size. The SDS sample buffer contains SDS, which disrupts secondary and tertiary protein structures, and detergent ß-mercaptoethanol, which reduces the covalent disulfide bonds. The negative charge provided by SDS enables the protein to migrate through an anode electrical field. Detection of the protein can be done via coloration with Coomassie blue or proteins can be transferred to an appropriate membrane (Western Blot) and detected by immunostaining.

For the SDS-PAGE, 12 % separating gels and 4.4 % stacking gels were prepared. The stacking gel enables the concentration of the protein, whereas the separating gel enables the separation of the proteins according to their size.

Composition of the gel:

12% separating solution (sufficient for two gels)

30% Acrylamide (Rotiphorese-Gel 30)	4 ml
1.5 M TRIS pH 8.8	2.5 ml
dH_2O	3.3 ml
10% SDS	100 µl
10% APS	100 µl
TEMED	10 µl

4.4% stacking solution (sufficient for two gels)

30% Acrylamide (Rotiphorese-Gel 30)	750 µl
0.5 M TRIS pH 6.8	1.3 ml
dH_2O	2.9 ml
10% SDS	100 µl
10% APS	60 µl
TEMED	10 µl

In the stacking gel pocket, 10 µl of each sample are added. As protein reference, 3.2 µl of a molecular weight marker (PageRuler Plus Prestained Protein Marker) is used. An electric field is applied (140 V, 300 mA) for 1h to separate the proteins according to their molecular size in a 1X SDS running buffer (diluted in water).

7.4.4 Western Blot: Transfer of proteins to PVDF-membranes

After electrophoretic separation by SDS-PAGE, proteins are transferred to a polyvinylidene fluoride (PVDF)-membrane via electro blotting. An electric field is applied allowing migration of the negatively charged proteins from the gel to the anode where they adhere irreversibly on the PVDF-membrane. The pile of electro-blotting layers is assembled in the following order:

Organisation of the pile:

Cathode

Three Whatman papers, imbued in transfer buffer

Gel, washed in transfer buffer

Membrane, activated in methanol and washed in transfer buffer

Three Whatman papers, imbued in transfer buffer

Anode

The transfer buffer, containing ethanol, removes SDS from the protein-detergent-complexes, resulting in adherence of protein on the membrane.

Transfer of proteins is performed at maximum voltage (300 V) and amperage of 40 mA per gel (0.8 mA/cm^2) for 70 min. For detection of specific proteins via immunostaining, the PVDF-membrane is incubated in blocking buffer (7 % skimmed milk diluted in Western Blot washing buffer) to avoid any unspecific signal.

7.4.5 Immunological detection of proteins on PVDF-membranes (Western Blot)

7.4.5.1 NP detection

After blocking of the membrane for 30 to 60 min on the plate shaker at RT, the membrane is incubated (in 5 ml antibody solution for Western Blot 7 %) with the primary rabbit α-H7N1 antibody (diluted 1:6000) for 1 h at RT or overnight at 4°C while shaking. Membranes are washed three times with Western Blot Washing buffer (10 min each washing step) to remove the remaining antibody-solution. The secondary swine α-rabbit antibody, coupled with Horseradish peroxydase (HRP) and diluted 1:2000 (in 5 ml antibody solution for Western Blot, 7 %) is then added to the membrane for 45 min on the plate shaker at RT. Three additional washing steps of 10 min are performed, in addition of one washing step with PBS^{def} for 5 min.

To detect the antibody-protein-complex by enhanced chemiluminescence, a specific substrate (Super signal West Femto Luminol), processed by the HRP, is added to the membrane according to manufacturer's protocol.

To normalize the amount of loaded protein, quantification with ß-actin as standard protein is performed.

7.4.5.2 Actin detection

After detection of the NP protein, the membrane is washed to remove any residual substrate. The membrane is dried in order to inactivate the HRP enzyme. Subsequently, the membrane is reactivated in methanol and washed in Western Blot washing buffer. The membrane is then incubated with the primary mouse α-actin antibody (diluted 1:1000, in 1 ml antibody solution for western blot, 1%) for 1 h at RT or overnight at 4°C, covered with parafilm. Membrane is washed three times with Western Blot Washing buffer (10 min each washing step) to remove the remaining antibody-solution. The secondary rabbit α-mouse antibody, coupled with HRP (diluted 1:2000, in 5 ml antibody solution for Western Blot, 7 %) is then added to the membrane for 45 min on the plate shaker at RT. Three additional washing steps of 10 min are performed, in addition to one washing step with PBS^{def} for 5 min.

The detection of actin protein is performed as for the NP proteins (see above).

7.5 Virological methods

7.5.1 Preparation of BSL-3 samples

All infections have been performed in a BSL-3 facility. Inactivation of BSL-3 samples is done following the current standard operating procedures of the BSL3 facility of the Institute for Virology, Philipps Universität, Marburg.

Immunofluorescence samples:

Infected cells are washed with PBS^{def} and fixed with 4 % paraformaldehyde (PFA) for a minimum of 16 h at 4°C. Cover slips are transferred into a new vessel with new PFA solution and transported out of the BSL-3 laboratory.

Plaque assay:

Infected cells are washed with PBS^{def} and fixed with 4 % paraformaldehyde (PFA) for a minimum of 16 h at 4°C. PFA is removed and fresh PFA is added to each plates and transported out of the BSL-3 laboratory.

Samples for Western Blot

Infected cells are lysed in presence of 1 % SDS and boiled for 10 min. Samples are then place into new tubes and transported out of the BSL-3 laboratory, and boiled once more at 100°C for 10 min.

RNA isolation

"*QiampViral RNA mini-kit*" is used for virus stock samples. Samples are mixed with the lysis buffer vortexed and incubated for 15 min at RT. One volume of ethanol is added according to the kit's protocol.

7.5.2 Infection of cells with influenza-A-virus

Subconfluent cells are washed with PBS^{def}, and infected with a virus dilution of required multiplicity of infection (MOI). Cells are incubated for 45 min at 37°C, 5% CO2. After adsorption of the viruses, cells are washed with PBS^{def}, and incubated in infection medium at 37°C, 5% CO2 for the required time, until harvest of the supernatants or cells.

$$\frac{\textbf{Amount of cells} \times \textbf{MOI}}{\textbf{Viral titer}\ [\textbf{PFU/ml}]} = \textbf{Inoculation Volume}\ [\textbf{ml}]$$

7.5.3 Recombinant virus (Rescue)

For the production of recombinant viruses, a reverse genetic system based on transfection of 8 plasmids [72] is used. Briefly, confluent HEK 293T cells are washed with PBS^{def}, and transfected with 8 plasmids each encoding for one segment of the influenza virus (Lipofectamine protocol). The plasmids are under the control of a polymerase-I-promoter for synthesis of negative-sense viral RNA and under the control of a polymerase-II-promoter for the transcription of messenger RNA (**Figure 17**).

After 6 h of incubation the transfection mix is replaced by 4 ml serum-free medium, containing trypsin/TPCK (1 µg/ml), and incubated for 48 h at 37°C and 5%CO_2. Supernatants of HEK 293T cells are then collected and treated with trypsin/TPCK (10 µg/ml) for 1 h at 37°C, to ensure cleavage of haemagglutinin from new viral particles. Activation of the HA enables the virus to infect new cells. In the meantime, MDCK cells (90 % confluent seeded in 25 cm^2 cell culture flasks) are washed with PBS^{def} and infected with 2 ml of trypsin-treated supernatant, followed by 2 h incubation at 37°C, 5% CO_2.

Supernatant is then discarded, cells are washed with PBS^{def} and incubated in 5 ml serum-free medium containing trypsin/ TPCK (1 µg/ml). After 48 hours of incubation, the supernatant is harvested and centrifuged at 2500 rpm at 4°C for three minutes to remove cells debris. Virus-solution is aliquoted in cryotubes and stored at -80°C until titration.

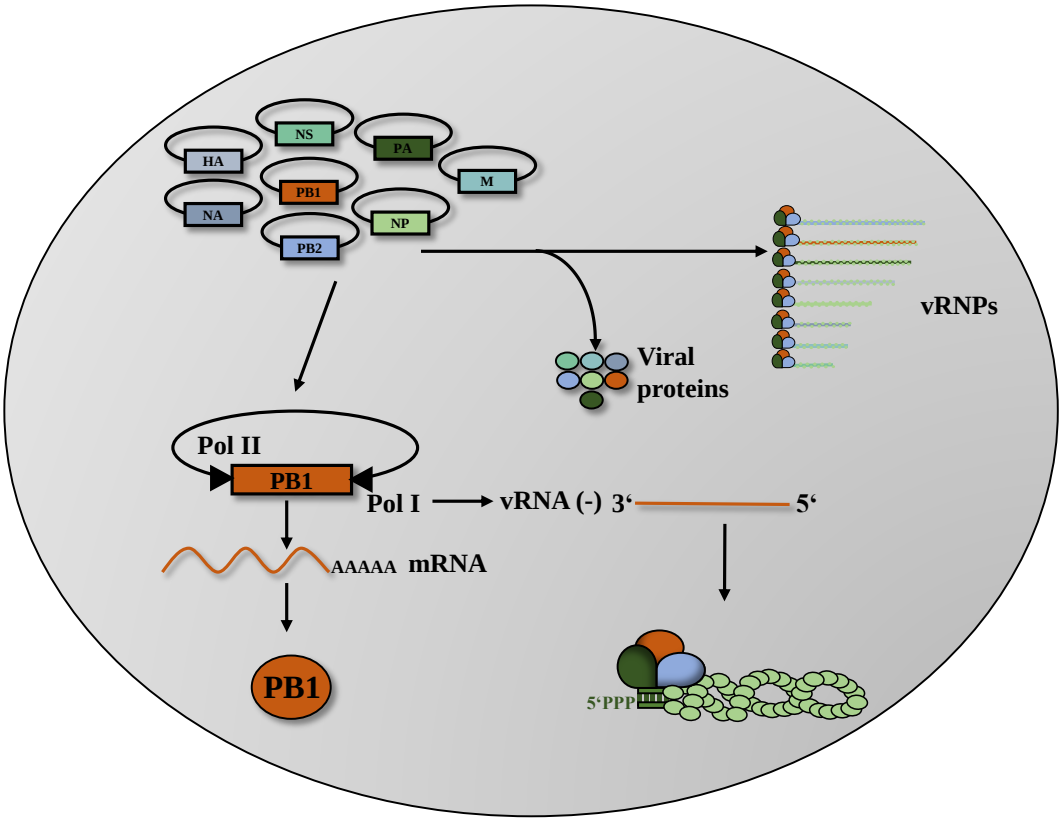

Figure 17: Schematic representation of recombinant virus generation. *Eight expression plasmids (pHW2000 vector) encoding the eight viral segments inserted between the human Pol I promoter and the Pol II promoter are transfected into HEK293T cells. The transcription of these plasmids by Pol I and Pol II results in the synthesis of viral mRNAs and vRNAs. The synthesis of the viral polymerase complex proteins (PB1, PB2, PA, NP) initiate the virus cycle, followed by the assembly of vRNPs and budding of new infectious influenza-A-virus.*

7.5.4 Haemagglutination assay

The haemagglutination assay is a common method for influenza viruses titration. The principle of this assay is based on the ability of influenza haemagglutinin to bind to N-acetylneuraminic acid of red blood cells and to form a lattice-structure. If the solution does not contain viral particles, the erythrocytes are not agglutinating and will form a spot at the bottom of the plate.

For the haemagglutination assay, a 96-well plate with U-shaped bottom is used. 100 µl of the virus-solution are 2-fold serially diluted in 50 µl PBS^{def}. Wells containing only PBS^{def} are used as negative control. In each well is added 50 µl of a 1% chicken-erythrocytes-suspension and the plate is incubated on ice for 30 min to inhibit the neuraminidase activity. The titre of the suspension corresponds to the inversed value of the dilution for the last haemagglutination well.

7.5.5 Plaque test

The avicel plaque-test enables the titration of virus samples and is indicated in plaque forming units (PFU) per millilitre. The overlay medium only allows viral diffusion from cell to cell, one plaque representing one infectious particle.

For this assay, titration is done in a 24-well plate with 90% confluent MDCK cells. A ten-fold serial dilution of the virus sample is done in serum-free medium. Cells are washed with PBS^{def}, and infected with 200 µl of diluted virus suspension. After 45 min of adsorption at 37°C and 5% CO_2, cells are washed with PBS^{def} (to remove non-adsorbed viral particles) and 0.5 ml of overlay medium containing trypsin/TPCK (1 µg/ml) are added to the cells followed by an incubation for 48 h at 37°C, 5%CO_2.

Two days post infection, overlay medium is removed and cells are washed with PBS^{def}. The cells are then fixed with PFA at 4°C for 24 h (BSL-3 conditions). PFA is discarded 24 h later and cells are washed with PBS^{def}. Permeabilisation of the cells is performed by adding 300 µl of 0.3% TritonX-100 for 30 min at RT, on shaker. After permeabilisation, 150 µl of primary antibody (α-H9N2; diluted 1:10.000 in 1% antibody solution for plaque test) are added to the cells, followed by an incubation of 90 min at RT, on shaker. Cells are washed three times with plaque test washing buffer and incubated with 150 µl of secondary antibody (swine α-rabbit; diluted 1:2000) coupled with HRP (Horseradish Peroxidase). After 75 min of incubation at RT and three additional washing steps, 125 µl of True Blue Peroxidase Substrate are added. The reaction is stopped with H_2O three washing steps and infected cells are detected as blue plaques. Virus titer is determined by the following formula:

$$\textbf{Plaque per well} \times \frac{\textbf{1}}{\textbf{dilution}} \times \frac{\textbf{1}}{\textbf{volume of virus suspension [ml]}} = \textbf{virus titer [pfu/ml]}$$

7.5.6 Isolation and Reverse Transcription of viral RNA

For isolation of viral RNA (vRNA), the Qiagen "*QIAmp viral RNA mini kit*" protocol is followed. Briefly, the vRNA is lysed under highly denaturing conditions to inactivate RNAse and to ensure isolation of intact viral RNA. After several washing step, RNA is eluted in AVE buffer (provided) and stored at -80°C.

To analyse the vRNA, reverse transcription need to be performed. For Reverse-Transcription-Polymerase-Chain-Reaction (RT-PCR), the Roche "Transcriptor One step RT-PCR kit" is used.

Standard Reaction

***Transcriptor One-Step RT-PCR kit* (Roche)**

Component	Volume/ Final concentration
5 X buffer	1 X
Primer fo	0.4 µM
Primer re	0.4 µM
Transcriptor enzyme mix	0.5 µl
template	10 µl
H_20	adjust to 25 µl

Cycle Parameters for PB2 Amplification

Transcriptor One-Step RT-PCR

Step	Temperature	Time	Cycles
Reverse transcription (RT)	50°C	30 min	1
Activation of the RT and activation of the polymerase	94°C	7 min	1
Denaturation	94°C	10 s	35
Annealing	60/**63°C**	30 s	
Elongation	68°C	3.5 min /**1.5 min**	
Final elongation	68°C	7 min	1

In bold are conditions for amplification of the C-terminal part of the PB2 using primers BA-PB2 re and H9N2 1694 fo, for full amplification of PB2, primer BA-PB2 re and BA-PB2 fo are used.

7.5.7 DNA separation on agarose gels

PCR-products are analysed for length and purity by electrophoresis on agarose gels. The migration of a DNA fragment is determined by its length. Because of the negative polarity of the phosphate at the 5' end, DNA is migrating from the cathode (-) to the anode (+) in the electrical field. DNA separation is performed with 0.8 % to 1 % agarose gel in 1 X TAE-Buffer, where samples are mixed with 6 X DNA sample buffer. A commercial marker "1 kb DNA Ladder" (NEB) is used to determine the size of DNA fragment. The electrophoretic separation is done under the following conditions: 150 V, 250 mA for 40 to 60 min. After migration, the gel is incubated in an ethidium bromide solution (10 µg/ml in 1 X TAE Buffer) for 10 to 20 min. ethidium bromide is an intercalating agent capable of binding double strand DNA. The exposition of DNA to UV light lead to the luminescence of the ethidium bromide and the detection of DNA fragment. Before sequence analysis of a DNA fragment, the sample is purified by using the "*QIAquick® PCR Purification kit*".

7.5.8 Virus propagation

7.5.8.1 Viral propagation in eggs

For the propagation of influenza A-viruses, eleven-day old chicken eggs are used. Area surrounding the air bladder is disinfected with iodine solution. A small hole is made using a hand brace and with a sterile syringe and cannula (0.55 x 25mm) 200 µl virus-solution (10 to 1000 PFU) are injected. The shell is resealed with a drop of glue (Pona Company). After infection, eggs are incubated for two days at 37°C with 80 % air moisture. Before virus isolation, eggs are stored at 4°C overnight to dispatch the embryo and restrict blood vessels. For isolation of allantoic fluid, the egg shell and the amnion are removed. The allantoic fluid is harvested with a cannula into 15 ml falcon tubes under sterile conditions. After centrifugation of the allantoic fluid (2500 rpm, 4°C for 3 min) to pellet cell debris, a haemagglutination assay is performed to check the presence of active virus. If the HA-test is positive, 500 µl of the virus solution are aliquoted in cryotubes and stored at -80°C.

7.5.8.2 Viral propagation in cells

Propagation of influenza A-viruses is performed on subconfluent MDCK cells (for H9N2 viruses) or DF-1 cells (for H5N1 virus, to avoid mutation E627K) seeded in 75 cm² flask. Cells are washed with PBS^{def} and infected with virus solution, diluted in serum-free medium with a multiplicity of infection (MOI) of 0.0001. Cells are incubated 45 min at 37°C, 5% CO_2 for adsorption of the virus and washed with PBS^{def} to remove non-adsorbed particles. After washing, 10 ml of infection medium containing 1 µg/ml of trypsin/TPCK are added, and cells are incubated at 37°C, 5%CO_2 for 48 h.

After 48 h, a cytopathic effect is recognized by the change of the medium-colour. Supernatant is harvested and centrifuged at 2500 rpm for 3 min to pellet cell debris. Virus suspension is aliquoted into cryotubes (500 µl per tube) and stored at -80°C until titration.

7.5.9 Detection of vRNP import by immunofluorescence

Subconfluent A549 cells (70 %) seeded in 24 well plate on cover slips are pre-treated with cycloheximide (CHX) or anisomycine (which block the translation machinery) and leptomycine B (LMB) (which blocks the export machinery) diluted in infection medium. Cells are incubated for 1 h at 37°C and 5%CO_2. After 1 h incubation the cells are washed with PBS^{def} and infected with 200 µl virus mix (MOI 1). Cells are incubated for 45 min at 4°C to synchronize the infection, then washed with PBS^{def} to remove spare virus particles. Cells are incubated with 500 µl of infection medium containing CHX-LMB.

The infected cells are incubated at 37°C, 5% CO_2 for several time points: 1 h and 6 h post infection. After each time point, cells are washed three times with PBS^{def}. Cells are fixed with 4% PFA for 24h at 4°C. After three steps of washing with PBS^{def}, cells are permeabilized with 250 µl of 0.3% Triton-X-100 for 30 min at RT on shaker. After permeablization, cells are incubated in blocking buffer for immunofluorescence and stored at 4°C overnight on the plate shaker to prevent non-specific binding.

Cells are then incubated in 500 µl of 1 % FCS/PBS for 1 h on the plate shaker. Each cover slip is incubated with 25 µl of the primary antibody (mouse α-NP diluted in 1%FCS/PBS 1:200) at RT in a dark humid chamber. After 1 h of incubation, slides are washed three times with PBS^{def}, 2 min each. Secondary antibody (α-mouse/FITC diluted in PBS/FCS 1:200), supplemented with DAPI (1:10.000) are added to the cover slips and incubated for 45 min at RT in a dark humid chamber. After three additional 5 min washing steps with PBS^{def} (in the dark to avoid excitation of the fluorochrome), the cover slips are washed three times with H_20 and dripped on paper towel. The slides are then mounted on objective slides with Fluoroprep and stored at RT to dry overnight and then transferred to 4°C until analysis with a confocal microscope.

The main principle of the confocal microscopy is based on scanning the sample with a focused laser beam in specific planes (confocal laser-scanning-microscope *CLSM*). A confocal microscope provides many advantages such as an increase of image resolution compared to images from a normal fluorescence microscope. Scanning of the object can be analysed in x/y direction as well as in z direction, which enables analysis of all sides of the object.

7.6 Animal experiment

All animal experiments have been done in collaboration with Dr. Gülsah Gabriel and Dr. Swantje Thiele at the Heinrich-Pette-Institut für Experimentelle Virologie in Hamburg, under BSL-3 conditions. The experiments have been performed according to the guidelines of the German animal protection law. All animal protocols are approved by the relevant German authority (Behörde für Stadtentwicklung und Umwelt Hamburg).

7.6.1 Infection of animals

BALB/C mice are sedated with a short inhalative narcosis with isoflurane. Mice are then anesthetized via an intra peritoneal injection of ketamine-xylazine (100 mg/kg and 10 mg/kg, respectively) diluted in NaCl. After 20 min, mice are infected intranasally with 50 µl of PBS-diluted virus (dose 10^6 PFU for each virus). Animals are monitored over 14 days, for weight loss and survival. In case of 25 % weight loss, the mice are euthanized.

7.6.2 Organ titration

Three days post infection, BALB/C mice are sedated with a short inhalative narcosis with isoflurane and euthanized by cervical dislocation. The lung and brain of three animals per group are harvested and weighed. The organs are then incubated with 200-300 µl of glass beads and 1ml of PBS. The homogenate is grinded in RETSCH mixer for 10 min, at 4°C by 20 Hz. The cell debris is discarded after centrifugation at 6000 g for 7 min at 4°C. The supernatant is conserved at -80°C until titration by plaque assay.

8 RESULTS

8.1 Characterization of adaptive PB2 mutations of H9N2 virus

Influenza-A-viruses have aquatic birds as natural reservoir. Due to a constant evolution, they can nevertheless be transmitted to terrestrial birds or mammals. Transmission to a new species leads to the adaptation to cellular receptors and intracellular host factors to enable efficient replication in the new host. Important mutations are located in the glycoproteins hemagglutin (HA) [71, 106, 173] or neuraminidase (NA) [108], the nuclear export protein (NEP) [103] and PB2, among others [53]. PB2 is a subunit of the polymerase complex responsible for cap binding from cellular messenger RNA enabling viral transcription [16]. The PB2 subunit has been described as an important host range factor that is also able to modulate the virulence of influenza viruses. Several mutations conferring a mammalian signature to the PB2 subunit have been identified. They include amino acid exchanges at position 591, 627, 701 and 714 that have been described to enhance polymerase activity, viral replication in mammalian cells and mice pathogenicity [36, 50, 159, 160, 194]. This thesis focuses on the impact of mammalian signatures when introduced into an avian H9N2 virus.

8.1.1 Effect of mutations Q591K and D253N on polymerase activity

First, mutations Q591K and D253N were tested in two H9N2 isolates: A/Quail/Shantou/2061/2000 (H9N2-2061) and A/Quail/Shantou/782/2000 (H9N2-782). These viruses have been isolated from quail in the province of Shantou (South of China) in 2000. Q591K and D253N mammalian signatures have been observed and characterized in another H9N2 isolate: A/Quail/Hong-Kong/G1/1997 (G1/97). They both are responsible for an enhanced polymerase activity, viral replication in mammalian cells and pathogenicity in mice [113]. In H5N1 virus, mutation Q591R has also been described to enhance viral replication in mammalian cells and pathogenicity in mice [192]. Isolate G1/97 is phylogenetically related to H9N2-2061 and H9N2-782 and their PB2 genes show 98% sequence identity and differ only by nine amino acids (**Table 3**).

Protein	Amino acid position	Amino acids in A/Quail/Shantou/2061/2000	Amino acids in A/Quail/HongKong/G1/1997
PB1	213	P	T
	423	V	I
	430	K	R
	455	S	N
PA	63	L	V
	101	N	D
	208	K	T
	618	V	T
PB2	8	R	W
	91	V	E
	106	A	T
	161	E	D
	263	A	V
	264	R	G
	441	N	D
	448	I	T
	505	Q	R
NP	33	I	V
	41	I	V
	52	H	Q
	136	I	M
	186	I	V
	210	E	D
	211	S	N
	350	A	T
	423	A	S

Table 3 : Amino acid differences between H9N2-2061 and H9N2-G1/97 in their polymerase and NP proteins.

To test the effect of mutations Q591K and D253N in strains H9N2-2061 and H9N2-782 PB2 mutants were generated and polymerase activity was tested in minigenome assay. The activity of the mutant polymerases was compared to WT polymerase activity (containing avian signature 253D-591Q) that was used as internal standard (**Figure 18**).

As expected, introduction of mutation D253N increased the polymerase activity 8-fold for H9N2-2061 and 12-fold for H9N2-782. Surprisingly, mutation Q591K led to a complete loss of activity in both H9N2-2061 and H9N2-782 isolates.

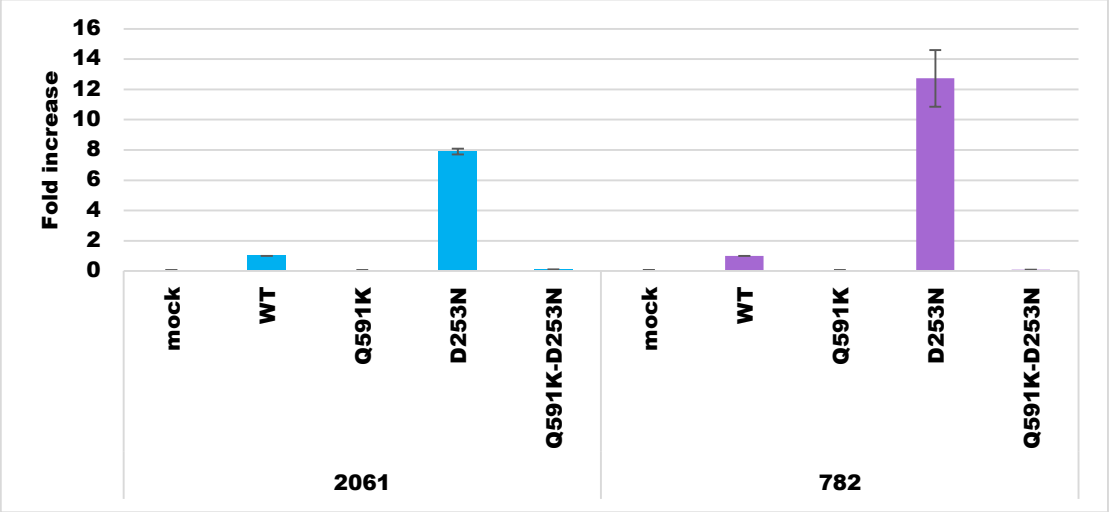

Figure 18 : Polymerase activity of the reconstituted polymerase complex of strains H9N2-2061 and H9N2-782 with mutations D253N and Q591K in PB2 subunit. *293T cells were cotransfected with pHW2000 plasmids encoding PB1, PA, PB2 and NP, in addition to plasmids encoding Firefly and Renilla luciferase. Quantification of Firefly luciferase normalized by Renilla luciferase enables determination of the polymerase activity with PB2 mutants. Activities of mutants were compared to the activity of the respective WT used as internal standard. WT represent the polymerase complex in presence of PB2 containing the avian signature 253D-591Q.*

To check whether the mutation Q591K was detrimental for a functional polymerase, a plasmid containing functional mutation D253N was mutated to introduce Q591K mutation (**Figure 18**). This introduction of Q591K resulted in a loss of activity when compared to single mutant D253N. These results indicate that mutation D253N increases the polymerase activity as previously described [113], in contrast to Q591K.

8.1.2 Effect of mutations E627K, D701N, S714I and S714R on polymerase activity

8.1.2.1 Effect of adaptive mutations in A/Quail/Shantou/2061/2000 H9N2

Mutations E627K, D701N, S714I and S714R in PB2 are well described in other subtypes such as H3N2, H5N1, H7N7, H1N1pdm09 [36, 50, 110, 159, 192]. Therefore the polymerase activity of H9N2-2061 and H9N2-782 with mutations at these positions was investigated. The adaptive mutations were first introduced and tested in the H9N2-2061 backbone (**Figure 19**). The nomenclature for each mutant is listed in **Table 4**. A WT virus contains PB2 subunit with avian signature 627E-701D-714S. In contrast each mutant is characterized by the introduced mutation.

Name of the mutants	Positions			
	253	627	701	714
WT	D	E	D	S
E627K	D	K	D	S
E627K D701N	D	K	N	S
E627K S714I	D	K	D	I
E627K S714R	D	K	D	R
E627K D701N S714I	D	K	N	I
E627K D701N S714R	D	K	N	R
D701N	D	E	N	S
D701N S714I	D	E	N	I
D701N S714R	D	E	N	R
S714I	D	E	D	I
S714R	D	E	D	R
D253N	N	E	D	S
D253N S714I	N	E	D	I
D253N S714R	N	E	D	R

Table 4 : Nomenclature of viruses containing PB2 WT or mutant. *WT represents a virus with the PB2 subunit containing the avian signature at each position of interest. Each mutant virus is characterized by the mutation introduced in PB2 subunit. The avian signatures for position 253, 627, 701, 714 are shown in grey.*

Introduction of mutation E627K increased the polymerase activity 20-fold, mutation D701N 6-fold, mutation S714I 7-fold and mutation S714R 8-fold. Double mutants containing mutations E627K with D701N or S714I/R increased the activity 20 to 27-fold. Nevertheless, it is important to note that combinations of E627K with D701N or E627K with S714I did not increase the polymerase activity when compared to E627K alone. In contrast, combination of E627K with S714R raised the activity 27-fold. Introduction of mutations S714I or S714R together with D701N increased polymerase activity 8-fold and 11-fold, respectively. Furthermore, combination of mutation D253N with S714I or S714R induced a 12-fold and a 17-fold increase, respectively (**Figure 19**). Finally, triple mutants E627K-D701N-S714I and E627K-D701N-S714R led to 27-fold and 38-fold increase respectively (**Figure 19**).

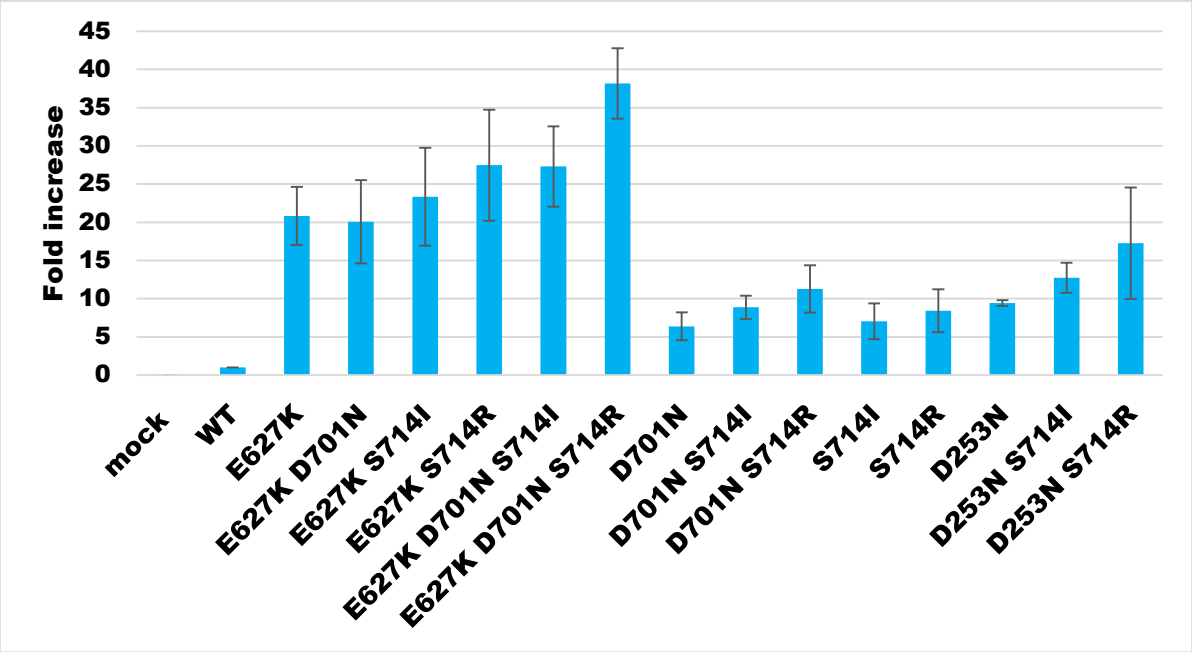

Figure 19 : Polymerase activity of the reconstituted polymerase complex of strain H9N2-2061 with mutations E627K, D701N, S714I/R in PB2 subunit. *293T cells were cotransfected with pHW2000 plasmids encoding PB1, PA, PB2 and NP, in addition to plasmids encoding Firefly and Renilla luciferase. Quantification of Firefly luciferase normalized by Renilla luciferase enables determination of the polymerase activity with PB2 mutants. Activities of mutants were compared to the activity of the respective WT used as internal standard. WT represents the polymerase complex in presence of PB2 containing the avian signature 627E-701D-714S.*

To summarize, these data show that introduction of adaptive mutations into the PB2 subunit of H9N2-2061 virus led to a significant enhancement of the polymerase activity in mammalian cells. Furthermore, it appears that the increase was more pronounced in combinations with mutation S714R than in combination with mutation S714I.

8.1.2.2 Effect of adaptive mutations in A/Quail/Shantou/782/2000 H9N2

Isolate H9N2-782 has the same PB2, NP and M sequences as H9N2-2061 and only a few amino acids changes in other viral proteins (**Table 5**). These two isolates are phylogenetically related, but present slight differences. While H9N2-782 presents a dibasic HA cleavage site sequence (RSSR), H9N2-2061 has a tribasic sequence (RSRR). In addition, the previous data with Q591K (**cf. Figure 18**) pointed out that even if closely related, the effect of the same mutation varies within H9N2 isolates. Therefore, it was interesting to investigate the impact of these adaptive mutations in H9N2-782 backbone.

Protein	Amino acid position	Amino acids in A/Quail/Shantou/2061/2000	Amino acids A/Quail/Shantou/782/2000
PB1	191	M	V
	213	T	P
	455	N	S
	571	K	R
	722	G	A
PA	63	V	L
	101	D	N
	618	A	V
NS	143	T	A
	186	K	E
NA	70	N	H
	126	L	P
	263	S	V
	468	S	P
HA	12	L	V
	147	I	T
	337	S	R

Table 5 : Amino acid differences between H9N2-2061 and H9N2-782 per proteins.

Introduction of adaptive mutations E627K, D701N and S714I/R in PB2 of H9N2-782 increased the polymerase activity of reconstituted polymerase as for H9N2-2061 (**Figure 20**). Introduction of mutation E627K enhances the activity 28-fold, mutation D701N 9-fold, mutation S714I 9-fold and mutation S714R 11-fold. Double mutants containing mutation E627K together with D701N or S714I/R increased the activity 34-fold, 40-fold and 48-fold, respectively (**Figure 20**).Combination of mutation D701N with S714I/R led to a 17 and 21-fold increase, respectively. Mutation D253N raised the polymerase activity 15-fold, and in combination with S714I/R 21-fold and 34-fold, respectively. The triple mutant E627K-D701N-S714I and E627K-D701N-S714R showed the strongest increase 57 and 65-fold, respectively (**Figure 20**).

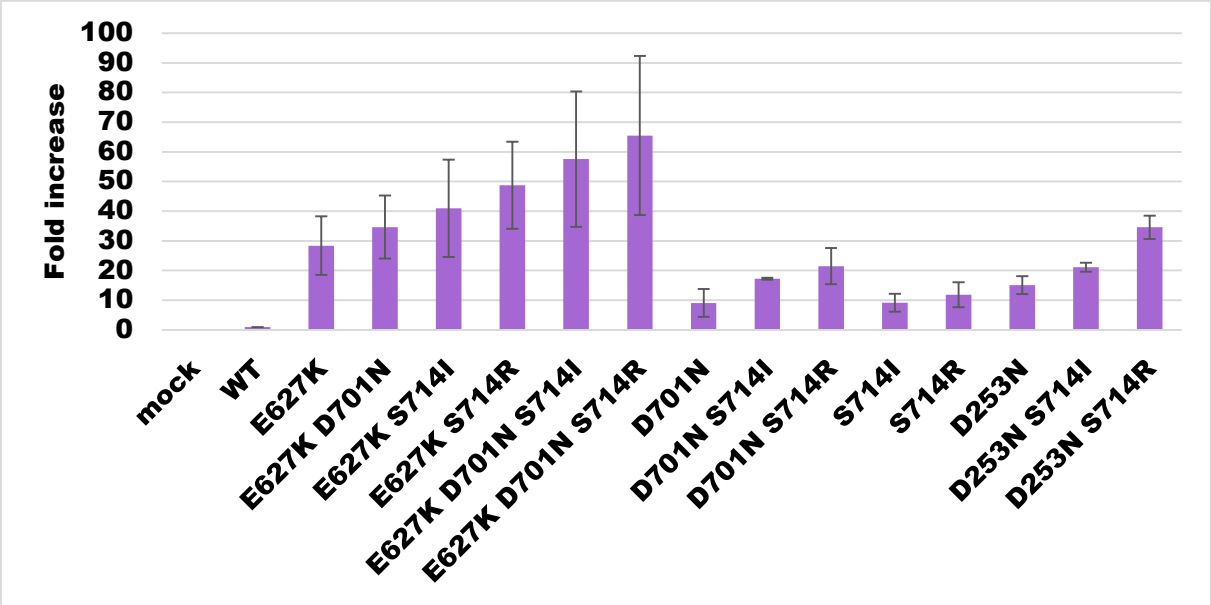

Figure 20 : Polymerase activity of the reconstituted polymerase complex of strain H9N2-782 with mutations E627K, D701N, S714I/R in PB2 subunit. *293T cells were cotransfected with pHW2000 plasmids encoding PB1, PA, PB2 and NP, in addition to plasmids encoding Firefly and Renilla luciferase. Quantification of Firefly luciferase normalized by Renilla luciferase enables determination of the polymerase activity with PB2 mutants. Activities of mutants were compared to the activity of the respective WT used as internal standard. WT represents the polymerase complex in presence of PB2 containing the avian signature 627E-701D-714S.*

These data reinforce the results obtained for H9N2-2061 and confirmed that introduction of adaptive mutations in PB2 of an avian H9N2 virus leads to an increase of polymerase activity in mammalian cells. Mutation S714R, alone or in addition to another adaptive mutation, has a higher impact on polymerase activity than S714I. Although the PB2 sequences of H9N2-782 and H9N2-2061 are identical, introduction of adaptive mutations leads to a stronger increase of activity in H9N2-782.

8.2 Impact of adaptive mutations on virus replication

8.2.1 Production of recombinant H9N2 viruses containing adaptive mutations in the PB2 subunit.

Introduction of adaptive PB2 mutations increases the polymerase activity of reconstituted ribonucleoprotein (**cf. Figure 19** and **Figure 20**). Nevertheless, further investigations needed to be conducted regarding efficiency of viral replication with these adaptive mutations. Previous studies have shown that an optimum, not a maximum, of polymerase activity is a precondition for efficient replication and high pathogenicity [50, 144]. To examine if the increased polymerase activity correlates with increased viral replication in mammalian cells, recombinant viruses with adaptive PB2 mutations were generated according to Hoffmann et al [72], where cells are transfected with plasmids encoding each viral segment. H9N2-2061 and H9N2-782 viruses with mutations E627K, E627K-D701N, E627K-S714I, E627K-S714R, E627K-D701N-S714I, E627K-D701N-S714R, D701N-S714I, D701N-S714R, S714I, S714R, D253N, D253N-S714I, D253N-S714R were obtained.

All recombinant viruses were titrated on MDCK cells under BSL-3 conditions. In contrast to published data [113], viruses containing mutation D253N did not grow efficiently, resulting in low titers compared to other H9N2 viruses with adaptive mutations. Recombinant viruses with the H9N2-782 backbone, replicated less efficiently than viruses with the H9N2-2061 backbone. As explained previously, these two isolates present some differences as observed with their plaque size (**Figure 21**). Therefore, the following experiments were conducted with viruses generated in the H9N2-2061 backbone.

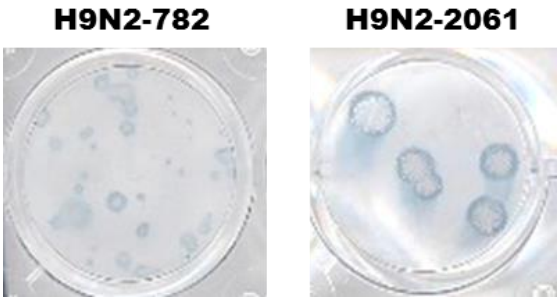

Figure 21 : Plaque size of H9N2-782 and H9N2-2061. *MDCK cells were infected with H9N2-782 or H9N2-2061. Detection of plaques was performed by immunostaining against NP.*

8.2.2 Growth kinetics of A/Quail/Shantou/2061/2000 H9N2 mutant viruses in human airway epithelial cells

Influenza-A-viruses are divided in two classes regarding their HA cleavage site: viruses with a monobasic or multibasic cleavage site. Viruses bearing a monobasic cleavage site are cleaved by trypsin-like protease such as TMPRSS2 and HAT [18, 19]. Viruses with multibasic cleavage sites are cleaved by a ubiquitously expressed protease such as furin [158]. For an efficient viral growth HA needs to be cleaved to obtain its correct conformation [87]. This cleavage enables the virus to fuse with the endosomal membrane after endocytosis [152]. H9N2-2061 virus has a multibasic cleavage sequence, but behaves as a virus with a monobasic one [9]. Additionally, it has been already described that HA of H9N2 is cleaved by TMPRSS2, HAT and matriptase proteases [10].

To study the effect of PB2 mutation on the viral life cycle, an appropriate cell line is required. MDCK cells are commonly used to grow influenza viruses. However, they are not suitable for investigating advantages provided by adaptive mutations for viral growth. Influenza viruses infect cells of the respiratory tract, therefore cell lines such as human alveolar epithelial cells (A549) or human airway epithelial cells (Calu-3) are more suitable for this assay. As mentioned above, H9N2-2061 virus behaves like a virus with as monobasic HA cleavage site, and thus needs the trypsin or trypsin-like proteases for an efficient replication in cells. A549 cells are very sensitive to trypsin and loose adherence after trypsin treatment, additionally they do not express the proteases TMPRSS2, HAT or matriptase capable of activating H9N2 virus [10]. In contrast, Calu-3 cells express TMPRSS2, which cleaves HA and fully activates the virus. Thereby, all growth kinetics experiments were performed with human airway epithelial cells. Calu-3 cells were infected with a MOI 0.0001 and supernatants harvested at 10, 24, 48 and 72 h post infection.

Infections with viruses containing only one mutation show an increase of growth on human airway epithelial cells (**Figure 22**). The effect of the adaptive mutations was more prominent during the first 24 h. Viruses with single mutations E627K, D701N, S714I or S714R reached viral titers of $3.5.10^4$ PFU/ml, $1.7.10^5$ PFU/ml, $1.1.10^4$ PFU/ml and $3.5.10^3$ PFU/ml, respectively, compared to WT virus (containing avian signature 627E-701D-714S) with $5.2.10^2$ PFU/ml.

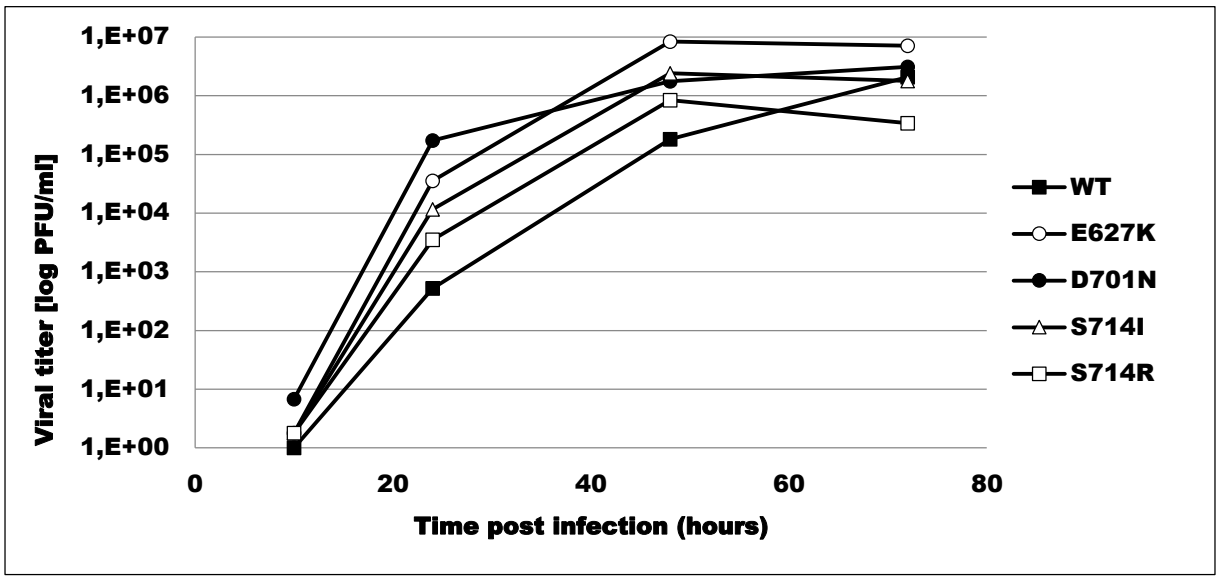

Figure 22: Growth kinetics in human airway epithelial cells upon H9N2-2061 infection. *Calu-3 cells were infected with H9N2-2061 viruses (MOI 0,0001) containing PB2 WT or with adaptive mutation E627K, D701N, S714I, S714R. Supernatants were harvested at 10, 24, 48 and 72 h post infection. WT represents viruses containing PB2 with the avian signature 627E-701D-714S. Titration was performed in MDCK cells. Titers are shown in PFU/ml and are representative of 3 independent experiments.*

Double mutants E627K-D701N, E627K-S714I, E627K-S714R, D701N-S714I and D701N-S714R exhibited titers of $1.8.10^4$ PFU/ml, $4.8.10^4$ PFU/ml, $1.6.10^6$ PFU/ml, $1.1.10^5$ PFU/ml and $3.4.10^4$ PFU/ml at 24 h, respectively (**Figure 23**).

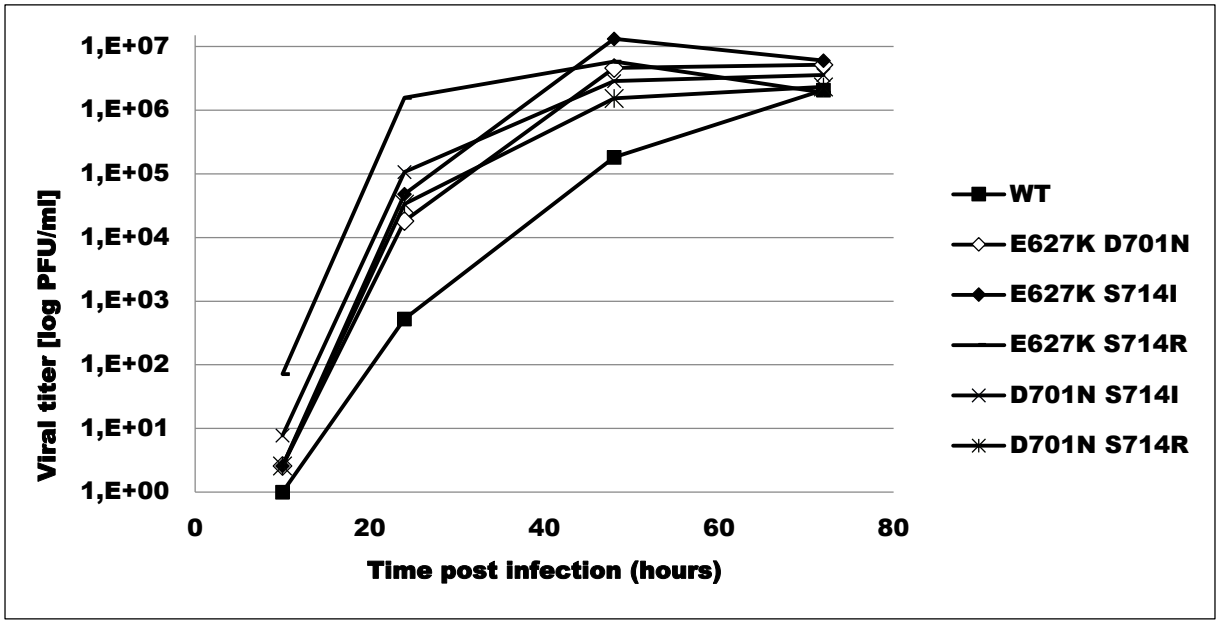

Figure 23: Growth kinetics on human airway epithelial cells upon H9N2-2061 infection. *Calu-3 cells were infected with H9N2-2061 viruses (MOI 0,0001) containing PB2 WT or with adaptive mutation E627K and D701N in combination S714I and S714R in PB2. Supernatants were harvested at 10, 24, 48 and 72 h post infection. WT represents viruses containing PB2 with the avian signature 627E-701D-714S. Titration was performed in MDCK cells. Titers are shown in PFU/ml and are representative of 3 independent experiments.*

Finally, infection with triple mutants E627K-D701N-S714I and E627K-D701N-S714R led to viral titres of $7.7.10^4$ PFU/ml and $3.9.10^5$ PFU/ml respectively. The differences observed for viral replication between the different viruses were more striking at 24 h and became less pronounced at 72 h (**Figure 24**).

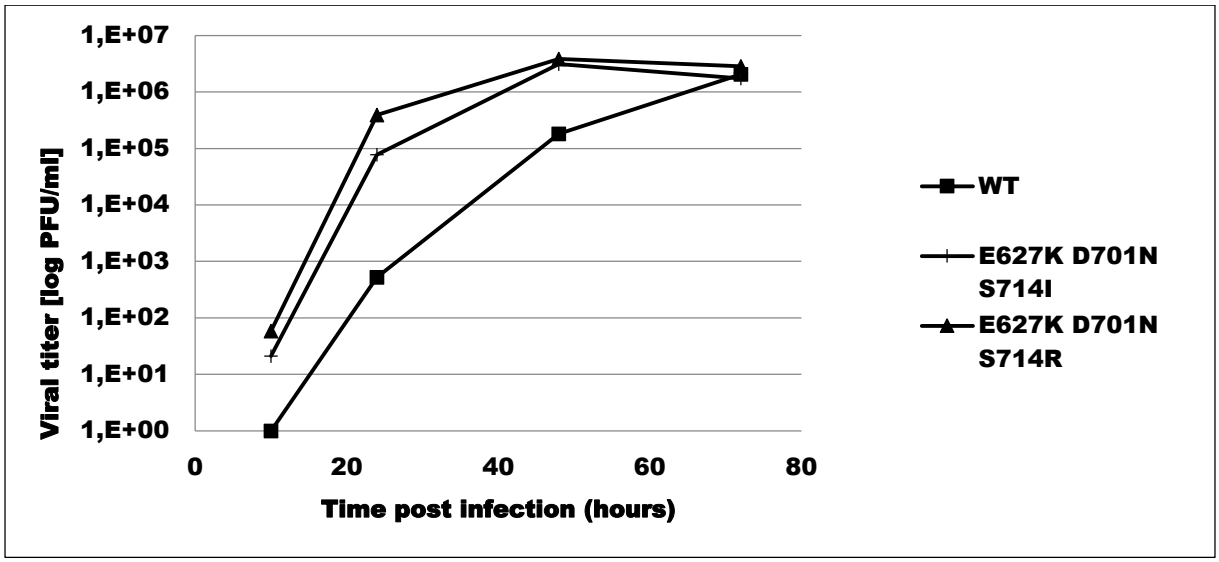

Figure 24: Growth kinetics in human airway epithelial cells upon H9N2-2061 infection. *Calu-3 cells were infected with H9N2-2061 viruses (MOI 0,0001) containing PB2 WT or with adaptive mutation E627K-D701N-S714I and E627K-D701N-S714R in PB2. Supernatants were harvested at 10, 24, 48 and 72 h post infection. WT represents viruses containing PB2 with the avian signature 627E-701D-714S. Titration was performed in MDCK cells. Titres are shown in PFU/ml and are representative of 3 independent experiments.*

Similar to the polymerase assay results, the viruses containing the mammalian signature E627K-S714R reached the highest titre at 24 h post infection among the single and double mutants.

In conclusion, these data indicate that introduction of adaptive mutations in H9N2-2061-PB2 increases the viral growth, consistent with the results of the polymerase activity. Furthermore, the triple mutant E627K-D701N-S714R showed the highest increase in viral growth.

8.2.3 Comparison of H9N2 viral growth in avian and human cell lines

Mutation E627K does not alter polymerase activity in avian cells in contrast to mammalian cells. To confirm the growth kinetic results and investigate the role of adaptive mutations in mammalian cells compared to avian cells, DF-1 cells (chicken fibroblasts) and Calu-3 cells (human airway epithelial cells) were infected. DF-1 cells are trypsin sensitive and do not express the proteases TMPRSS2, HAT or matriptase (able to cleave H9N2 HA [10]). Therefore, NP expression was monitored over 8 h infection (single infection cycle). This assay does not require addition of trypsin. Both cell lines were infected with MOI 1, and every 2 h cells were harvested and analysed for NP expression by Western Blot. Only single mutants E627K, D701N, S714R and triple mutant E627K-D701N-S714R were tested. NP expression indicated that mammalian adaptive mutations did not affect viral replication in DF-1 cells (**Figure 25**). For all viruses, including WT, NP expression was detected at 4 h post infection and increased over time.

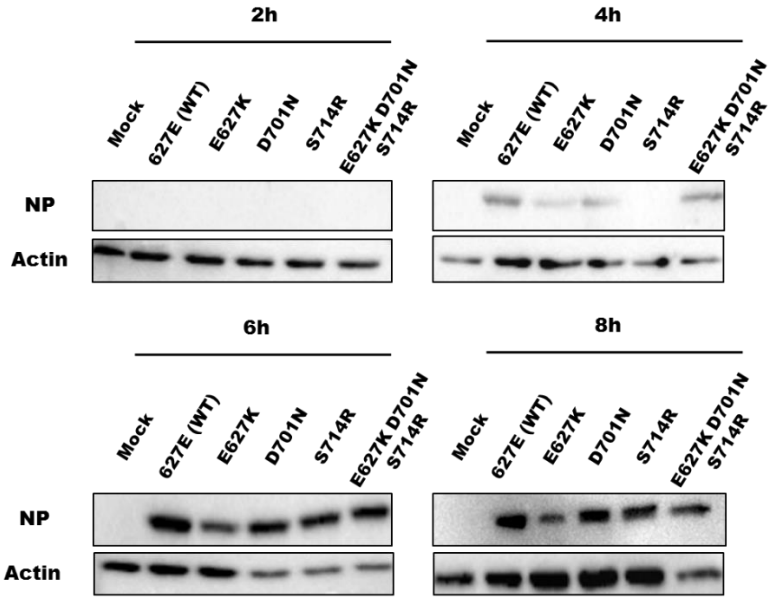

Figure 25 : Expression of NP in an avian cell line. *DF-1 cells (chicken fibroblast) were infected with H9N2-2061 (MOI 1) viruses containing PB2 WT (627E-701D-714S) or with adaptive mutations E627K, D701N, S714R and E627K-D701N-S714R. Cells were harvested at 2, 4, 6, 8 h post infection. Protein samples were separated on a 12% SDS-gel and detected by immunostaining.*

In comparison, in Calu-3 cells, NP detection was delayed for WT virus at 8 h post infection (**Figure 26**). However, viruses with adaptive mutations revealed NP production starting at 6 h post infection.

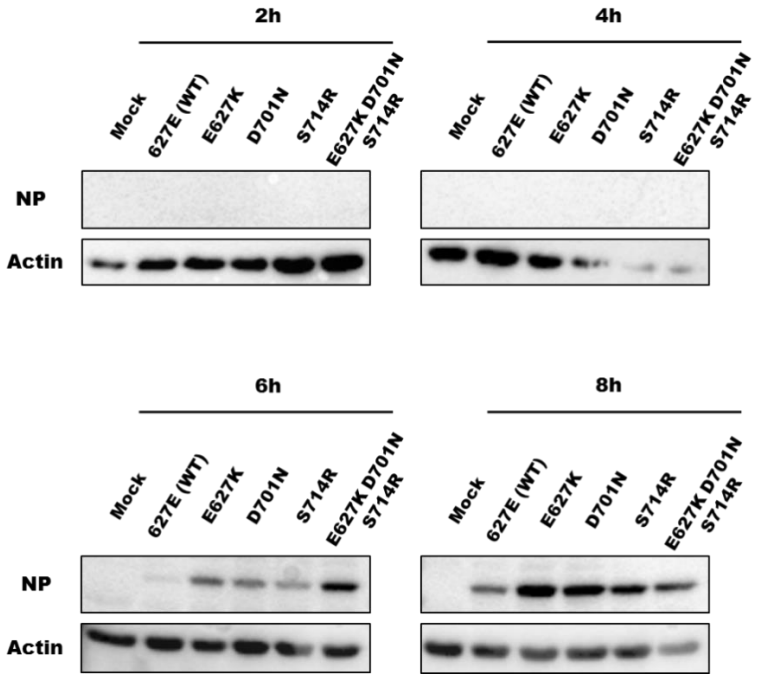

Figure 26 : Expression of NP on human airway epithelial cells. *Calu-3 cells were infected with H9N2-2061 (MOI 1) viruses containing PB2 WT (627E-701D-714S) or with adaptive mutations E627K, D701N, S714R and E627K-D701N-S714R. Cells were harvested at 2, 4, 6, 8 h post infection. Protein samples were separated on a 12% SDS-gel and detected by immunostaining.*

Taken together, these data confirm that introduction of adaptive mutations provides advantage for viral growth in mammalian cells.

8.3 Impact of adaptive mutations on mice pathogenicity

8.3.1 Monitoring of weight loss upon H9N2 infection

The previous data proved that introduction of adaptive mutations increase polymerase activity and viral growth in mammalian cells. Several studies have shown that adaptive mutations also increased pathogenicity in mice, when introduced in H5N1, H7N7 and H9N2 viruses [36, 174, 187]. In H9N2 virus, it has been described that mutation E627K in the PB2 subunit was lethal for mice. To deepen the understanding of the adaptive mutations, it was relevant to study if the effect observed for polymerase activity and viral replication was reflected by pathogenicity in mice.

Balb/C mice were infected with WT or mutant viruses containing PB2 with E627K, D701N, S714R and E627K-D701N-S714R and monitored for weight loss and survival. Monitoring the weight indicated that infection upon WT, D701N and S714R viruses did not affect body weight compared to control mice (**Figure 27**). However, infection with E627K and E627K-D701N-S714R induced a mild to strong loss of weight (10% to 20 %) at day 4 post infection, followed by a partial recovery to initial weight.

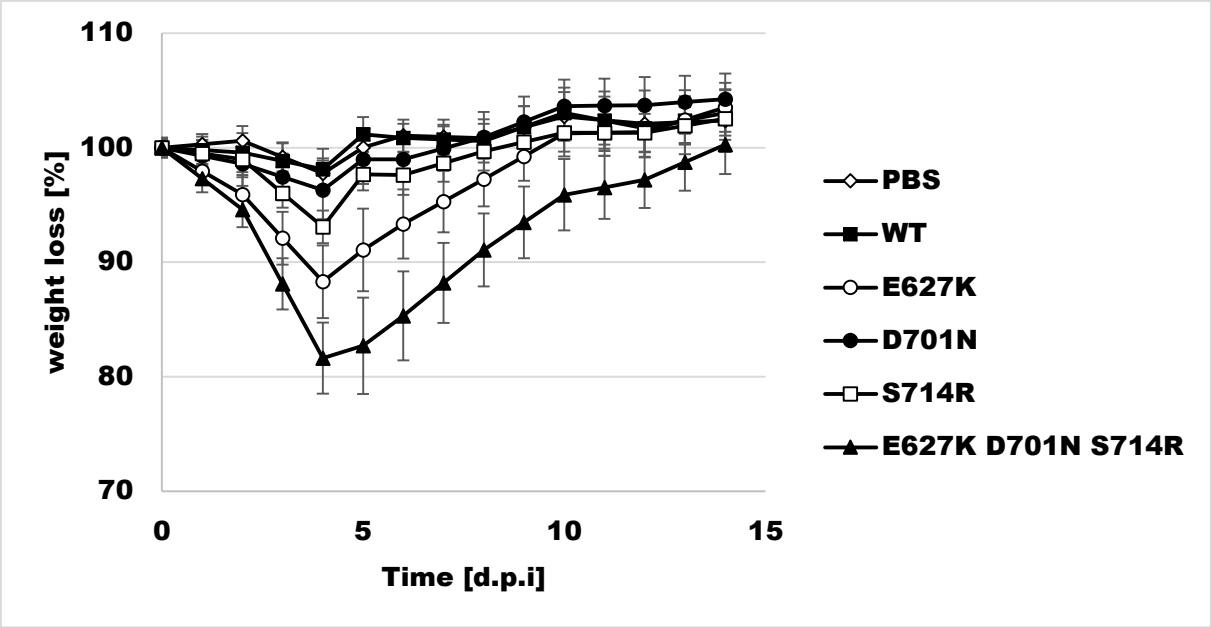

Figure 27 : Weight loss of Balb/C mice. *Six to eight weeks old Balb/C mice were infected with 10^6 PFU of H9N2-2061 viruses containing PB2 WT (627E-701D-714S) or with adaptive mutations E627K, D701N, S714R and E627K-D701N-S714R. Weight loss was monitored for 14 days post inoculation (d.p.i). Collaboration project with S. Thiele and G. Gabriel.*

8.3.2 Monitoring of survival rate upon H9N2 infection

To further analyse mice pathogenicity, survival of infected mice was monitored over 14 days. Mice infected with WT, D701N or S714R viruses did not present any signs of illness (ruffled fur, sunken sides) and recovered from the infection (**Figure 28**). In contrast, mice infected with viruses containing mammalian signature E627K or E627K-D701N-S714R showed strong sign of illness and viruses with the triple mammalian signatures showed 40% lethality, starting at day 5 post infection and reflecting the weight loss.

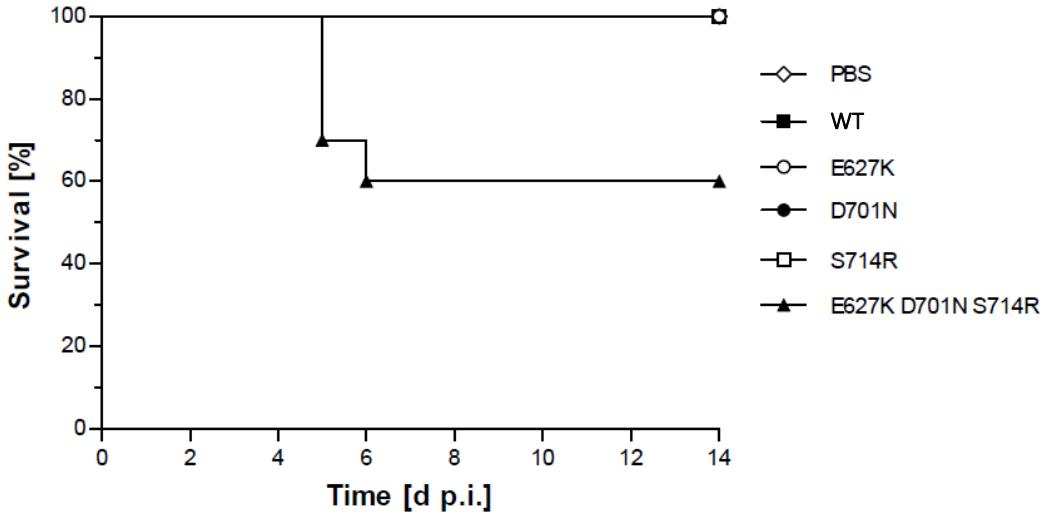

Figure 28: Survival rate upon H9N2-2061 infection*. six to eight weeks old Balb/C mice were infected with 10^6 PFU of H9N2-2061 viruses containing PB2 WT (627E-701D-714S) or with adaptive mutations E627K, D701N, S714R and E627K-D701N-S714R. Survival was monitored for 14 days post inoculation (d.p.i). Collaboration project with S. Thiele and G. Gabriel.*

8.3.3 Organ tropism upon H9N2 infection

To observe the viral replication of the recombinant virus in mice, titrations of lung and brain was performed (**Figure 29**). Lungs of mice infected with WT and S714R viruses contained the lowest viral titers ($2.6.10^3$ PFU/ml and $4.4.10^3$ PFU/ml respectively) whereas E627K and triple mutant E627K-D701N-S714R viruses presented titers of $1.1.10^5$ PFU/ml and $5.1.10^4$ PFU/ml respectively. Surprisingly, mice infected with virus containing adaptive mutation D701N had a high viral titer ($5.6.10^4$ PFU/ml) in the lung, when no weight loss was observed. This mutation had no effect on pathogenicity, but the virus still reached a titer as high as E627K-D701N-S714R virus. Infection of mice with all recombinant viruses did not lead to dissemination into the brain (**Figure 29**).

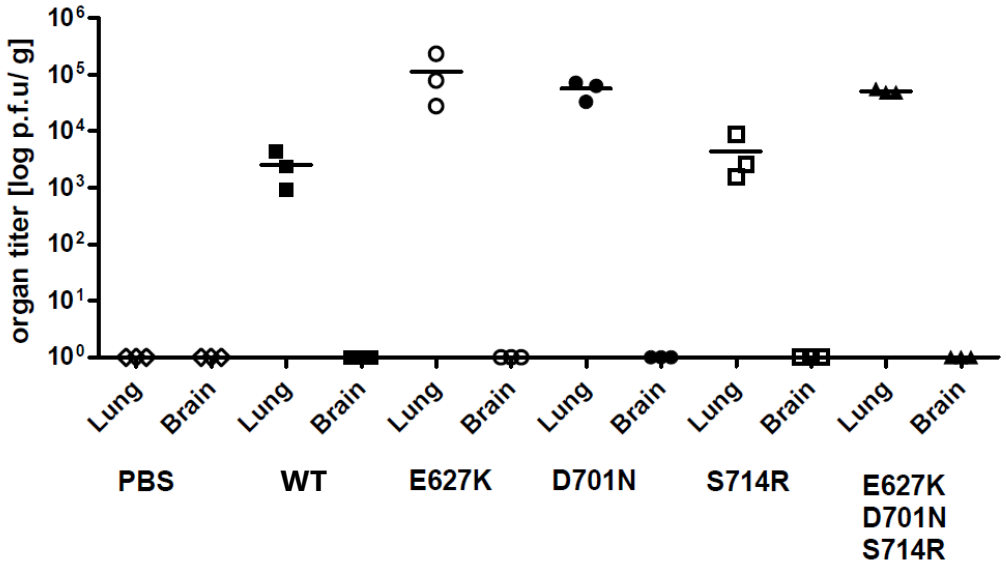

Figure 29: Organ titration of infected Balb/C mice upon H9N2-2061 infection*. Six to eight weeks old Balb/C mice were infected with 10^6 PFU of H9N2-2061 viruses containing PB2 WT (627E-701D-714S) or with adaptive mutations E627K, D701N, S714R and E627K-D701N-S714R. Organs homogenates were titrated on MDCK cells. Collaboration project with S. Thiele and G. Gabriel.*

Introduction of adaptive mutation in avian H9N2-PB2 increase pathogenicity in mice, with most pronounced effect with the triple mutant E627K-D701N-S714R.

To conclude this part, the results have proved that introduction of mutations E627K, D701N and S714R in the PB2 of avian H9N2-2061 virus increase polymerase activity and viral replication in mammalian cells. Furthermore, viruses with adaptive mutations E627K-D701N-S714R also show an increased pathogenicity in mice.

8.4 Characterization of adaptive mutations in different influenza subtypes

8.4.1 Impact of adaptive mutations E627K, D701N, S714R on polymerase activity

8.4.1.1 Effect of adaptive mutations in H1N1pdm09 and H7N7 polymerase complexes

The results presented in the first part showed that introduction of adaptive mutations strongly increased the polymerase activity of H9N2-2061 in mammalian cells. Consequently it was essential to compare the effect of these mutations in other influenza strains. To address this question, the effect of adaptive mutations on polymerase activity of H7N9, H1N1pdm09 and H7N7 viruses was analyzed. First, A/Seal/Massachusetts/1/1980 (H7N7), A/Hamburg/05/2009 (H1N1pdm09) and A/Quail/Shantou/2061/2000 (H9N2) were compared. These three viruses are not related phylogenetically and are clearly different regarding their sequences (**Table 6**).

H7N7 was derived from a seal isolate by serial passages in chicken embryo and presents avian signatures at positions 627, 701 and 714 in PB2. H1N1pdm09 is a human virus (responsible for the last pandemic in 2009), which presents two characteristic mutations at position 590/591 supposed to compensate for the lack of mutation E627K. Mutations E627K, D701N and S714R were introduced in PB2 of H7N7 [50] and of H1N1pdm09 (F. Schwalm thesis).

Protein	Amino acid positions	Amino acids in H9N2-2061	Amino acids in H1N1pdm09	Amino acids in H7N7
NP	21	N	D	N
	33	I	I	V
	52	H	Y	Y
	53	E	D	E
	77	R	K	K
	100	R	V	R
	105	V	M	M
	119	I	V	I
	133	L	I	L
	136	I	I	L
	183	I	V	V
	186	I	I	V
	189	M	I	M
	190	V	A	V
	211	S	N	N
	217	I	V	I
	284	A	A	S
	289	Y	H	Y
	305	R	K	R
	313	F	V	F
	316	I	M	I
	350	A	K	A
	351	R	K	R
	353	I	I	V
	357	Q	K	Q
	371	V	V	M
	373	A	I	T
	375	D	D	E
	377	S	N	S
	400	R	K	R
	425	I	V	I
	430	K	S	T
	433	T	N	T
	444	I	V	I
	450	S	S	N
	452	R	K	R
	456	V	L	V
	482	S	S	N
	497	D	D	N
	498	S	S	N

Protein	Amino acid positions	Amino acids in H9N2-2061	Amino acids in H1N1pdm09	Amino acids in H7N7
PB2	54	K	R	K
	65	E	D	E
	106	A	T	T
	125	L	L	M
	147	M	T	I
	161	E	D	D
	184	T	A	T
	190	R	K	K
	192	E	E	K
	194	K	Q	Q
	195	N	D	D
	197	N	K	K
	225	S	G	I
	255	V	V	I
	271	T	A	T
	292	V	V	I
	299	K	R	R
	315	M	I	M
	318	K	R	R
	334	K	S	S
	340	R	K	R
	355	K	R	R
	381	M	L	L
	441	N	D	D
	453	P	S	P
	478	V	I	I
	508	Q	R	R
	524	M	T	T
	526	K	R	K
	547	V	V	I
	559	T	I	T
	567	E	D	D
	588	A	T	A
	590	S	S	G
	591	Q	R	Q
	645	M	L	M
	649	V	V	I
	655	A	V	V
	661	T	A	A
	667	I	V	V
	684	A	S	A
	717	T	A	A

Protein	Amino acid positions	Amino acids in H9N2-2061	Amino acids in H1N1pdm09	Amino acids in H7N7
PB1	12	V	I	I
	13	P	P	L
	54	R	K	K
	56	T	T	K
	92	M	M	V
	102	L	I	I
	114	V	V	I
	166	F	F	L
	168	K	K	R
	172	E	E	D
	175	D	N	D
	179	M	I	M
	211	K	R	R
	213	P	N	N
	215	K	R	R
	216	S	G	S
	253	H	Y	Y
	257	A	T	T
	298	L	I	L
	302	V	I	I
	317	I	M	M
	336	V	I	V
	339	I	M	I
	361	S	R	S
	364	L	I	L
	375	N	S	N
	386	R	K	R
	398	E	D	D
	423	V	I	I
	430	K	K	R
	435	T	I	T
	455	S	N	N
	486	R	K	R
	517	I	V	I
	581	E	D	E
	584	R	Q	R
	587	A	V	A
	618	E	D	E
	621	Q	R	Q
	637	V	I	I
	638	E	D	E
	694	T	N	N
	715	M	V	V
	728	I	V	I
	741	A	S	A
	744	L	M	M
	754	G	R	R
	757	G	K	K

Protein	Amino acid positions	Amino acids in H9N2-2061	Amino acids in H1N1pdm09	Amino acids in H7N7
PA	20	T	A	A
	54	I	I	V
	63	L	V	V
	85	A	I	A
	100	V	V	I
	101	N	E	E
	118	T	I	I
	186	G	S	G
	204	R	K	R
	208	K	T	T
	213	R	K	R
	216	D	D	N
	237	K	E	E
	256	R	K	R
	262	K	R	K
	272	D	D	E
	275	P	L	P
	277	S	H	S
	318	R	K	K
	323	I	V	V
	336	L	M	L
	352	D	E	E
	356	K	R	K
	362	K	R	K
	367	M	K	K
	382	E	D	E
	387	I	V	V
	388	G	G	S
	394	E	D	E
	400	L	P	Q
	407	I	V	I
	409	S	N	S
	452	H	H	R
	474	C	C	S
	545	V	I	I
	547	E	D	D
	581	M	L	M
	602	I	V	V
	615	R	K	K
	618	V	T	T
	626	K	R	K
	651	S	A	A
	684	E	G	G
	688	G	E	E
	716	R	K	K

Table 6 : Amino acid differences comparing H9N2-2061 with H1N1pdm09 and H7N7 within the different polymerase subunits and NP. *In grey are indicated the amino acid corresponding to the avian signature and similar to H9N2-2061 amino acid sequences.*

Each reconstituted polymerase was compared to mock transfection. This normalization enables the comparison between all tested polymerase complexes at once and shows the basic polymerase activity within the different mutants. The WT polymerase represents the polymerase complex with PB2 containing the avian signature 627E-701D-714S. WT polymerase of H7N7 shows a higher activity than H9N2 or H1N1pdm09 WT polymerase (**Figure 30**). However, H7N7 and H9N2 polymerase with mutation E627K appeared with a similar activity, in contrast to a 4-fold decline in H1N1pdm09. Similar results were observed with D701N. Finally, reconstituted polymerase with mutation S714R exhibited the highest activity when introduced in H9N2.

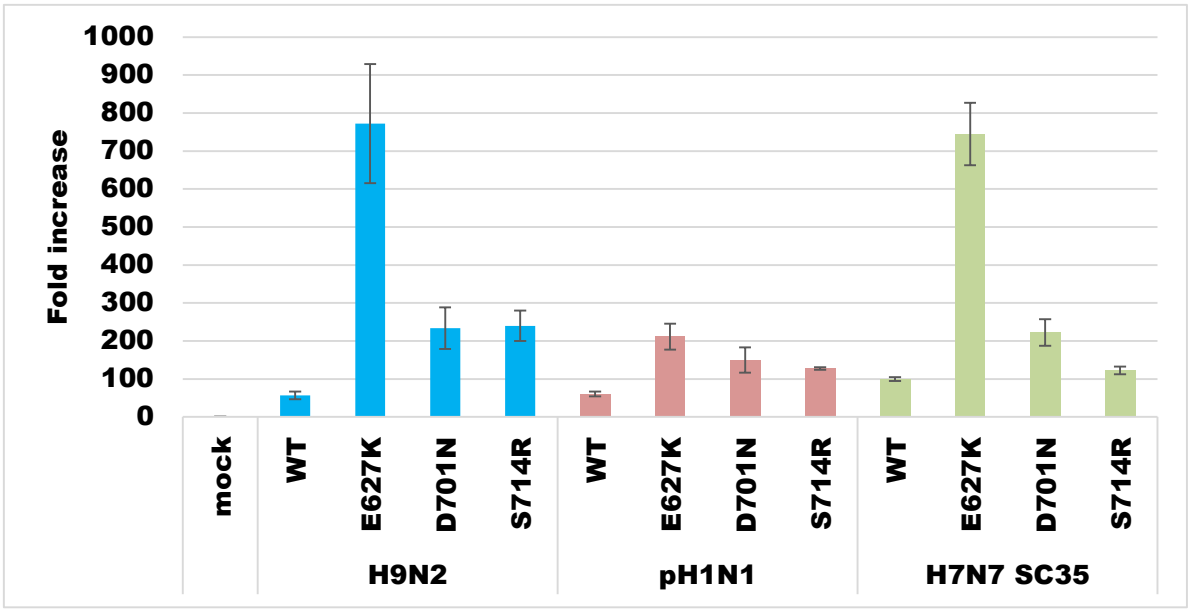

Figure 30 : Polymerase activity of the reconstituted H9N2, H1N1pdm09 and H7N7 polymerase complexes with mutations E627K, D701N, S714R in the PB2 subunit compared to mock. *293T cells were cotransfected with pHW2000 plasmids encoding PB1, PA, PB2 and NP, in addition to plasmids encoding Firefly and Renilla luciferase. Quantification of Firefly luciferase normalized by Renilla luciferase enables determination of the polymerase activity with PB2 mutants. For each polymerase complex, activities of mutants were compared to mock transfection used as internal standard. WT represents the polymerase complex in presence of PB2 containing the avian signature 627E-701D-714S.*

In addition, for each virus, the activity of the mutant polymerases was compared to their respective WT polymerase activity, used as internal standard. Thus, the impact of each mutation in the specific backbone was determined (**Figure 31**). Introduction of mutation E627K resulted in a 3-fold increase of H1N1pdm09, a 7-fold increase of H7N7, and a 20-fold increase of H9N2 polymerase activity. Mutation D701N induced a 2-fold increase with H1N1pdm09 and H7N7 as compared to a 5-fold increase with H9N2. Finally introduction of S714R induced a 2-fold increase with H1N1pdm09 and H7N7, in contrast to a 6-fold increase with H9N2.

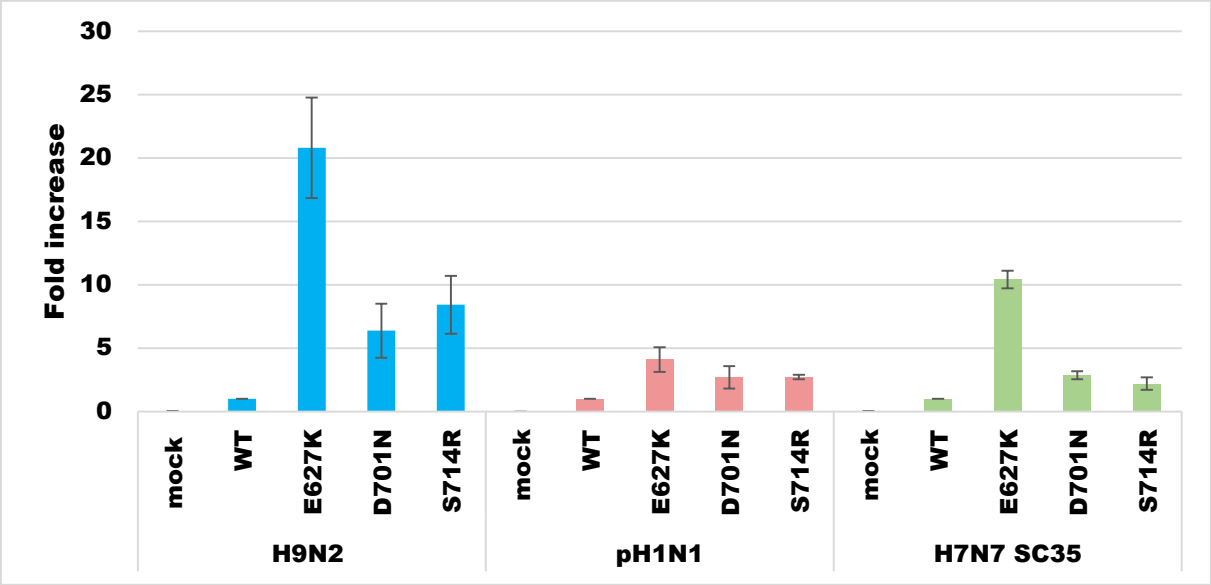

Figure 31: Polymerase activity of the reconstituted H9N2, H1N1pdm09 and H7N7 polymerase complexes with mutations E627K, D701N, S714R in the PB2 subunit. *293T cells were cotransfected with pHW2000 plasmids encoding PB1, PA, PB2 and NP, in addition to plasmids encoding Firefly and Renilla luciferase. Quantification of Firefly luciferase normalized by Renilla luciferase enables determination of the polymerase activity with PB2 mutants. Activities of mutants were compared to the activity of the respective WT used as internal standard. WT represents the polymerase complex in presence of PB2 containing the avian signature 627E-701D-714S.*

These results demonstrate that introduction of adaptive mutation E627K, D701N and S714R increase the polymerase activity in different backbones but have a higher impact on reconstituted ribonucleoprotein activity in H9N2 than in H1N1pdm09 or H7N7.

8.4.1.2 Effect of adaptive mutations in H7N9 polymerase complex

Unlike H7N7 and H1N1pdm09 viruses, H7N9 is closely related to H9N2 viruses regarding its internal genes, where it has been demonstrated that the polymerase genes of H7N9 virus derived from H9N2 [45]. It was therefore of interest to compare the effects of the adaptive mutations in H9N2 related polymerase.

Since H7N9 WT already contains adaptive mutation 627K in PB2, mutation K627E was introduced to generate an avian signature virus and analysed by minigenome assay. In addition, PB2 mutant containing mutation S714R was also generated (**Table 7**).

	Positions		
Name of the mutants	**627**	**701**	**714**
K627E	**E**	**D**	**S**
627K	**K**	**D**	**S**
627K S714R	**K**	**D**	**R**

Table 7 : Nomenclature of PB2 mutation in H7N9 virus. *K627E represents a PB2 subunit containing the avian signature at each position of interest. Each mutant virus is characterized by the mutation present in PB2 subunit. The avian signatures are shown in grey.*

When compared to revertant K627E mutation 627K led to a 15-fold increase in H7N9 polymerase activity and a 25-fold in combination with mutation S714R (**Figure 32**). The effects of the mutations are similar to those observed with H9N2 polymerase, where the increases are 20-fold and 27-fold, respectively (**cf. Figure 19**).

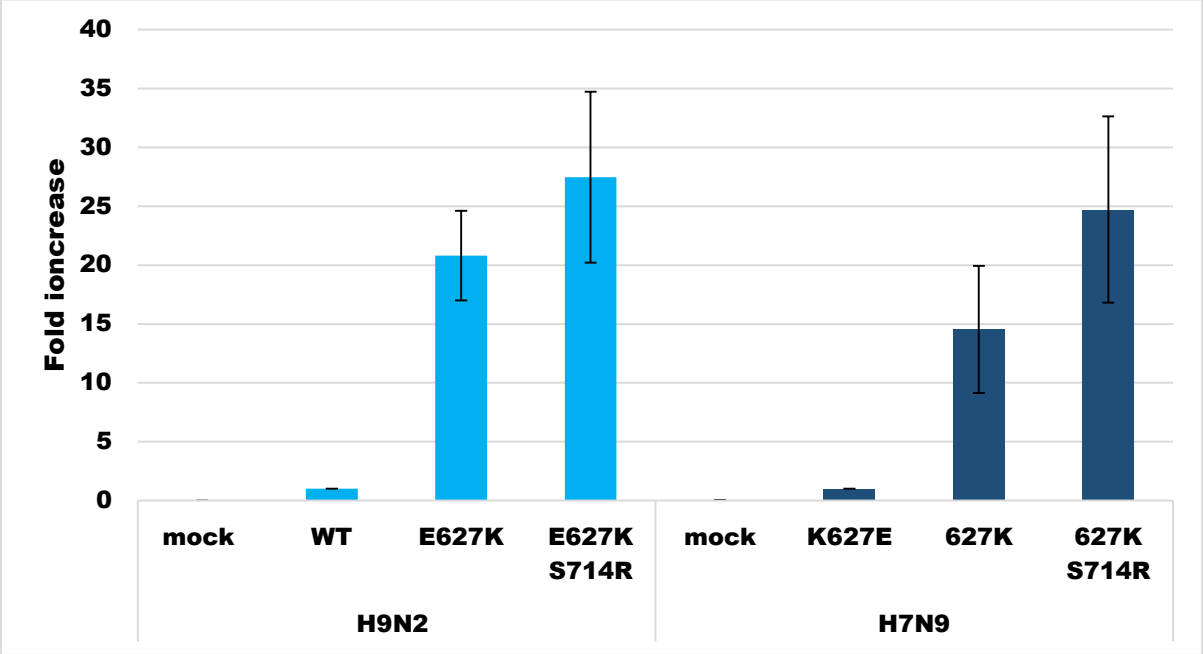

Figure 32 : Polymerase activity of the reconstituted polymerase complexes of H9N2 and H7N9 viruses with mutations E627K and S714R in the PB2 subunit. *293T cells were cotransfected with pHW2000 plasmids encoding PB1, PA, PB2 and NP, in addition to plasmids encoding Firefly and Renilla luciferase. Quantification of Firefly luciferase normalized by Renilla luciferase enables determination of the polymerase activity with PB2 mutants. Activities of mutants were compared to the activity of the respective WT or K627E avian signature used as internal standard. WT and K627E represent the polymerase complex in presence of PB2 containing the avian signature 627E-701D-714S.*

When polymerase activity of reconstituted polymerase was compared to mock transfection, polymerase activities for K627E, 627K and 627K-S714R were higher in H7N9 backbone than H9N2 (**Figure 33**).

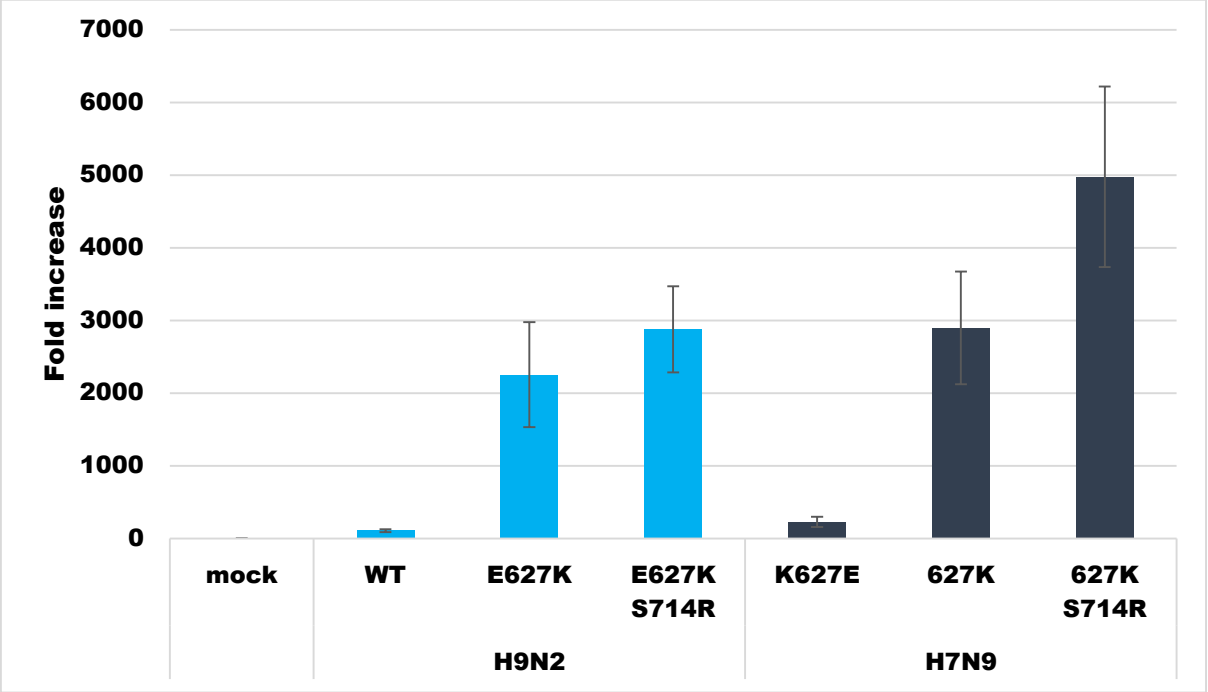

Figure 33: Polymerase activity of the reconstituted H9N2 and H7N9 polymerase complexes with mutations E627K, D701N, S714R in the PB2 subunit compared to mock. *293T cells were cotransfected with pHW2000 plasmids encoding PB1, PA, PB2 and NP, in addition to plasmids encoding Firefly and Renilla luciferase. Quantification of Firefly luciferase normalized by Renilla luciferase enables determination of the polymerase activity with PB2 mutants. For each polymerase complex, activities of mutants were compared to mock transfection used as internal standard. WT and K627E represent the polymerase complex in presence of PB2 containing the avian signature 627E-701D-714S.*

To summarize, these results confirm that introduction of adaptive mutations leads to an increased polymerase activity in H7N9. Moreover, these mutations have the same impact on the polymerase activity for H7N9 (related to H9N2 polymerase) and H9N2, in contrast to H7N7 and H1N1pdm09 (non-related to H9N2 polymerase).

8.4.2 Impact of adaptive mutations E627K, D701N, S714R on viral replication

The impact of adaptive mutations on polymerase activity is different within a backbone. Consequently, investigations of their impact on viral replication were conducted. Calu-3 cells were infected with H5N1, H9N2 and H1N1pdm09 viruses containing mutation E627K or D701N in the PB2 subunit. Viral titres of each virus subtype containing PB2 WT (627E-701D-714S) were used as internal standard.

Effects on viral titres were determined by comparing WT viruses to E627K or D701N at 24 h post infection (**Figure 34**). Adaptive mutation in H5N1 led to an increase of viral replication of 2.5 log, for H9N2 of 4 log and of 0.5 log decrease for H1N1pdm09 when mutation E627K was introduced. Introduction of mutation D701N led to a 2.5-log increase with H5N1, a 4.5-log with H9N2 and 0.5-log with H1N1pdm09.

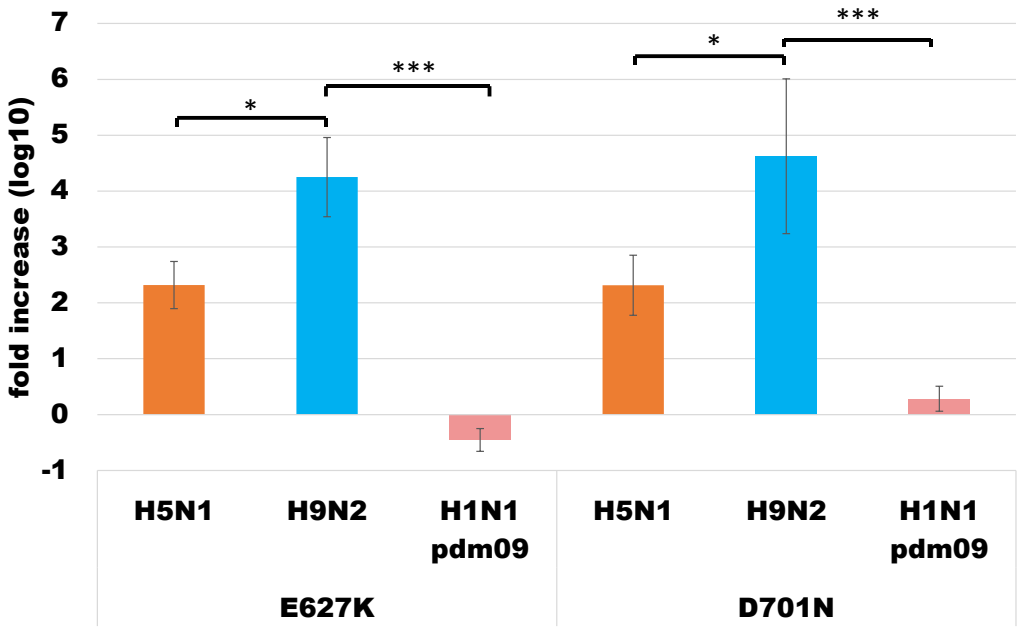

Figure 34 : Impact of adaptive mutations on virus replication in human airway epithelial cells upon H9N2, H5N1 and H1N1pdm09 infection. *Calu-3 cells were infected with H9N2, H5N1 or H1N1pdm09 viruses (MOI 0,0001) containing avian signature 627E-701D-714S or adaptive mutations E627K or D701N in PB2 subunit. Results for H1N1pdm09 kinetics were performed by* ***Folker Schwalm****. Supernatants were harvested at 24 h post infection. Titration was performed on MDCK cells. Viral titers were compared to the respective WT viruses containing PB2 with the avian signature 627E-701D-714S. Results are representative of 3 independent experiments.*

These results confirm that the impact of adaptive mutations is more potent in H9N2, than H5N1 or H1N1pdm09 regarding viral growth.

8.5 Adaptive PB2 mutations in heterologous polymerase complexes.

8.5.1 Impact of adaptive mutations in H7N7 and H1N1pdm09 heterologous polymerase complexes

According to the results presented above, introduction of adaptive mutations into H9N2-PB2 had the strongest impact on polymerase activity. It was now of interest to determine if PA and PB1 contributed to this effect. For this purpose, heterologous polymerase complexes of H1N1pdm09, H7N7 and H7N9 viruses were generated in which PA, PB1 and PB2 were individually replaced by the respective H9N2 subunit (**Figure 35**). Minigenome assays were performed to assess the polymerase activity of these reassortants as depending on the adaptive PB2 mutations. For each virus, the activity of the mutant polymerases was analysed and compared to the homologous polymerase complex activity that was used as internal standard.

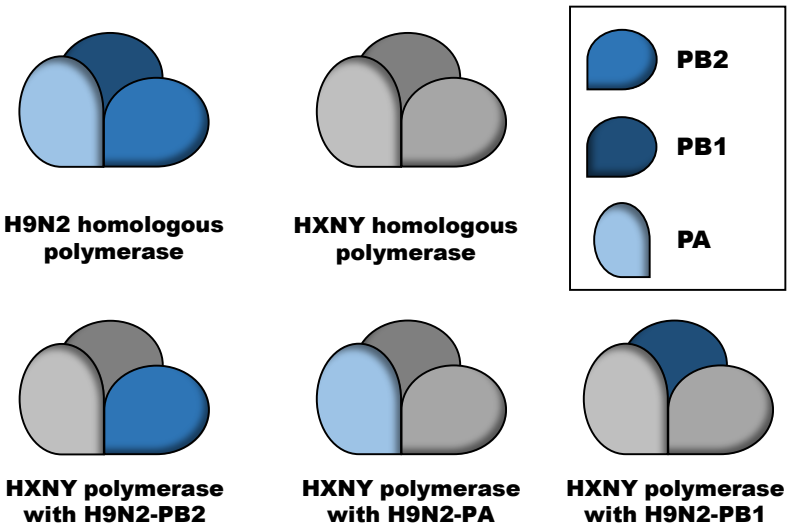

Figure 35 : Polymerase subunit exchange between H9N2 and other influenza viruses. *Here are represented the different heterologous polymerases composed of H9N2, H1N1pdm09, H7N7and H7N9.*

There was a strong decrease of the activity of the H1N1pdm09 polymerase, when PA was replaced by the H9N2 subunit (**Figure 36**). On the contrary, replacement of PB1 did neither significantly change the polymerase activity, nor did it alter the effects of the PB2 mutations. There was also no significant change in activity after reassortment with H9N2-PB2 WT. However, there was a distinct effect when H9N2-PB2 contained adaptive mutations. When compared to H1N1pdm09-PB2, introduction of H9N2-PB2 with mutation E627K increased the activity from 4-to-14 fold, mutation D701N from 3-to-4-fold, and mutation S714R from 3-to-5-fold.

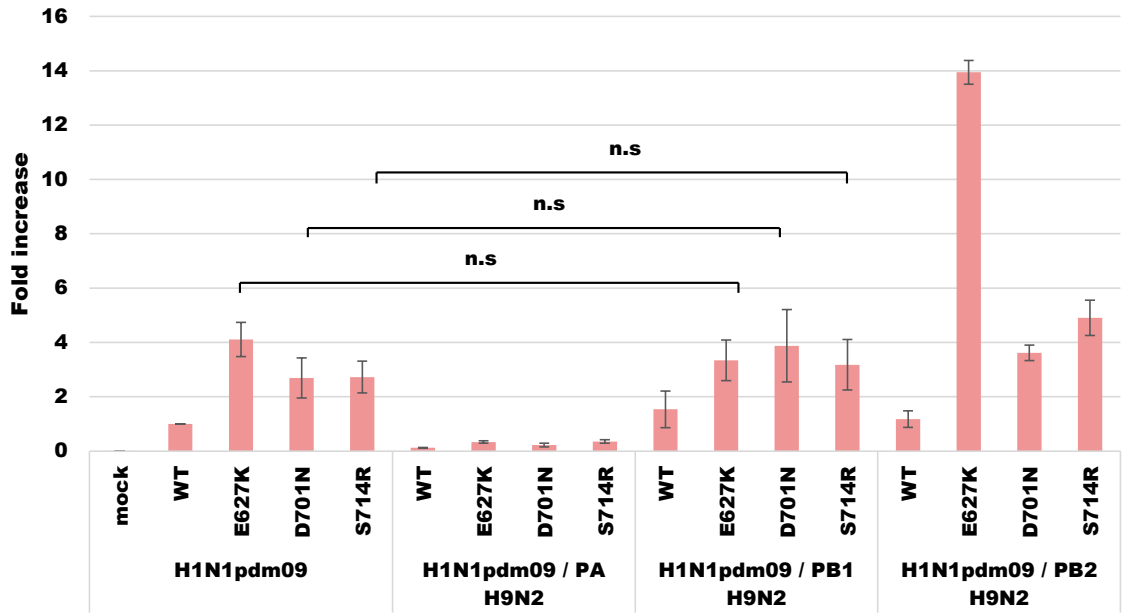

Figure 36 : Polymerase activity of the reconstituted polymerase complexes of H1N1pdm09 with H9N2 polymerase subunit. *293T cells were cotransfected with pHW2000 plasmids encoding PB1, PA, PB2 and NP, in addition to plasmids encoding Firefly and Renilla luciferase. Quantification of Firefly luciferase normalized by Renilla luciferase enables determination of the polymerase activity with PB2 mutants. Activities of reassortants were compared to the activity of the homologous H1N1pdm09 polymerase used as internal standard. WT represents the polymerase complex in presence of PB2 containing the avian signature 627E-701D-714S. ns: non-significant indicates a P value of > 0.05 (Student's t test).*

These increased activities reflected the raise observed in H9N2 reconstituted polymerase when adaptive mutations were introduced (**cf. Figure 19**)

Similar results were obtained for H7N7 (**Figure 37**). Introduction of PA and PB1 of H9N2 into H7N7 polymerase led to a decrease of activity when compared to the homologous reconstituted H7N7 polymerase. This decrease was stronger with exchange of PA than with PB1. Introduction of PB2 subunit led, as for H1N1pdm09, to a strong increase of the polymerase activity. When compared to H7N7-PB2, introduction of H9N2-PB2 with mutation E627K increased the activity from 10 to 17-fold, mutation D701N from 3-to-9-fold, and mutation S714R from a 2-to-10-fold. Similar to H1N1pdm09, introduction of H9N2-PB2 led to an increased activity corresponding to the homologous H9N2 polymerase results (**cf. Figure 19**). There was, however, a slight (3-fold) increase when H9N2-PB2 WT was combined with PA and PB1 of H7N7 (**Figure 37**).

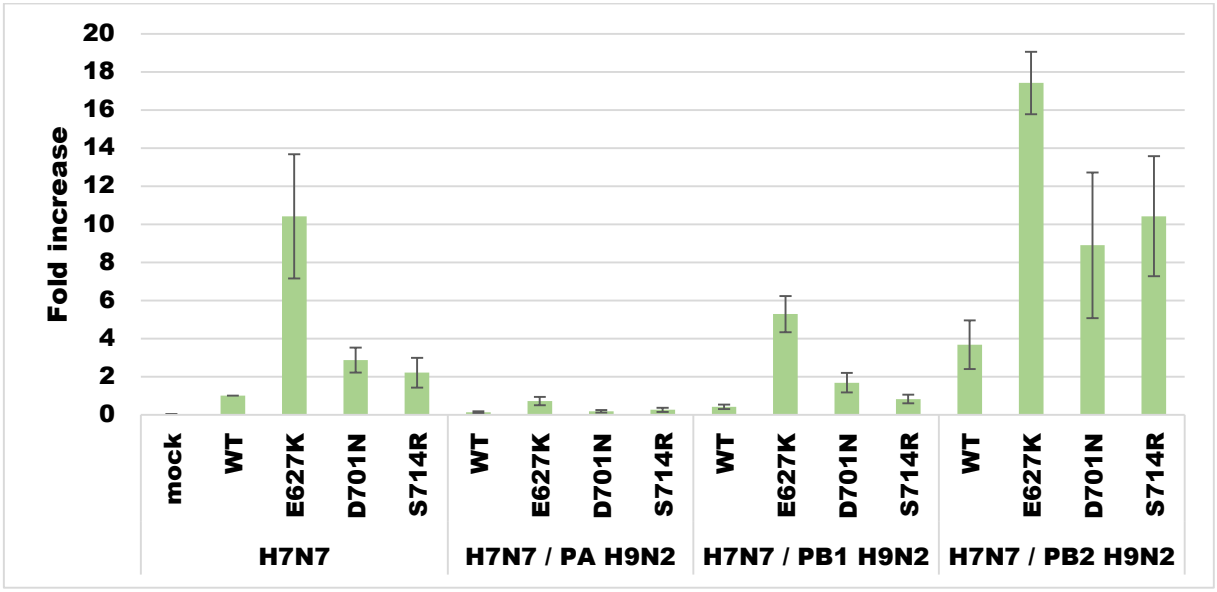

Figure 37: Polymerase activity of the reconstituted polymerase complexes of H7N7 with H9N2 polymerase subunit. *293T cells were cotransfected with pHW2000 plasmids encoding PB1, PA, PB2 and NP, in addition to plasmids encoding Firefly and Renilla luciferase. Quantification of Firefly luciferase normalized by Renilla luciferase enables determination of the polymerase activity with PB2 mutants. Activities of reassortants were compared to the activity of the homologous H7N7 polymerase used as internal standard. WT represents the polymerase complex in presence of PB2 containing the avian signature 627E-701D-714S.*

Altogether, these data indicated that the subunits PA and PB1 decrease the polymerase activity when introduced in H1N1pdm09 or H7N7, whereas PB2 leads to a strong increase of the activity.

8.5.2 Impact of adaptive mutations in H7N9 heterologous polymerase complex

It was furthermore relevant to investigate the role of each H9N2 polymerase subunit in the context of the related H7N9 polymerase (**Figure 38**). When H7N9-PB1 and H7N9-PA were replaced by the H9N2 subunits, there was a moderate reduction in the polymerase activity, but there was no complete loss of activity as observed after introduction of H9N2-PA into H1N1pdm09 and H7N7 polymerases (**cf.**

Figure 36 and **Figure 37**). The enhancing effect of the adaptive mutations was also clearly visible in H7N9/PA H9N2 and H7N9/PB1 H9N2

Introduction of H9N2-PB2 into the H7N9 polymerase did not lead to significant differences when compared to the homologous H7N9 polymerase. Introduction of PB2 E627K of H9N2 led to an increase of 12-fold, whereas PB2 627K of H7N9 induced a 14-fold increase. Introduction of PB2 E627K-S714R of H9N2 led to an increase of 31-fold whereas PB2 627K-S714R of H7N9 induced a 24-fold increase (**Figure 38**).

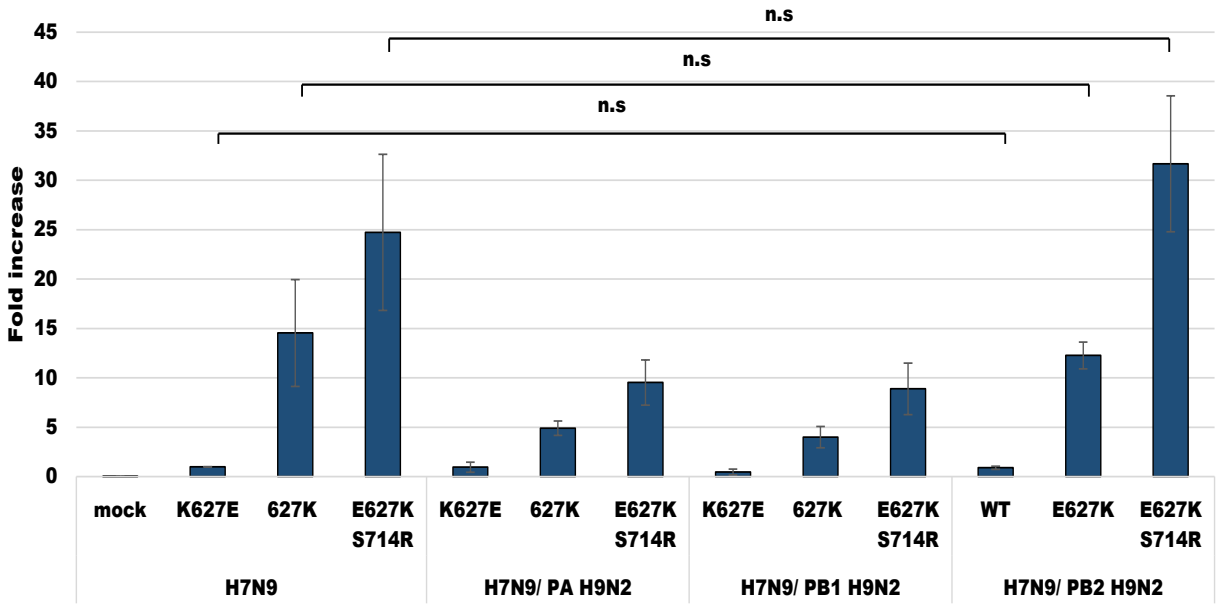

Figure 38: Polymerase activity of reconstituted polymerase complex of H7N9 with H9N2 polymerase subunit. *293T cells were cotransfected with pHW2000 plasmid encoding for PB1, PA, PB2 and NP, in addition to plasmids encoding minigenome expressing Firefly and plasmid encoding Renilla luciferase. Quantification of Firefly luciferase normalized by Renilla luciferase enables determination of the polymerase activity, within PB2 mutants. Each subunit of H7N9 polymerase complex were exchange by H9N2 corresponding subunit. Activities of reassortants were compared to the activity of the homologous H7N9-K627E polymerase used as internal standard. WT and K627E represent the polymerase complex in presence of PB2 containing the avian signature 627E-701D-714S. ns: non-significant indicates a P value of > 0.05 (Student's t test).*

In brief, these data demonstrated that the H9N2 subunits PA and PB1 lead to a decrease of polymerase activity when introduced in H7N9, in contrast to H9N2-PB2 which does not alter the polymerase activity when compared to the homologous H7N9 reconstituted polymerase.

In conclusion of this part, the results describe in **Figure 36**, **Figure 37** and **Figure 38** provide further evidence for the concept that enhancement of polymerase activity, by adaptive PB2 mutations, is most distinct in the H9N2 polymerase and the related H7N9 polymerase. They also demonstrate that this effect is a specific trait of H9N2-PB2 without significant contribution of PA and PB1.

8.6 Modulation of RIG-I recognition by PB2-627K

8.6.1 Impact of adaptive mutation E627K on RIG-I activation

The gene segments of influenza virus have partially complementary 5' - 3' end sequences, that form the so called "panhandle" structure. On this panhandle sits the polymerase complex, composed of PB1, PB2 and PA [131, 136].

Influenza viruses have developed several strategies to escape the immune system. For instance, NS1 is known to counteract RIG-I activation by targeting TRIM25 late in the life cycle of the virus [55]. RIG-I is a double-stranded RNA sensor present in the cytoplasm. It recognizes 5'ppp double-stranded RNA structures as described for bunyavirus and influenza virus segmented genomes [12, 147, 178, 179]. Early in the viral life cycle, influenza virus vRNPs are translocated to the nucleus after their release in the cytoplasm (**cf. Figure 5, step 4**). The short trafficking through the cytoplasm raises the question whether RIG-I recognizes also incoming influenza virus RNA, before NS1 synthesis and despite the presence of the polymerase on the panhandle region (collaboration project with M.Weber, AG Weber, [181]).

A549 cells were pre-treated with cycloheximide (CHX) and leptomycin B (LMB) to ensure that only incoming vRNP could activate RIG-I. CHX is an inhibitor of the translation machinery (by blocking translational elongation) and LMB the export machinery (by inhibiting CRM1, a protein required for nuclear export). Infection was performed with H9N2 or H5N1 viruses, containing avian 627E or mammalian 627K signatures in PB2, no other mutations were present. After 1 h infection, cells were harvested and subjected to limited trypsin digestion. The presence of a 30kDa fragment of RIG-I (reflecting a partial trypsin resistance) indicates a conformational switch and thus activation of RIG-I [143, 180]. During infection with H9N2 or H5N1 containing the avian signature (627E), the trypsin resistant fragment was observed, indicating that influenza virus RNA is recognized by RIG-I (**Figure 39**). Infection with viruses containing the mammalian signature (627K) in PB2 exhibited a faint or no 30kDa fragment, reflecting that viruses with 627K polymerase were less sensitive to RIG-I recognition (**Figure 39**).

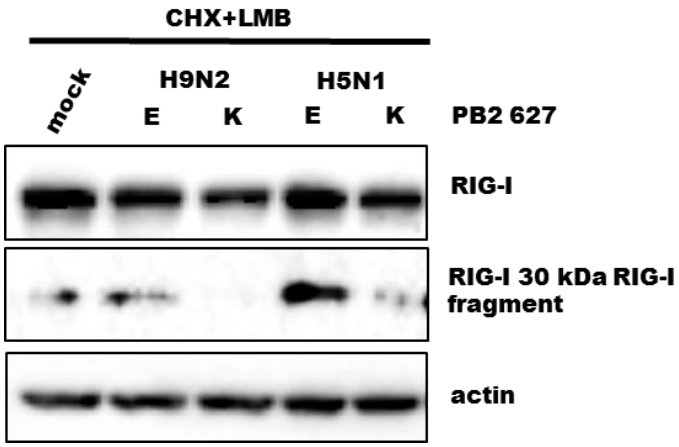

Figure 39: Activation of RIG-I upon H9N2 and H5N1 infection*. A549 cells were pretreated with CHX-LMB, followed by infection with 627E or E627K viruses in H9N2 and H5N1 backbone for 1 h. Cells were harvested and treated for limited trypsin digestion. Protein samples were separated on 12% SDS-gel and detected by immunostaining. Presence of 30kDa fragment indicates RIG-I activation. 627E viruses present the avian signature 627E-701D-714S. 627K viruses present only this mutation and the remaining avian signature 701D-714S. (collaboration project with M.Weber, AG Weber, [181])*

These results demonstrate that the incoming influenza virus genome activates RIG-I if PB2 has the avian signature (627E).

8.6.2 Impact of RIG-I activation on viral replication upon H9N2 and H5N1 infection

RIG-I can directly recognize incoming vRNPs. This recognition can affect viral replication and thus explain the differences between the polymerase activity and viral growth of 627E and 627K polymerases in mammalian cells. Indeed, results showed above (**cf. Figure 25**) indicated that in chicken fibroblasts cells (DF-1), which lack RIG-I [7], levels of NP production are similar with viruses containing the avian signature (627E) and polymerase with the mammalian signature (627K) [105, 128]. However, a difference in NP production is observed in the mammalian cell lines (**cf. Figure 26**). HEK293 WT cells or RIG-I deficient HEK293 cells (del-RIG-I) were infected with H9N2 or H5N1 viruses containing PB2 627E or E627K. Viral infection was monitored by quantification of NP protein over a period of 8 h after infection. Briefly, 2, 4, 6, 8 h post infection, cells were harvested and NP production analysed by Western Blot (**Figure 40**). For H9N2 and H5N1 viruses containing the mammalian signature (627K), NP was detected at 4 h post infection in both cell types. In contrast, for H9N2 and H5N1 viruses containing the avian signature (627E), NP was detected at 8 h post infection in WT cells, but at 6 h in del-RIG-I cells.

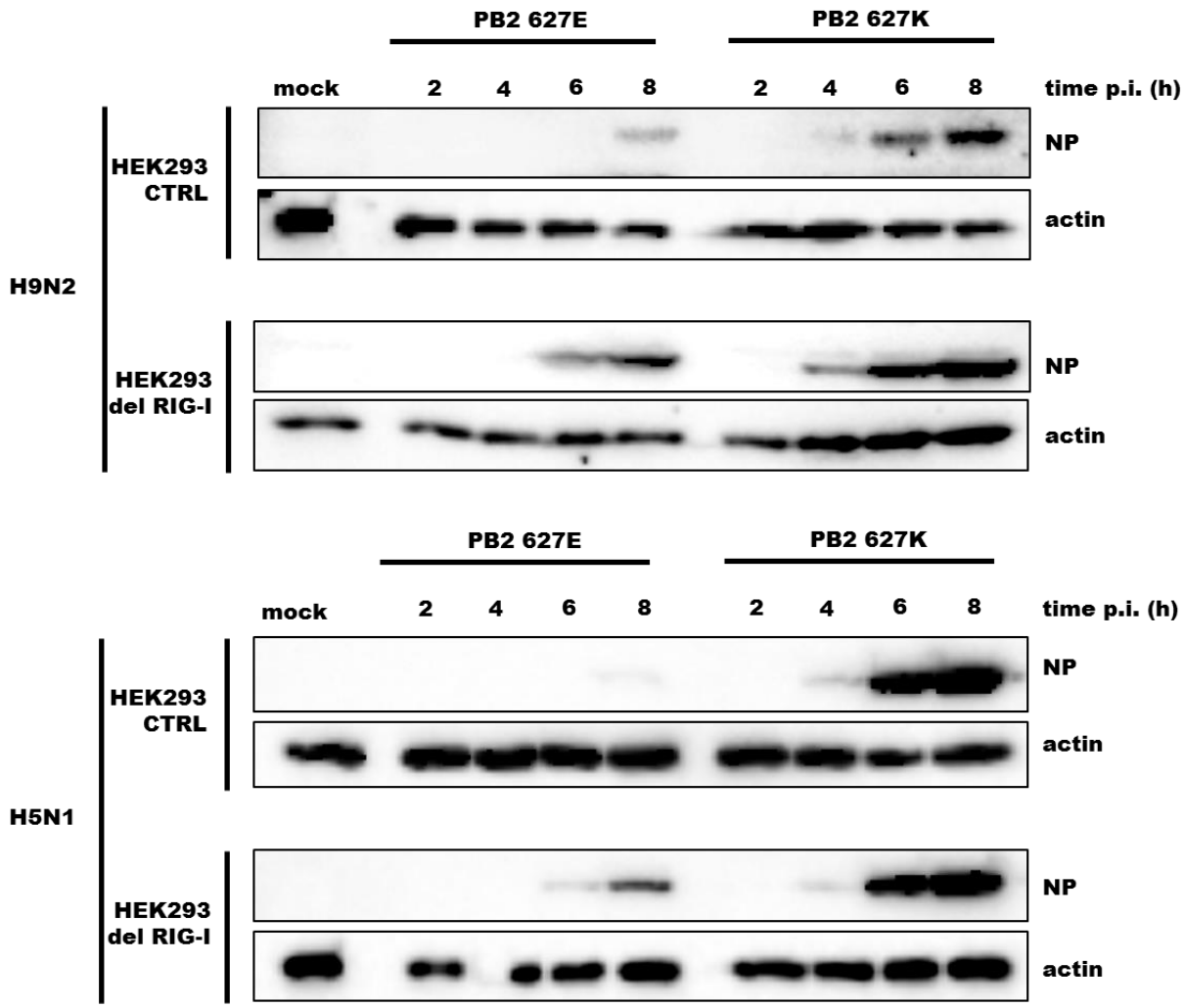

Figure 40: Expression of NP on RIG-I expressing cells or del-RIG-I cells. *HEK293 control cells or RIG-I depleted cells were infected with 627E or E627K viruses of H9N2 and H5N1 backbone (MOI 1). Cells were harvested at 2, 4, 6 and 8 h post infection. Protein samples were separated on a 12% SDS-gel and detected by immunostaining. 627E viruses present the avian signature 627E-701D-714S. 627K viruses present only this mutation and the remaining avian signature 701D-714S (collaboration project with M.Weber, AG Weber, [181])*

To sum up, these results confirm the impact of RIG-I at an early stage of infection and its role as a restriction factor for viruses presenting avian signature (627E) in PB2.

In the context of multicycle replication, WT cells and del-RIG-I cells were infected with avian (627E) or mammalian (627K) H5N1 viruses for 24 h (**Figure 41**). H5N1 was selected because of its multibasic cleavage site, which does not require addition of proteases to enable multicycle replication. Supernatants were collected at 8, 10 and 24 h post infection and titrated in MDCK cells (Fig.24). Titration showed that at 24 h in absence of RIG-I, virus with avian signature (627E) was rescued with a higher titer ($2.3.10^3$ PFU/ml) than in presence of RIG-I (1.10^2 PFU/ml). Overall, the absence of RIG-I increased by one logarithm the viral titre of avian (627E) H5N1 virus. Conversely, virus with mammalian signature (627K) grew to similar titre on cells expressing RIG-I ($8.5.10^6$ PFU/ml) or RIG-I depleted ($1.29.10^6$ PFU/ml).

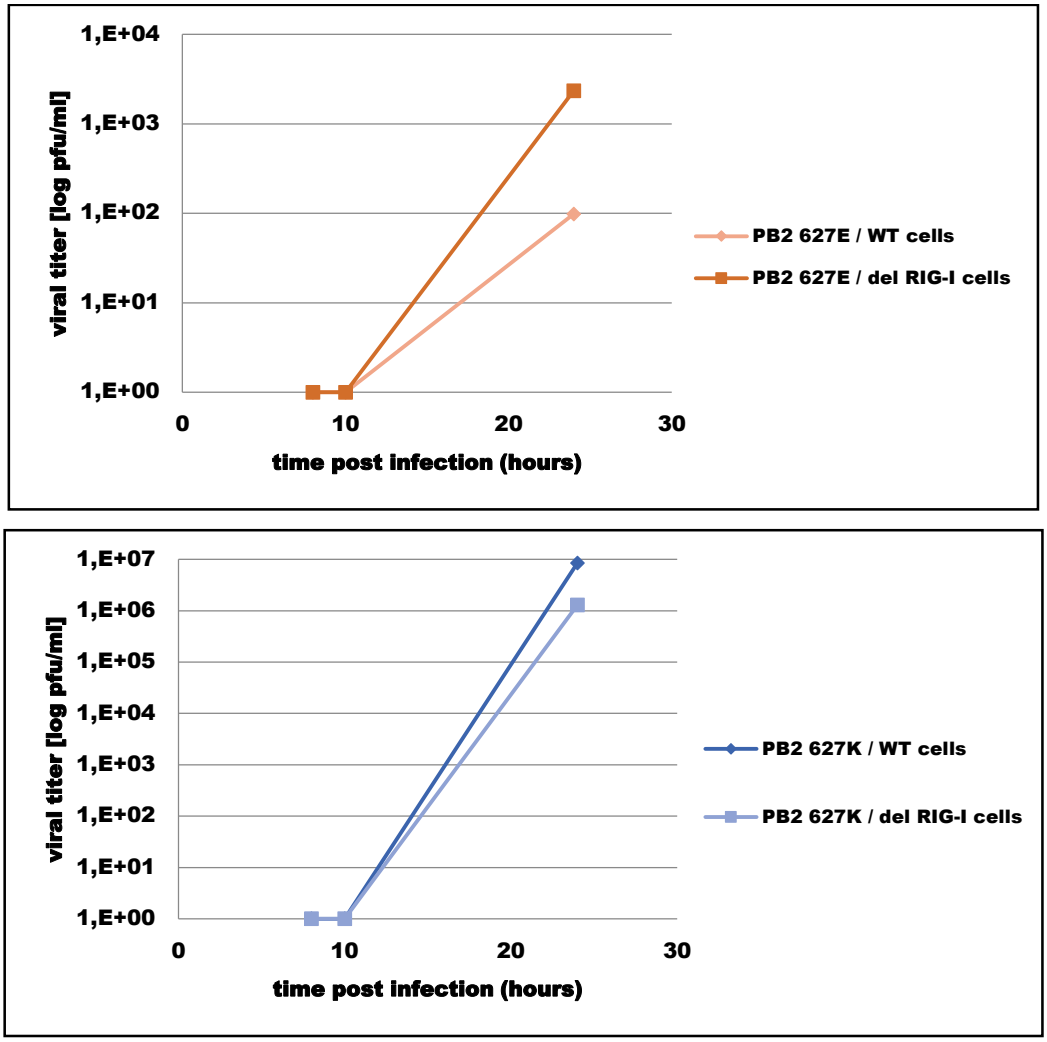

Figure 41: Growth kinetics on control or RIG-I deficient cells upon H5N1 infection. *HEK293 control cells or RIG-I depleted cells were infected with H5N1 627E or E627K viruses (MOI 0,0001). Supernatant were harvested at 8, 10 and 24 h post infection. Titration was performed on MDCK cells. Titres are expressed in PFU/ml and are representative of 3 independent experiments. 627E viruses present the avian signature 627E-701D-714S. 627K viruses present only this mutation and the remaining avian signature 701D-714S*

These results confirm that RIG-I affects replication of viruses containing the avian signature (627E) in PB2, whereas it does not influence replication of mammalian viruses (627K).

8.6.3 Mechanism of RIG-I evasion mediated by mutation E627K

It was of interest to investigate the mechanistic role of mutation E627K for RIG-I counteraction. It has been demonstrated that mutation E627K in PB2 led to an increased binding of NP in mammalian cells [93, 109, 135]. Therefore it was hypothesized that a weaker interaction between avian (627E) polymerase and NP enables the access of RIG-I to the panhandle structure, in contrast to mammalian (627K) polymerase.

To test this hypothesis, the viral polymerase was disassembled from the nucleocapsid by using a peptide inhibitor: T6Y (**Figure 42**). In absence of the peptide inhibitor, the same results as for **Figure 39** were observed. H9N2 and H5N1 viruses containing the mammalian signature (627K) did not activate RIG-I,

in contrast to viruses containing the avian signature (627E). In presence of the peptide inhibitor, both viruses were sensitive to RIG-I independently of the avian or mammalian signature.

From this observation it can be concluded that the disassembly of the polymerase complex from the panhandle results in the exposure of RIG-I recognition site and thus allows activation of RIG-I.

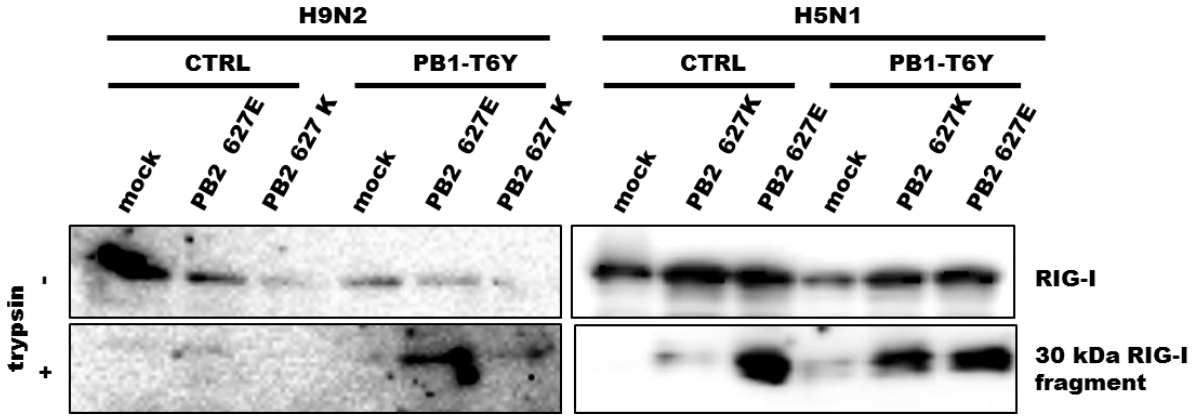

Figure 42: Activation of RIG-I upon H9N2 and H5N1 infection in presence of PB1-T6Y inhibitor*. A549 cells were pretreated with CHX-LMB. Cells were infected with 627E or E627K viruses in H9N2 or H5N1 backbone, for 1 h under treatment with control inhibitor or PB1-TY6. Cells were harvested and treated for limited trypsin digestion. Protein samples were separated on 12% SDS-gel and detected by immunostaining. Presence of 30 kDa fragment indicate RIG-I activation. 627E viruses present the avian signature 627E-701D-714S. 627K viruses present only this mutation and the remaining avian signature 701D-714S (collaboration project with M.Weber, AG Weber, [181])*

Taken together, these data show that mutation E627K interferes with RIG-I activation by preventing dissociation of the polymerase from the influenza gene segments in mammalian cells.

8.7 Transport of incoming vRNP

Another well described adaptive mutation in the PB2 subunit is D701N. It has been described to enhance polymerase activity, viral replication and pathogenicity in mice [50, 157]. It has also been characterized to increase interaction with human, but not avian importin proteins. This increased interaction leads to an enhanced nuclear localisation of newly synthesized PB2 protein into the nucleus [52]. Structural data indicated that mutation D701N led to a conformational change within PB2, which resulted in a better exposure of the NLS domain and improved interaction with importins [162]. Translocation of vRNP from the cytoplasm to the nucleus is driven by NP protein associated to the viral RNA [35, 125, 188]. The question was to evaluate if, in addition to NP, mutation D701N in PB2 subunit affects incoming vRNP transport.

8.7.1 Detection of vRNP traffic in infected cells

8.7.1.1 Establishment of vRNP immunodetection

To allow detection of vRNPs several parameters required optimization. vRNPs are composed of viral RNA of negative polarity, PB2, PB1, PA which compose the polymerase complex, and NP. One of these proteins had to be used for detecting the vRNPs. PB2, PA and PB1 are present as single monomers on

vRNPs, whereas NP covers the viral RNA. In addition, NP is a highly conserved protein among influenza viruses, which facilitates its detection. Therefore, a specific antibody against NP of H1N1pdm09 was tested. This antibody has been validated for immunostaining in plaque assays and is known to cross-react with NP of several strains. The staining of infected cells (as observed in **Figure 43**) revealed a strong signal allowing the detection of vRNP.

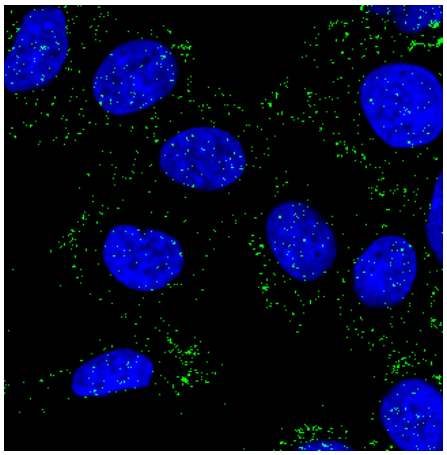

Figure 43: Optimisation of vRNP detection*. A549 cells were pretreated with CHX-LMB and infected for 1 h with H9N2 WT. Cells were fixed in 4% PFA for 24 h and stained against NP with primary antibody NP of H1N1pdm09 virus (secondary antibody FITC-coupled (green) and DAPI (blue)).*

To ensure the specific detection of NP with this antibody, 293T cells were transfected with plasmids encoding for the different proteins of the virus and the minigenome plasmid. Analysis of the transfected cells revealed specific detection in cells transfected with the plasmid encoding for NP (**Figure 44**). To generate vRNP (as for the minigenome assay), cells were transfected with plasmids encoding for PB2, PA, PB1, NP and minigenome plasmid (Firefly luciferase) (**Figure 44**). The staining shows here again detection of NP protein, when associated to the vRNA.

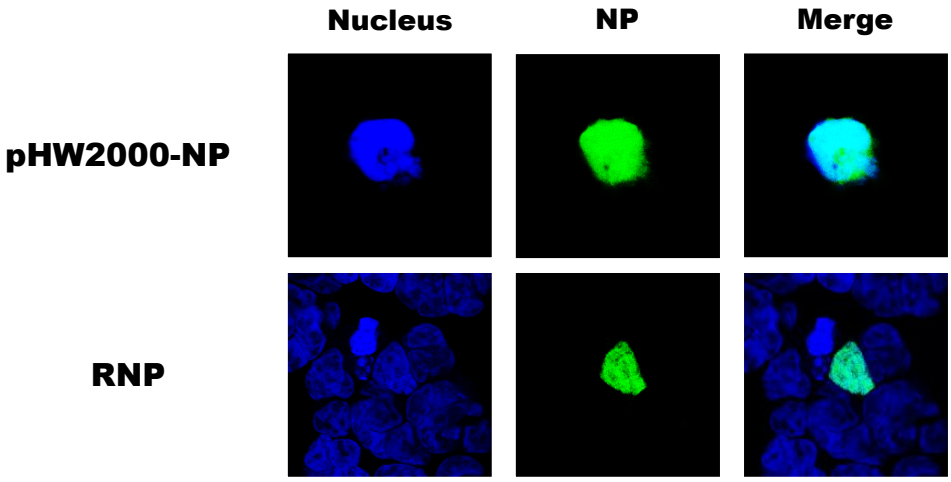

Figure 44: Confirmation of NP antibody specificity*. 293T cells were transfected with plasmids used for the polymerase assay: Firefly luciferase plasmid (flanked with NP sequence), PB1, PA, PB2 and NP (Ribonucleoprotein complex). Cells were fixed in 4% PFA for 30 min and stained with an antibody directed against NP of H1N1pdm09 virus (secondary antibody FITC-coupled (green) and DAPI (blue)).*

Finally, no staining was observed when cells were transfected with plasmids encoding for PB1, PB2, PA, HA, NA, M and NS segments (**Figure 45**). This confirms that this antibody specifically recognize NP and that no cross reaction can be observed with the other viral proteins.

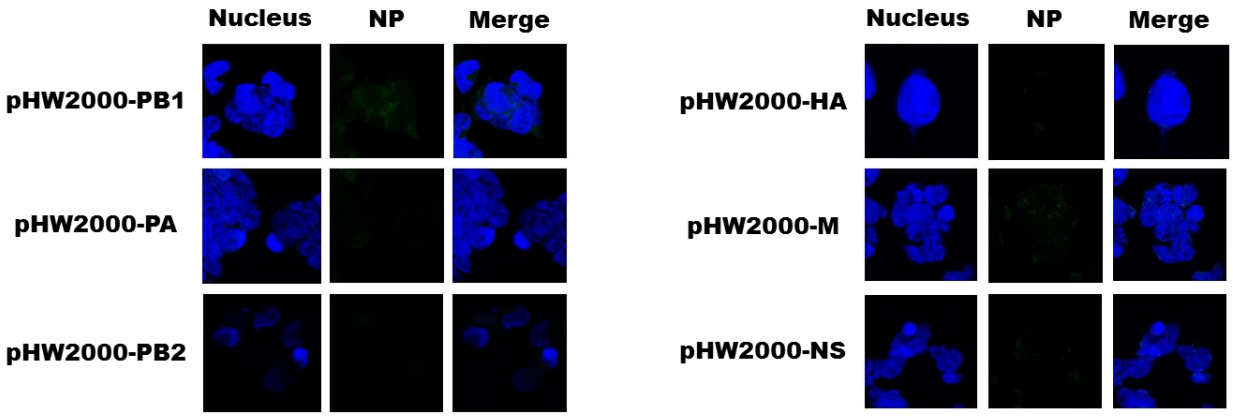

Figure 45: Confirmation of NP antibody specificity*. 293T cells were transfected with plasmids encoding each protein of H9N2 virus : PB1, PA, PB2, HA, M, NS. Cells were fixed in 4% PFA for 30 min and stained with an antibody directed against NP of H1N1pdm09 virus (secondary antibody FITC-coupled (green) and DAPI (blue)).*

8.7.1.2 Confirmation of the translation and export inhibitors efficiency

To determine the role of mutation D701N on nucleocapsid import, a procedure for detection of incoming vRNPs was established. For this purpose, cells were pre-treated with CHX and LMB, which impede the viral replication cycle at the primary transcription and retain newly synthesized mRNA into the nucleus. As translation is blocked, NP proteins are not synthesized, which ensures the recognition of NP only present on incoming vRNP. By blocking the export machinery, re-export of incoming vRNP from the nucleus to the cytoplasm is also prevented.

To test the efficiency of the inhibitor for different viruses, A549 cells were infected with H9N2, H1N1 (PR8) and H3N2 (Aichi) viruses in presence or absence of CHX-LMB (**Figure 46**). In the absence of inhibitors, the viral life cycle is not obstructed, and translation of new viral mRNA occurs. Therefore, newly synthesized NP is present into the nucleus, explaining the strong staining of the nucleus. In contrast, the presence of CHX-LMB interrupts at the primary transcription step and enables specific staining of incoming vRNP, represented by dot-like staining.

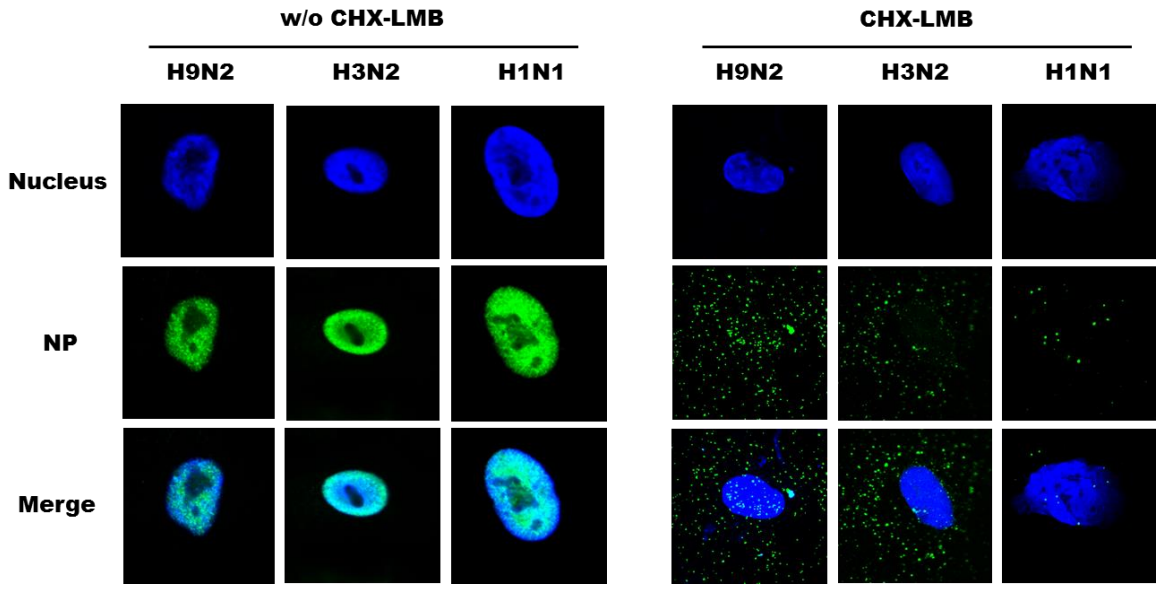

***Figure 46: Confirmation of inhibitors efficiency**. A549 cells were or were not pre-treated with CHX-LMB and infected with H9N2, H3N2 and H1N1 viruses for six hours. Cells were fixed in 4% PFA for 30 min and stained with an antibody directed against NP of H1N1pdm09 virus (secondary antibody FITC-coupled (green) and DAPI (blue)).*

To validate that this dot-like staining is due to the translation arrest, another inhibitor of the translation machinery, anisomycin was used in combination of LMB (**Figure 47**). In the presence of anisomycin, the staining in a dot-like shape is also observed, as detected in the presence of CHX (**cf. Figure 46**).

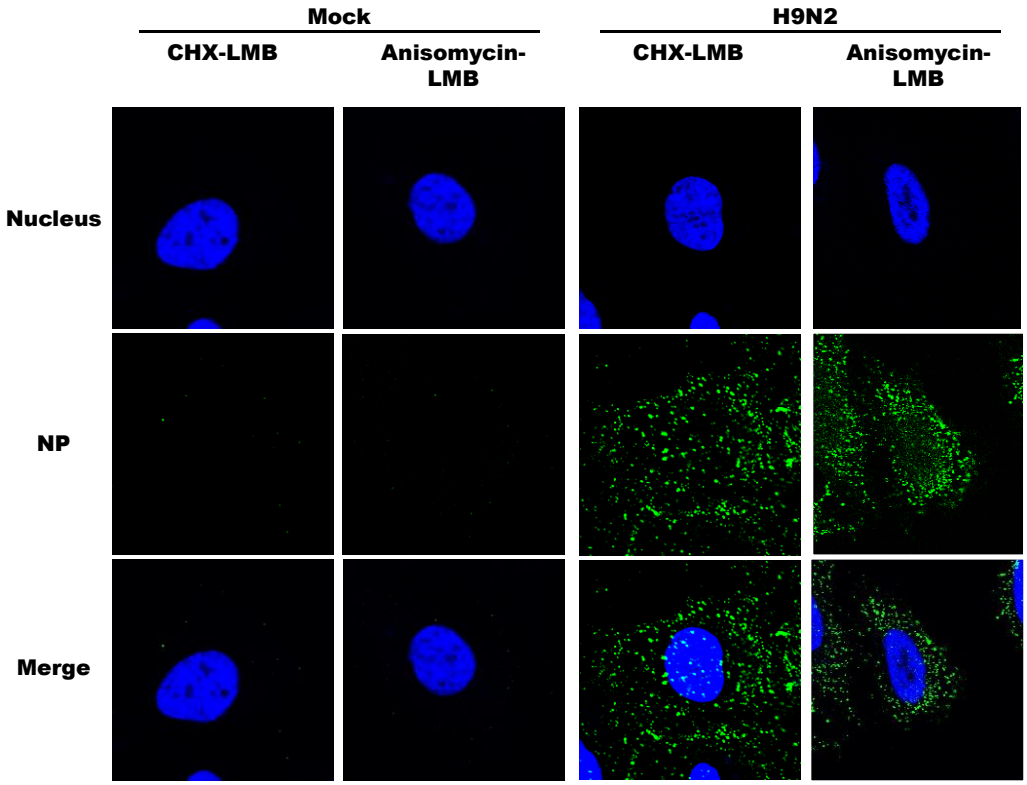

***Figure 47: Confirmation of inhibitors efficiency.** A549 cells were pre-treated with CHX-LMB or Anisomycin-LMB and infected with H9N2, H3N2 and H1N1 viruses for 6 h. Cells were fixed in 4% PFA for 30 min and stained with an antibody directed against NP of H1N1pdm09 virus (secondary antibody FITC-coupled (green) and DAPI (blue)).*

To validate the immunofluorescence data, infected cells were harvested 2, 4, 6, 8 h post infection and levels of NP production were monitored by Western Blot (**Figure 48**). Treatment of the cells with CHX-LMB completely aborted the synthesis of NP protein, compared to untreated cells. This quantification of NP supports the immunofluorescence observations, and demonstrates the effect of the inhibitor on the virus life cycle.

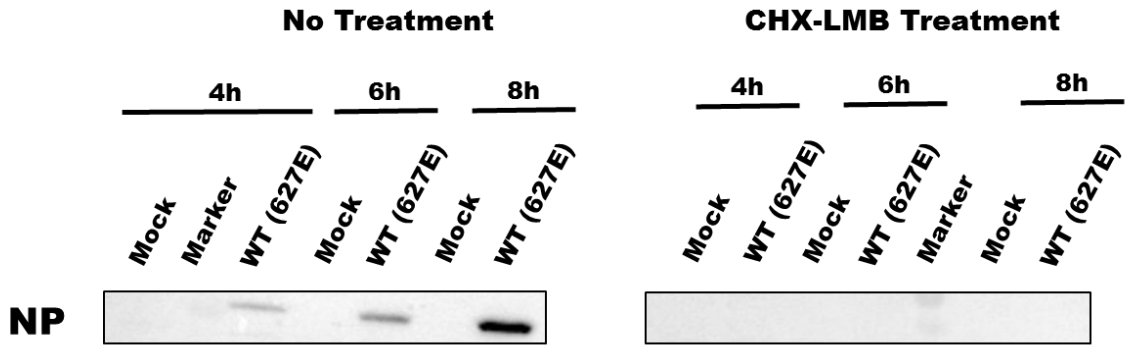

Figure 48: Confirmation of inhibitor efficiency by monitoring NP expression*. A549 cells were pre-treated or not with CHX-LMB. Cells were then infected with H9N2 WT virus. Cells were harvested 2, 4, 6, 8 h post infection. Protein samples were separated on a 12% SDS-gel and detected by immunostaining. H9N2 WT virus contains PB2 with avian signature 627E-701D-714S.*

In brief, detection of NP and pre-treatment with CHX-LMB is the relevant procedure for the detection of incoming vRNP.

8.7.2 Role of adaptive mutations E627K, D701N and S714R on incoming vRNP transport upon H9N2 infection

Mutation 627K has been described to interact with importin-α without affecting intracellular localisation of the PB2 protein [139]. Furthermore, mutation D701N has also been characterized to have an enhanced interaction with human but not with avian importins, which led to an increased nuclear localisation of PB2 in mammalian cells [52]. In addition, mutation S714R has been described to play a role in increased polymerase activity. A model has been proposed where this mutation would cooperate with mutation D701N for PB2 unfolding [36]. It was then hypothesized that mutations D701N could play a role in vRNP import, where, consequently, the increased nuclear localisation could explain the enhanced viral replication in mammalian cells.

To test this hypothesis, A549 cells were infected with recombinant virus WT (627E-701D-714S) or with viruses containing adaptive mutations in PB2, under CHX-LMB treatment. After 1 to 6 h of infection, cells were fixed for 24 h with 4% PFA, and immunodetection of NP was performed. The vRNP entry of H9N2 WT depicted that 6 h post infection vRNPs were present into the nucleus, but several remained in the cytoplasm mostly localized at the cell membrane (**Figure 49**).

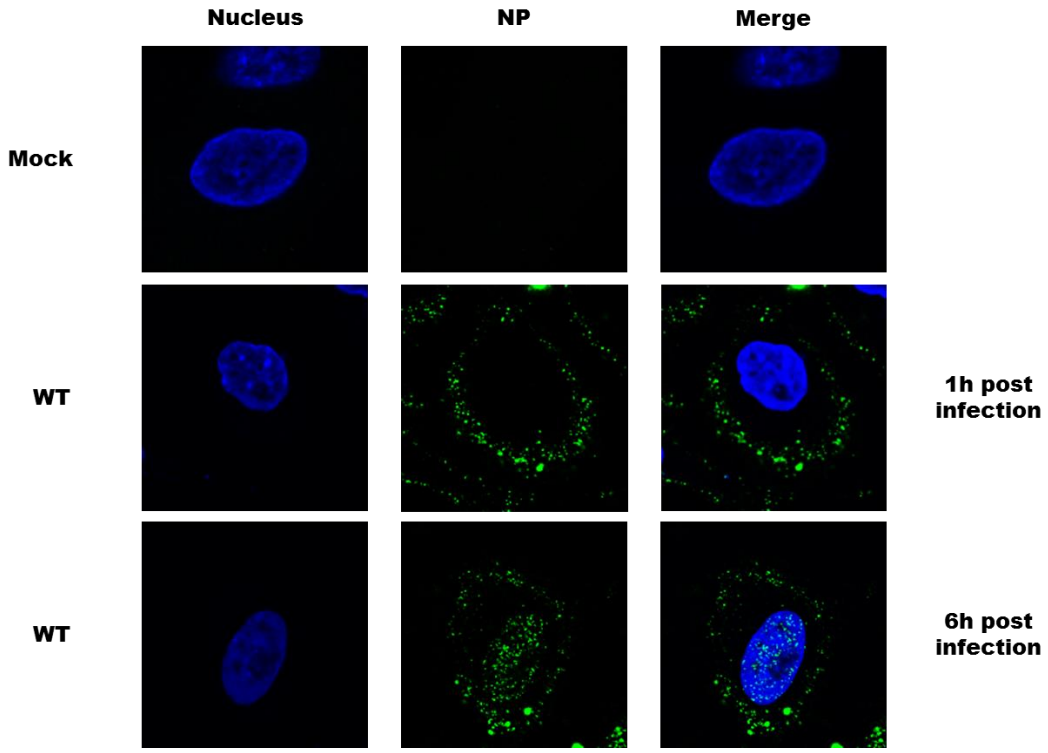

Figure 49: vRNP trafficking upon H9N2 infection in human cell line. *A549 cells were pre-treated with CHX-LMB and infected with H9N2 WT for 1 to 6 h. Cells were fixed in 4% PFA for 24 h and stained with an antibody directed against NP of H1N1pdm09 virus (secondary antibody FITC-coupled (green) and DAPI (blue)). H9N2 WT virus contains PB2 with avian signature 627E-701D-714S.*

Cells were infected with H9N2 E627K virus (containing PB2 with E627K-701D-714S signature) revealed a similar phenotype of vRNP import as H9N2 WT (**Figure 50**). Here as well, vRNP are present into the nucleus but mostly in the cytoplasm at the cell membrane.

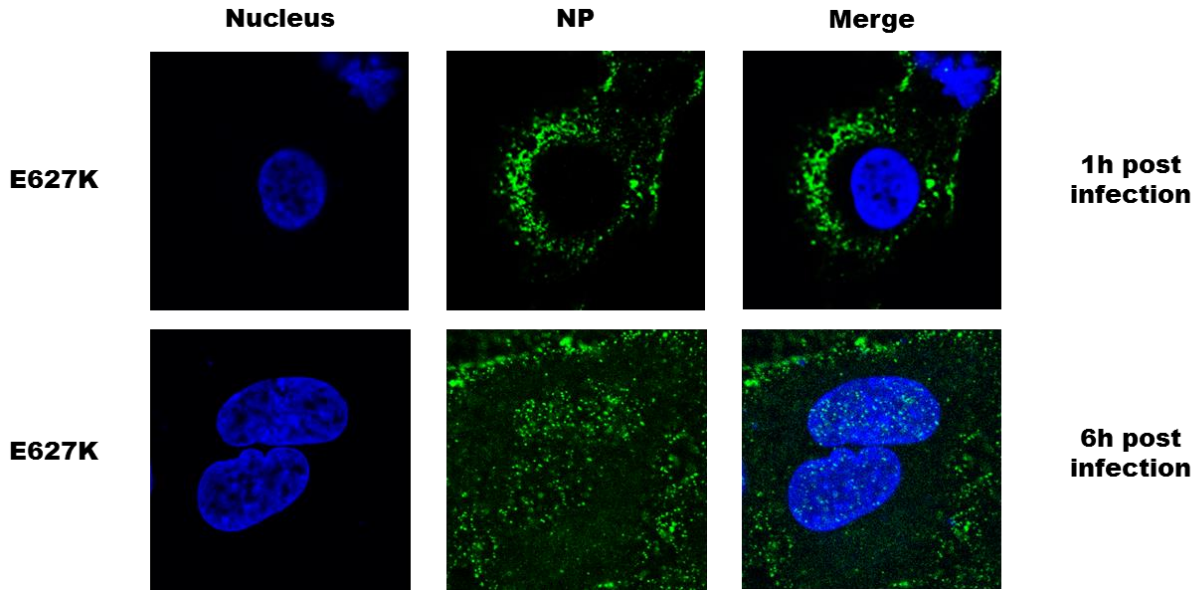

Figure 50: vRNP trafficking upon H9N2 infection in human cell line. *A549 cells were pre-treated with CHX-LMB infected with H9N2 E627K for 1 to 6 h. Cells were fixed in 4% PFA for 24 h and stained with an antibody directed against NP of H1N1pdm09 virus (antibody FITC-coupled (green) and DAPI (blue)). H9N2 E627K virus contains PB2 with mutation E627K only and the remaining avian signature 701D-714S.*

Interestingly infection with H9N2 D701N virus (containing PB2 with 627E-D701N-714S signature) showed the presence of vRNPs almost exclusively in the nucleus (**Figure 51**).

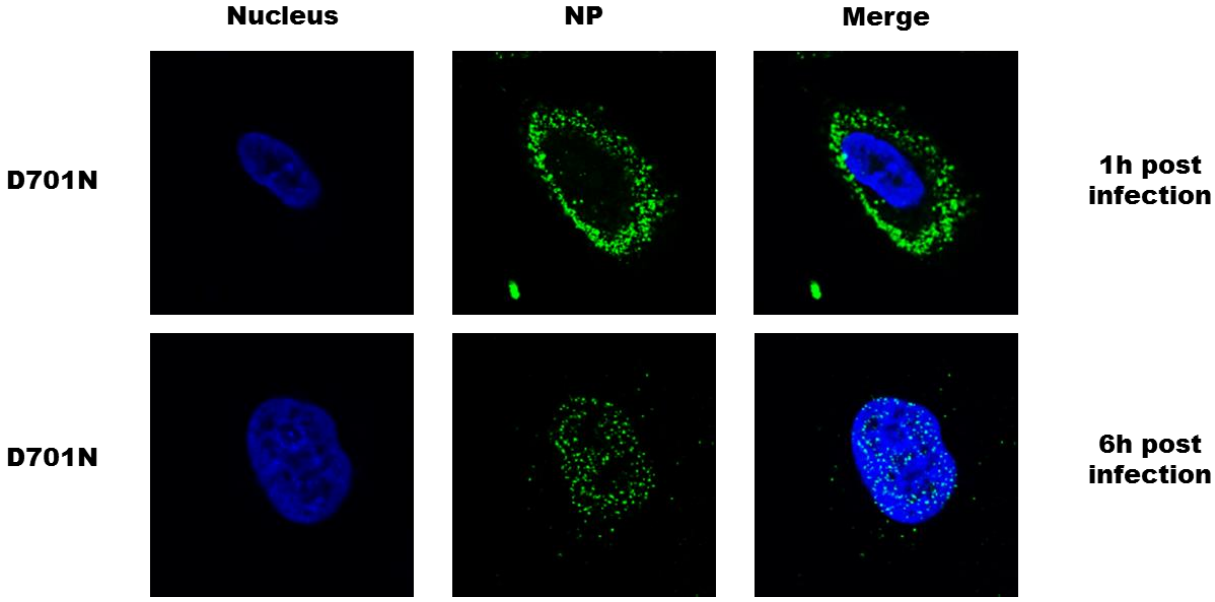

Figure 51: vRNP trafficking upon H9N2 infection in human cell line. *A549 cells were pre-treated with CHX-LMB infected with H9N2 D701N for 1 to 6 h. Cells were fixed in 4% PFA for 24 h and stained with an antibody directed against NP of H1N1pdm09 virus (secondary antibody FITC-coupled (green) and DAPI (blue)). H9N2 D701N virus contains PB2 with mutation D701N only and the remaining avian signature 627E-714S.*

Infection with H9N2 S714R virus (containing PB2 with 627E-701D-S714R signature) indicated the same phenotype of nuclear import as H9N2 WT and H9N2-E627K, where vRNPs remained mostly in the cytoplasm, close to the cell membrane (**Figure 52**).

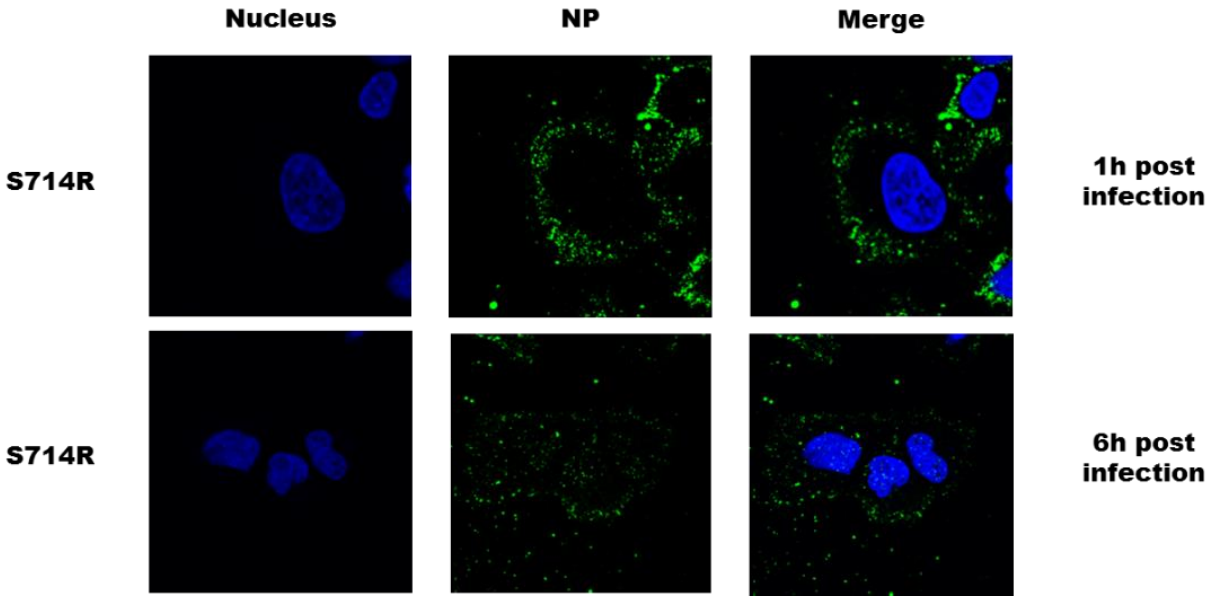

Figure 52: vRNP trafficking upon H9N2 infection in human cell line. *A549 cells were pre-treated with CHX-LMB infected with H9N2 S714R for 1 to 6 h. Cells were fixed in 4% PFA for 24 h and stained with an antibody directed against NP of H1N1pdm09 virus (secondary antibody FITC-coupled (green) and DAPI (blue)). H9N2 S714R virus contains PB2 with mutation S714R only and the remaining avian signature 627E-701D.*

Additional infections with double and triple mutants were performed. H9N2 D701N-S714I, D701N-S714R (with only avian signature at position 627) (**Figure 53**) and E627K-D701N-S714R (**Figure 54**) exhibited import into the nucleus 6 h post infection. Localization of vRNPs was increased into the nucleus and very few remained in the cytoplasm.

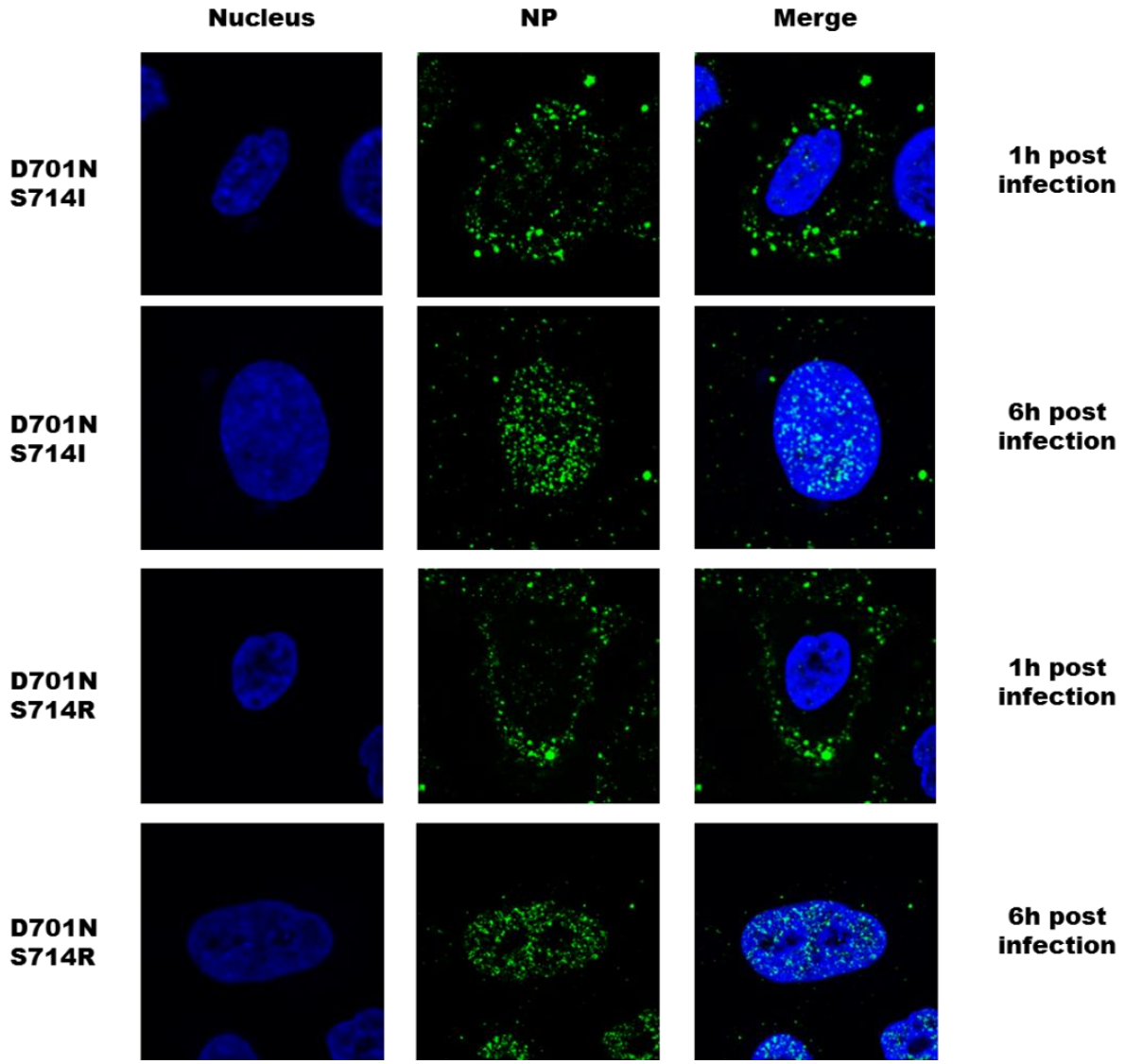

Figure 53: vRNP trafficking upon H9N2 infection in human cell line. *A549 cells were pre-treated with CHX-LMB infected with H9N2 D701N-S714I or D701N-S714R for 1 to 6 h. Cells were fixed in 4% PFA for 24 h and stained with an antibody directed against NP of H1N1pdm09 virus (secondary antibody FITC-coupled (green) and DAPI (blue)). H9N2 D701N-S714I and H9N2 D701N-S714R viruses contain PB2 with mutations D701N-S714I/R only and the remaining avian signature 627E.*

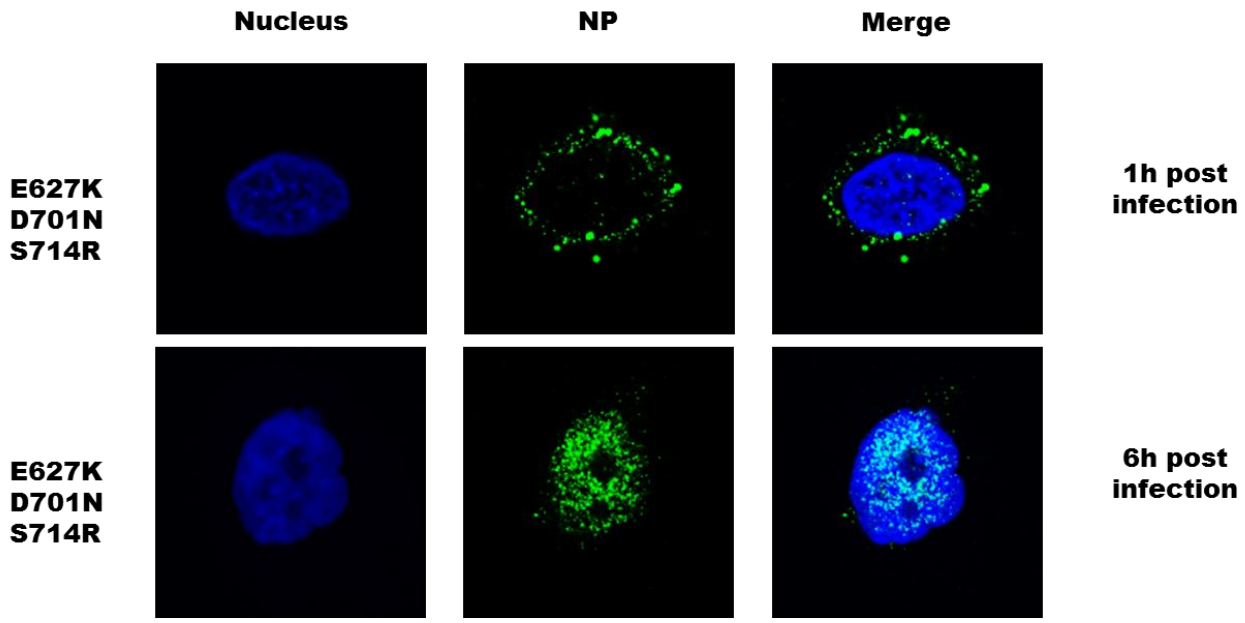

Figure 54 : vRNP trafficking upon H9N2 infection in human cell line. *A549 cells were pre-treated with CHX-LMB infected with H9N2 E627K-D701N-S714R for 1 to 6 h (under CHX-LMB treatment). Cells were fixed in 4% PFA for 24 h and stained with an antibody directed against NP of H1N1pdm09 virus (secondary antibody FITC-coupled (green) and DAPI (blue)).*

To sum up, these results support the concept that mutation D701N affects vRNPs nuclear localization and can provide the same advantage in combination with mutations E627K, S714I and S714R. Mutation D701N promotes not only the nuclear import of newly synthesized PB2 proteins, as described by others [52], but promotes also the nuclear entry of PB2 bound to the incoming nucleocaspids.

8.7.3 Role of mutation D701N in H7N7 viruses

To confirm the role of D701N on vRNP import in another influenza subtype, detection of nucleocapsid of H7N7 virus was performed. The same procedure of vRNP detection, applied after H9N2 infection, was conducted with H7N7 WT (containing PB2 627E-701D-714S)) and H7N7 D701N (containing PB2 with 627E-701N-714S) (**Figure 55**). Infection with H7N7 WT presents a similar phenotype of import as H9N2 WT, where vRNP entered the nucleus, but a high amount remained in the cytoplasm. Addition of mutation D701N induced an increased localization of vRNP into the nucleus. Nevertheless, it has to be pointed out that a high amount of H7N7 vRNP remained in the cytoplasm.

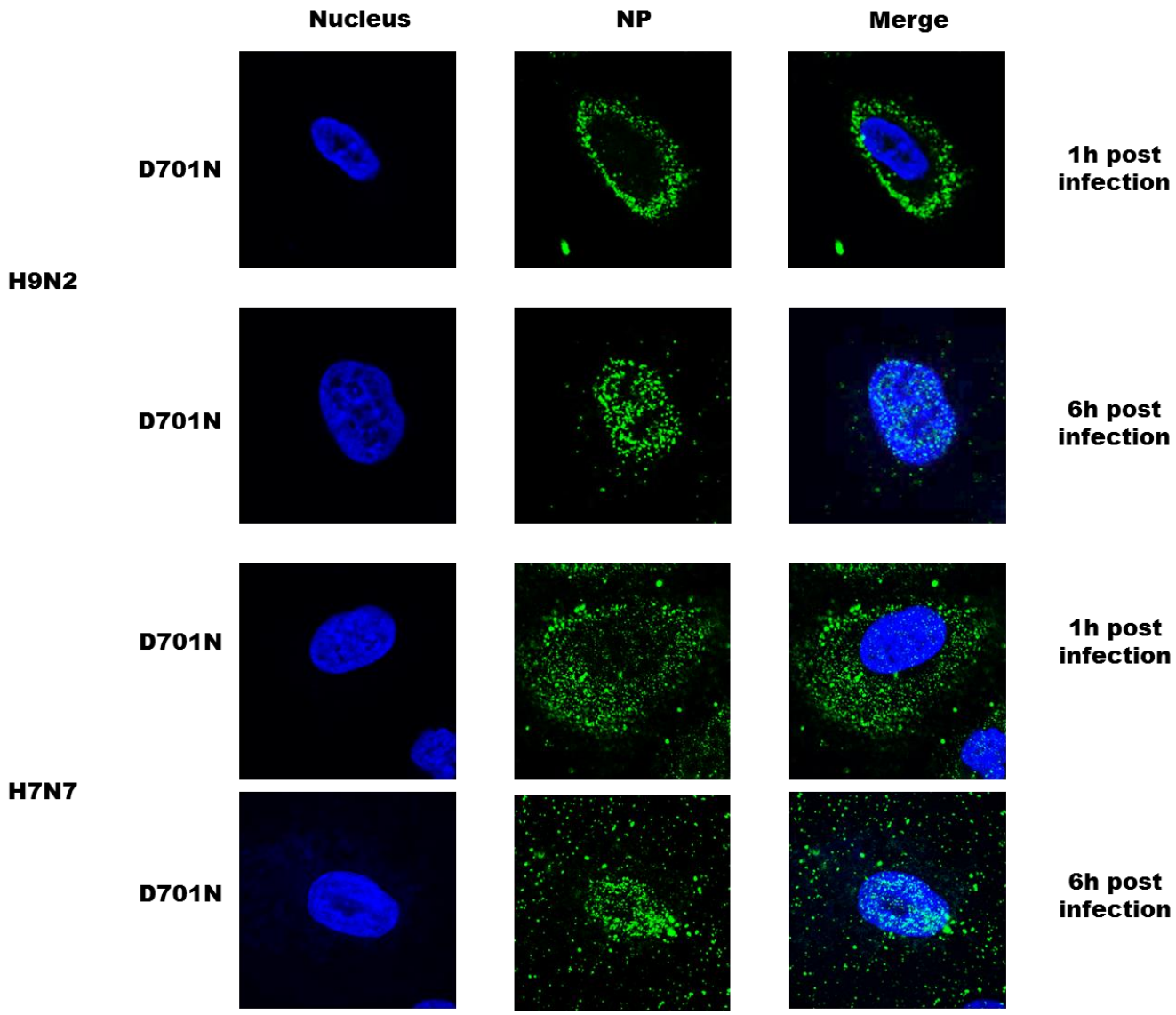

Figure 55 : vRNP trafficking upon H9N2 and H7N7 infection in human cell line. *A549 cells were pre-treated with CHX-LMB infected with H9N2 D701N or H7N7 D701N for 1 to 6 h.. Cells were fixed in 4% PFA for 24 h and stained with an antibody directed against NP of H1N1pdm09 virus (secondary antibody FITC-coupled (green) and DAPI (blue)). H9N2 D701N and H7N7 D701N viruses contain PB2 with mutation D701N only and the remaining avian signature 627E-714S.*

In conclusion, these data illustrate that mutation D701N induces import of vRNP in both H9N2 and H7N7 strains.

To summarize this part, the data demonstrate on one hand that mutation E627K is involved in RIG-I counteraction by preventing exposure of the genomic double-stranded RNA. On the other hand, mutation D701N in PB2 is directly active when associated to vRNP and enhances nuclear localisation. These mutations promote adaptation to mammalian host via evasion of the innate immune system and increase the interaction of incoming vRNPs with the nuclear import machinery.

9 DISCUSSION

Some viral proteins are particularly important for host adaptation. Mutations which occur in the surface glycoprotein HA enable the virus to adapt to the new host receptor [71, 173]. Mutations in the PB2 gene enable the virus to adapt to intracellular host factors that mediate import into the nucleus where transcription and replication of influenza viruses occurs. Mutations in PB2 have been linked to enhanced polymerase activity, viral growth and pathogenicity [36, 50, 113, 155, 159, 160, 162, 194].This work addresses the role of adaptive mutations introduced into an avian H9N2 influenza virus. The results showed that mutations E627K, D701N and S714R promote adaptation of A/Quail/Shantou/2061/2000 influenza virus to mammalian hosts. Furthermore, it is demonstrated that the H9N2-PB2 subunit plays an important role in increased polymerase activity during reassortment of polymerase subunits. This work also describes the mechanism of action of mutation E627K in PB2 and its function in innate immune evasion, as well as the role of mutation D701N for the import of incoming vRNP into the nucleus.

9.1 Mutations E627K, D701N, S714R and D253N promote adaptation to mammals.

9.1.1 Variations within two H9N2 isolates: H9N2-782 and H9N2-2061

The introduction of the mutations E627K, D701N and S714R led to different enhancement of the polymerase activity with the isolates H9N2-782 and H9N2-2061. With H9N2-782, the polymerase activity was always higher than with H9N2-2061. These two isolates show the same amino acid sequence in segments 1 and 5. The differences in polymerase activity have therefore to be attributed to PB1 (differing by 5 amino acids) and PA (differing by 3 amino acids) subunits (**cf. Table 5**).

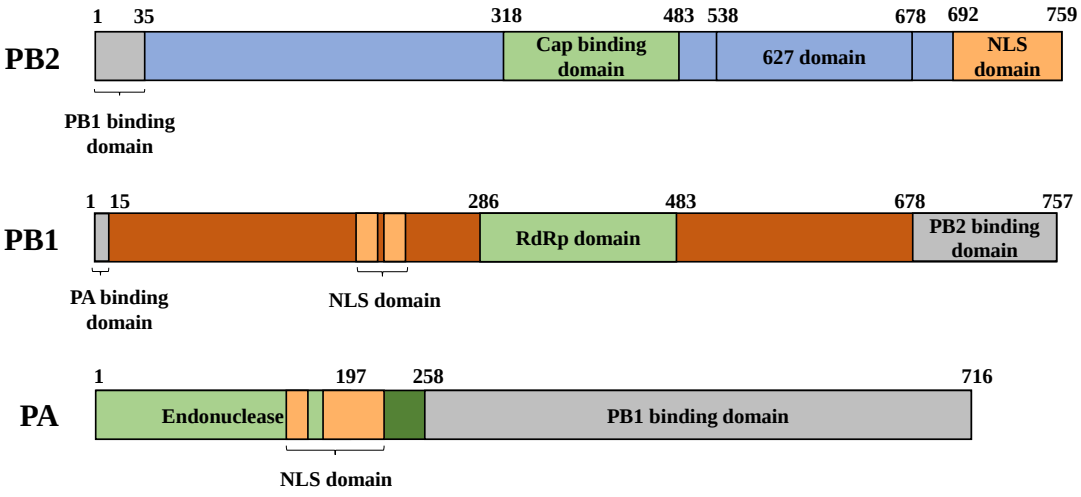

***Figure 56: Domains of influenza polymerase subunits PB2, PB1 and PA**. In green are represented the functional domain of each subunit for the transcription and replication steps: PA and its endonuclease domain, PB1 and its RdRp catalytic domain and PB2 with its cap binding domain. Binding domains for each subunit are coloured in grey. In orange are represented the NLS domains of PB2, PB1 and PA.*

The amino acid changes present at positions 63 and 101 in PA are both localised in the endonuclease domain (**Figure 56**). The amino acid change at position 618 is localized in the PB1 binding domain. These substitutions may affect the enzymatic activity or the import of the heterodimer PA/PB1 into the nucleus. The mutations present in PB1 are localized at positions 191, 213, 455, 571, 722. Position 722 is localized in the PB2 binding region and may have an impact on the transcription or replication efficiency. Position 455 is localized in the RNA-dependent-RNA-polymerase (RdRp) catalytic domain, and positions 191 and 213 are in the NLS region (**Figure 56**). These few changes could be responsible for an altered polymerase activity in H9N2-782 and H9N2-2061. It would be of interest to exchange the subunits between the two isolates in order to find out if PB1 or PA are responsible for the differences in polymerase activity. Consequently, the results could describe critical positions involved in the transcription/replication efficiency of the virus.

9.1.2 Adaptive mutations E627K, D701N, S714I, S714R and D253N increase the polymerase activity in contrast to mutation Q591K.

Mutations E627K, D701N and S714R have already been described to promote adaptation of other viruses, such as H3N2, H7N7 and H5N1 viruses [17, 36, 50, 99, 159] to mammalian hosts. Mutation E627K has already been characterized to enhance polymerase activity and viral growth in mammalian cells, as well mice pathogenicity of H9N2 virus. This is the first time that mutations D701N and S714R are described to increase polymerase activity and viral replication in mammalian cells, when introduced into an avian influenza virus of subtype H9N2.

Introduction of mutation S714R into PB2 subunit has a higher impact on polymerase activity than mutation S714I (**cf. Figure 19 and Figure 20**). This effect was also observed when virus growth in mammalian cells was analysed, where viruses containing the mutation S714R grew to higher titres compared to virus with the mutation S714I (**cf. Figure 22, Figure 23 and Figure 24**). These results are consistent with the data published by Czudai et al. The authors suggested that S714R would cooperatively work with D701N to induce a conformational change of PB2 and that an uncharged amino acid, such as isoleucine, will not be as efficient for an increase polymerase activity or viral growth [36].

Mutation D253N (localized in the N-terminal part of PB2) also leads to an increase of polymerase activity confirming results obtained previously by Mok et al for strain H9N2 G1/97 [113]. Despite the increased polymerase activity *in vitro*, this mutation was not beneficial for viral growth. The mutation D253N has already been observed by Li et al. The authors investigated restriction factors that prevent influenza virus genes reassortment. They have demonstrated that polymerase complex subunit PB2 and PA of different origins were responsible for a restricted viral growth. However, after several passages of this virus, adaptive point mutations in PB2 (D253N) and PA (A448V) emerged, leading to an increased viral replication. These mutations were suggested to compensate the PA and PB2 incompatibility [96]. Therefore it can be assumed that the presence of mutations A448V in PA, in addition to mutation D253N in PB2, is mandatory for an efficient viral growth. As PA of both H9N2

isolates do not present mutation A448V, it could explain the deficient replication of H9N2 viruses containing mutation D253N.

The results have demonstrated that mutation Q591K in PB2 leads to a loss of activity in the two H9N2 isolates in contrast to the data published by Mok et al. Mutation Q591K has been described to enhance the polymerase activity and viral growth in mammalian cells, as well as cytokine response in mice infected with H9N2 G1/97 virus [113]. Furthermore the mutation Q591R has been described in a H5N1 isolate to enhance mice pathogenicity [192]. These two publications demonstrate that basic amino acid at position 591 enhances polymerase activity and mice pathogenicity. However, a recent study showed that a basic amino acid exchange at position 526 modulates polymerase efficiency. The presence of an arginine increased the polymerase activity, while the presence of a lysine led to a loss of activity [155]. These results provide an explanation for the abolished polymerase activity observed with mutation Q591K in H9N2-2061/H9N2-782. Therefore it would be interesting to investigate the impact of Q591R in H9N2-2061/782 and its potential to restore and enhance the polymerase activity. Sequencing of H9N2-2061/782 PB2 did not show additional mutations which could explain a counteracting effect. Mutation Q591K is localized in the C-terminal part of PB2 [162] more precisely in the 627-domain and therefore should not influence replication or cap snatching activity. It has been proposed by Reich et al that during the transcription process the viral messenger RNA passes through a basic channel between the cap-binding domain and the 627-domain (including position 591) [136]. This exit pathway avoids the endonuclease, protecting subsequently the viral mRNA from degradation. Therefore, it is conceivable that this mutation affects the release of viral messenger RNA.

9.1.3 Adaptive mutations increase viral growth in mammalian cells.

Most of the adaptive mutations conferring enhanced polymerase activity in mammals have been described in PB2 subunit. One of the most frequently observed mutation during mammalian adaptation is E627K [25] and is therefore one of the most characterized. Mutation E627K has not yet been described in natural H9N2 isolate. In contrast, in 2009 a human H9N2 isolate containing mutation D701N (A/Hong Kong/33982/2009, Genbank accession number: KF188313) has been reported. The results presented here confirm that introduction of adaptive mutations in PB2 of H9N2-2061 virus leads to an increase of viral growth in mammalian cells, corresponding to the increased polymerase activity data (**cf. Figure 19**, **Figure 22**, **Figure 23** and **Figure 24**). The recurring presence of H9N2 infections in humans raises concerns about the possibility of H9N2 viruses evolving into pandemic strains. Consequently, these observations underline the relevance to investigate the effects of adaptive mutations introduced into an avian H9N2 isolate and thereby evaluate the potential threat arising from H9N2 viruses.

9.1.4 Adaptive mutations increase mouse pathogenicity

Mice infections are a widely used animal model to study influenza pathogenicity in mammals. The virulence of H9N2 influenza viruses with the different PB2 mutations was therefore investigated in this

model. Viruses with mutation E627K alone or in combination with mutation D701N and S714R showed an increased pathogenicity in mice. Similar effects of mutation E627K on mice virulence have been observed in studies with different viruses, including other H9N2 isolates [99, 174, 187]. Nevertheless, it has to be pointed out that infection with H9N2 E627K was not lethal for the mice in contrast to the study of Li et al. The authors used the isolate H9N2 A/chicken/Guangdong/V/2008 (with mammalian signature E627K), which provoked 25% weight loss, and 100% lethality [99]. A possible explanation for this difference might be related to the isolates used in this study. Several viral proteins are involved in influenza virulence and PB2 is not the only viral determinant responsible for a severe infection. For example HA or NS1 also play a role in pathogenicity [148]. The polymerase assay data also suggest that the impact of mutations could differ between two related H9N2 isolates (**cf. Figure 19** and **Figure 20**) and could therefore affect the virulence in mice.

H9N2-2061 viruses with the mutations D701N or S714R showed a similar phenotype as WT. Despite high titres in the lung, mice infected with H9N2-D701N did not indicate signs of illness. This could be the result of an efficient replication in the lung without raising a strong immune response. Davidson et al have demonstrated that a strong IFN response upon influenza infection is responsible for an increased morbidity in mice [37]. Analysis of the cytokine response could thereby provide more insight for this phenotype. Mutation S714R alone did neither affect weight and survival nor organ titres. This leads to the conclusion, that mutation S714R alone does not promote adaptation to mammals and needs the combination with the mutation D701N. This was observed by Czudai et al, where combination of S714R with D701N was more effective than S714R alone regarding mice pathogenicity [36]. It has been demonstrated by Otte et al, that the genetic background of mice may also affect influenza virus pathogenicity. They demonstrated that H1N1pdm09 was less virulent in Balb/C than in C57BL/6J mice, whereas infection with a highly pathogenic H5N1 isolate led to higher pathogenicity in Balb/C than in C57BL/6J mice [127]. Therefore it would be interesting to evaluate the virulence of H9N2-D701N or H9N2-S714R viruses in C57BL/6J mice in comparison to Balb/C mice. It is the first time that recombinant H9N2 virus with the triple mutation E627K, D701N and S714R has been studied and found to be lethal. Interestingly, although H9N2 is known to be at the origin of H5N1 virus in 1997, introduction of adaptive mutation in H9N2-PB2 did not provoke viral dissemination into the brain, as observed by Czudai et al [36].

To conclude, introduction of mutation E627K, D701N and S714R promotes adaptation of an avian H9N2 virus to mammals as demonstrated by the observations that it (i) enhances polymerase activity and viral growth in mammalian cells, and (ii) enhances mouse pathogenicity.

9.1.5 Adaptive mutation are more efficient in H9N2 and H7N9 virus than in H1N1pdm09 and H7N7

Adaptive mutations E627K, D701N and S714R were introduced into PB2 of H1N1pdm09, H7N7, H7N9 and H9N2 viruses. The results demonstrate that the mutations have a higher impact on polymerase activity, when introduced into H9N2 than into H7N7 or H1N1pdm09 PB2. Interestingly, these mutations had the same effect when introduced into PB2 of H7N9 virus. A possible explanation could be the avian origin of H9N2 and H7N9 viruses where the effect of a mammalian signature is more potent. In contrast, H7N7 and H1N1pdm09 are already, to some extent, adapted to a mammalian host (**cf. Table 6**), where therefore introduction of the adaptive mutations does not further enhance the polymerase activity. The differences within H9N2 and H7N7 or H1N1pdm09 in contrast to H7N9 could also be explained by phylogenetic analysis. H7N7 and H1N1pdm09 are evolutionary distant from H9N2, whereas H7N9 was generated from H9N2 internal genes [45].

This more potent effect of adaptive mutations in H9N2 was also observed in the context of viral growth. Comparison of viral replication of H9N2, H5N1 and H1N1pdm09 in human airway epithelial cells, demonstrated that the mutations E627K and D701N in H9N2 had a higher impact on viral growth than in H5N1 and H1N1pdm09. It has to be pointed out, that only the impact of the mutation was analysed and that this does not reflect the viral titres post infection, where H5N1 reached the highest titer.

9.1.6 PA and PB1 do not contribute to the enhancement effect of PB2 mutations in H9N2 viruses

Reassortment is an important mechanism in influenza virus evolution and played a critical role in the evolution of H5N1 viruses. In fact, the H5N1 influenza viruses, in 1997 in Hong Kong causing an outbreak in humans, contained internal genes of H9N2 virus G1/97 [30, 64]. Since H9N2 influenza viruses are endemic in Asia, the chances are high that reassortment events occur with high frequency. This concept is supported by observations that H7N9 [45, 56] and H10N8 [26, 134] viruses, recently isolated in China from human cases, contain also internal genes of H9N2 origin. Introduction of adaptive mutations in H9N2-PB2 has a higher impact on polymerase activity than in H7N7 or H1N1pdm09. It was therefore relevant to evaluate the role of PA and PB1 in this enhancement, by producing heterologous polymerases.

The loss of polymerase activity when PA of avian H9N2 was introduced in H1N1pdm09 and H7N7 could be the result of an incompatibility within the subunit (**cf. Figure 30**). Naffakh et al have proposed that differences in the endonuclease activity of PA could affect the polymerase efficiency [118]. Furthermore, Li et al suggested that the N-terminal part of PA is responsible for the incompatibility between the polymerase subunits during reassortment due to a defect of heterotrimer formation [96]. Introduction of H9N2-PA also led to a decreased polymerase activity in H7N9 virus which could also illustrate a difference of enzymatic activity. Chen et al have described that reassortment of PB2 and PA

of avian origin showed an improved polymerase efficiency [27]. This would therefore explain why the activity of reconstituted polymerase in H7N9 is not aborted in the presence of avian H9N2-PA. Consequently, PA of H9N2 is to some extend more compatible with PB1 and PB2 of H7N9 virus than with PB1 and PB2 of H7N7 and of H1N1pdm09 viruses. In addition, Naffakh et al proposed that PB1 of avian origin cooperates more efficiently with human PB2, PA and NP [118], and therefore explain why PB1 of avian H9N2 does not affect the polymerase activity of H1N1pdm09 (human isolate) (**cf. Figure 36**). As explained above, H9N2 is phylogenetically related to H7N9 in contrast to H1N1pdm09 and H7N7, and could thereby resolve the differences within the heterologous polymerase.

Several studies have investigated the reassortment process of influenza viruses and described some restriction mechanisms preventing combination of segments. They have observed that not all combinations were possible. There are in theory 254 possibilities of reassortant viruses between two different influenza isolates. However, only a few have been observed in nature or experimentally obtained, supporting the hypothesis of a mechanism preventing random reassortment [44, 60, 68, 118, 119].

The results demonstrate that H9N2-PA and PB1 do not contribute to the polymerase enhancement observed after introduction of adaptive mutations, but that this increase is a special characteristic of H9N2-PB2. The role of H9N2-PB2 in H1N1pdm09, H7N7 and H7N9 viruses during infection of mammalian cells or mice still remains to be investigated. However, the results with the heterologous polymerase suggest that these reassortants would have an enhanced viral growth and pathogenicity.

9.2 Mechanisms of adaptive mutations E627K and D701N

9.2.1 Mutation E627K modulates the evasion of innate immunity

The innate immune system is constantly challenged by pathogens, including viruses. These pathogens are rapidly evolving and adapting to new hosts and develop strategies to evade the recognition by the immune system. They also hijack the cellular machinery for their own purpose to either promote replication or to evade cellular sensors [52, 66, 67, 177, 178, 185].

Influenza virus have developed several strategies to evade RIG-I sensing, one of the major sensors during influenza infection. Nuclear transcription and replication is one of the most efficient mechanisms to avoid recognition by the innate immune system. Furthermore, the protein NS1 targets TRIM25 responsible for the ubiquitin-activation of RIG-I [55]. Proteins of the polymerase complex, PB1, PB2 and PA were also described to act on the RIG-I pathway via interaction with MAVS and thus blocking the signaling pathway leading to IFN production [63, 82]. Nevertheless, NS1 is not present at early stages of infection, and PB2, PB1 and PA are present as a heterotrimer on the incoming vRNP. The data presented in the thesis highlight that despite all the subversion mechanisms developed by the virus, RIG-I can still be activated by incoming vRNP exposed during translocation into the nucleus.

Activation of RIG-I is dependent on a short blunt 5'ppp double-stranded-RNA, as observed in the panhandle of negative strand viruses [147]. The particular structure of the influenza vRNP fulfil these criteria. Indeed, vRNP present a double stranded RNA structure formed by the 5' and 3' end of the genome (so called panhandle) with a 5'ppp group. However, the recently elucidated structure of the influenza promoter showed that nucleotide 1-10 of the 5' end are organized in a hook structure [131]. This hook is confined in a pocket formed by PA and PB1 and is required for enhancement or activation of the polymerase functions. The results presented in this thesis, clearly show the activation of RIG-I following the recognition of the incoming vRNP. It can therefore be hypothesized that despite the interaction of the hook structure with PB1/PA, RIG-I is still able to access and bind the 5'ppp because of the polymerase flexibility [136]. Furthermore, it can be proposed that the binding of the polymerase to the promoter is dynamic and can accordingly vary between the incoming vRNP and the initiation of the transcription step. This primordial interaction of RIG-I and the 5'ppp would trigger the destabilisation of the polymerase complex and lead to the binding of RIG-I to the panhandle structure of the influenza genome.

Mutation E627K in the PB2 subunit is one of the most frequently observed adaptive mutations in mammals. Recent studies provide new evidence for the role of E627K mutation in host adaptation in combination with importin-α. The latter plays a role as positive regulator for human (627K) but not avian (627E) polymerase activity, independently of its import function [80]. Other studies postulate that E627K is counteracting an unknown restriction factor in mammalian cells [109]. However, another study challenge this hypothesis, where the authors propose that the difference within 627E/627K polymerase activity is not due to a restriction factor but due to the absence or low expression of a positive factor in mammalian cells [114]. A particular feature of PB2 E627K is the strong interaction with NP compared to PB2 627E [93, 124]. This strong interaction is supposed to be responsible for an increased stability of the nucleocapsid. The presented results demonstrate that the unknown inhibitory factor is RIG-I and proved that the sensitivity of this sensor is dependent on the mammalian or avian signature at position 627. This reveals a new evasion mechanism developed by influenza viruses, to avoid recognition of incoming vRNP by RIG-I.

A recent publication from Song et al describes a new mutation K526R, which show similar host adaptation characteristics as E627K. Interestingly, mutation K526R is also described to increase interaction between PB2 and NP [155]. These data raise therefore the question of the potential role of K526R in RIG-I evasion.

The results described here point to a direct action of RIG-I which prevents transcription or replication of the virus, independently of the innate signaling pathway (**Figure 57**). The model of action is based on the binding of the 5'ppp end, which leads to the conformational change of RIG-I and destabilisation of the polymerase with 627E PB2 from the nucleocapsid. This destabilisation leads to exposure of the panhandle structure, which is recognized by the helicase domain of RIG-I. In contrast, the mutation

E627K increases the stability of the polymerase complex to the nucleocapsid, via a stronger interaction with NP, which restricts destabilisation and access to the panhandle structure, therefore RIG-I activation.

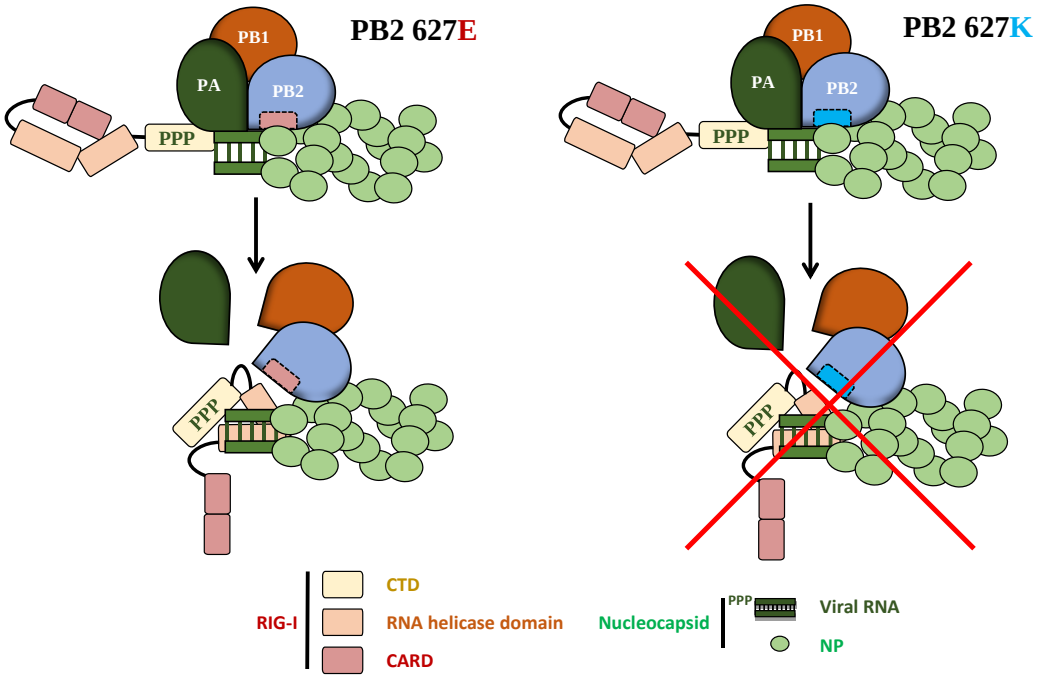

Figure 57: Counteraction of RIG-I activation by mutation E627K. *The scheme represents the RIG-I activation in presence of vRNP containing avian signature (627E) or mammalian signature (627K) in PB2. The recognition of the 5'ppp leads to the conformational change of RIG-I and destabilization of the viral polymerase (627E) from the vRNP. This destabilization gives access to the panhandle structure of influenza genome to RIG-I. In presence of a polymerase with mammalian signature (627K), the increased stability of the nucleocapsid prevents the destabilization of the polymerase and consequently RIG-I activation.*

Influenza viruses developed additional mechanisms to evade the immune system, such as strategies involving PB1-F2. This protein is a truncated form of PB1 composed of 90 amino acids. It has been shown to have different roles in the pro-apoptotic and pro-inflammatory pathway, but also in modulation of the innate immune response. PB1-F2 can modulate IFN response via binding to MAVS [42, 167] or modulate NF-κB signaling pathway via binding of the IKK-β protein [138].

Furthermore, influenza viruses have been demonstrated to use the cellular RNA helicase UAP56 and URH49 to promote transcription and replication of the viral genome [185]. These helicases are also diverted to prevent double stranded RNA formation. It has been described that RIG-I is also present into the nucleus [98]. Therefore it can be assumed that influenza viruses will hijack these RNA helicases to avoid formation of double-stranded RNA, between vRNA and cRNA during replication step and thus prevent RIG-I recognition.

RIG-I is a key determinant for the different immune response between mammalian and avian species. It has been demonstrated that RIG-I is absent in chicken (Galliformes) that possess however MDA-5 and its downstream signaling pathway, common to RIG-I [7]. The demonstrated role of RIG-I acting on incoming vRNP explains the differences in polymerase activity and viral growth within mammalian and avian cells.

Despite the absence of RIG-I, chicken possess a developed immune system including TLR, NLR and RLR. The expression of the chicken TLR (chTLR) varies within cells and tissues and has homologous functions as the mammalian TLRs. For example, mammalian TLR9 corresponds to chTLR21 in chicken, with the same function of sensing bacterial genomic DNA. In addition, chTLR15 is an avian specific TLR which senses specific patterns of viruses and bacteria as would, among others, mammalian TLR4 and TLR9. Finally the chTLR17 has been proposed to have a role during influenza infection, which could then compensate for RIG-I absence [28].

The RLR pathway with MDA-5 and LGP2 is still present in chicken. MDA-5 is ubiquitously expressed in different chicken tissues and plays an important role in IFN production. It has been demonstrated in mammalian cells that MDA-5 could compensate for the absence of RIG-I [151], upon influenza infection, which could also be the case in chicken cells. Karpala et al have demonstrated that chicken MDA-5 is active and induces a signaling pathway after recognition of synthetic RNA (poly I:C) or vRNA. However, chicken MDA-5 was not able to protect against an influenza infection [84].

TLRs preferentially activate the NF-κB signalling pathway, whereas RIG-I leads to the IFN-β synthesis [101]. The IFN pathway will lead to the activation of ISG as OAS, Mx protein, RNAse L, PKR among others [142]. In chicken, IFN-α can be synthesized via another pathway during influenza infection, but not IFN-β [101]. A study demonstrated that in IFN-β knock-out mice, the viral lung titer is considerably increased upon influenza infection. Despite the presence of IFN-α, the protective effect of IFN-β cannot be compensated [89]. Even if the chicken immune system protects against a broad spectrum of pathogens, the lack of RIG-I is one of the weaknesses in influenza recognition.

Interrestingly, RIG-I is present in ducks (Anseriformes), which are the natural reservoir of influenza-A-viruses [7]. This difference may explain why ducks are less sensitive to highly pathogenic influenza virus infection, in contrast to chicken. It remains unclear why only chicken have lost RIG-I during evolution.

9.2.2 Mutation D701N modulates the transport of incoming vRNP

There are several critical steps during influenza infection. Despite receptor binding, entry and uncoating, vRNPs need to be imported into the nucleus for completing transcription and replication. For this purpose the virus needs to adapt to the host import machinery. The size of the vRNP (10-20nm) cannot afford a passive passage through the nuclear pore [34, 126], and therefore needs the recruitment of the host import machinery. It has been shown that the entry of influenza vRNP was driven by the NLS signal of NP present in the N-terminal part and referred as unconventional NLS [35] (**Figure 58**).

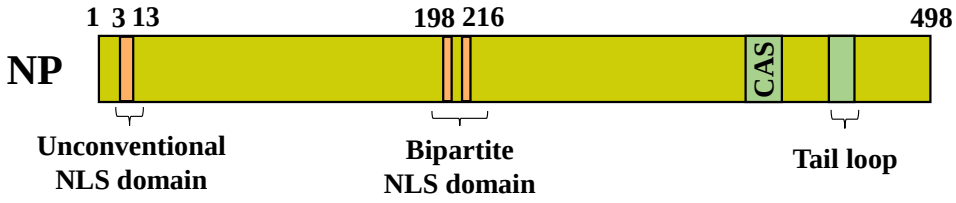

***Figure 58: Domains of influenza NP**. A scheme of the nucleoprotein and its domains is shown. In green are represented the functional domains for NP function: The cytoplasmic accumulation signal (CAS) and the tail loop, enabling the oligomerization. In orange is represented the NLS domains: the bipartite NLS as well as unconventional NLS.*

vRNPs use the classical nuclear import pathway via importin-α/β adaptors, as NP and PB2. In contrast, PB1/PA use the non-classical import pathway via RanBP5, independently of importin-α [139].

As described above influenza viruses have developed an efficient mechanism to counteract RIG-I activation. This evasion occurs during the short exposition in the cytosplasm before nuclear transport, thanks to the mutation E627K in PB2 subunit.

Mutation D701N in PB2 has also been shown to have an important role in adaptation [36, 50, 51]. D701N increases polymerase activity and viral growth, as well as pathogenicity in mice. The mechanistic role of D701N has been described in 2007 by Tarendeau et al, where the authors investigated the structure of the C-terminal domain of PB2. In this study, the authors observed that the PB2 structure is affected by mutation D701N. They show that the 701D residue forms a salt bridge with the arginine at position 753. This salt bridge leads to the closed conformation of the C-terminal part (containing the NLS domain) of PB2. The presence of mutation D701N provokes the disruption of the salt bridge and the switch to an open conformation of PB2. This conformational change exposes the NLS domain, which enables a better interaction with importin-α [162] (**Figure 59**).

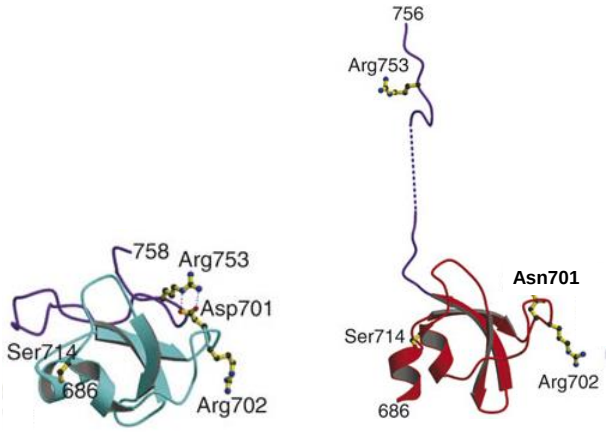

***Figure 59: Structure of the NLS domain of PB2 subunit.** Here are represented the structure of the NLS. Residue Asp701 forms a salt bridge with Arg753 of the major NLS motif and tethers the C terminus to the core of the domain in the unbound state. The presence of residue Asn701 demonstrates unfolding of residues 736–759 (purple) leading to the exposure of the NLS domain. Figure from Tarendeau et al 2007.*

Thus, mutation D701N plays an important role in PB2 import into the nucleus. Gabriel et al have demonstrated the interaction between PB2 and importins. They observed that PB2 with mutation D701N had an enhanced interaction with mammalian importin-α1 and -α7, leading to an increased nuclear localisation of the newly synthesized PB2 protein [52] (**Figure 60**).

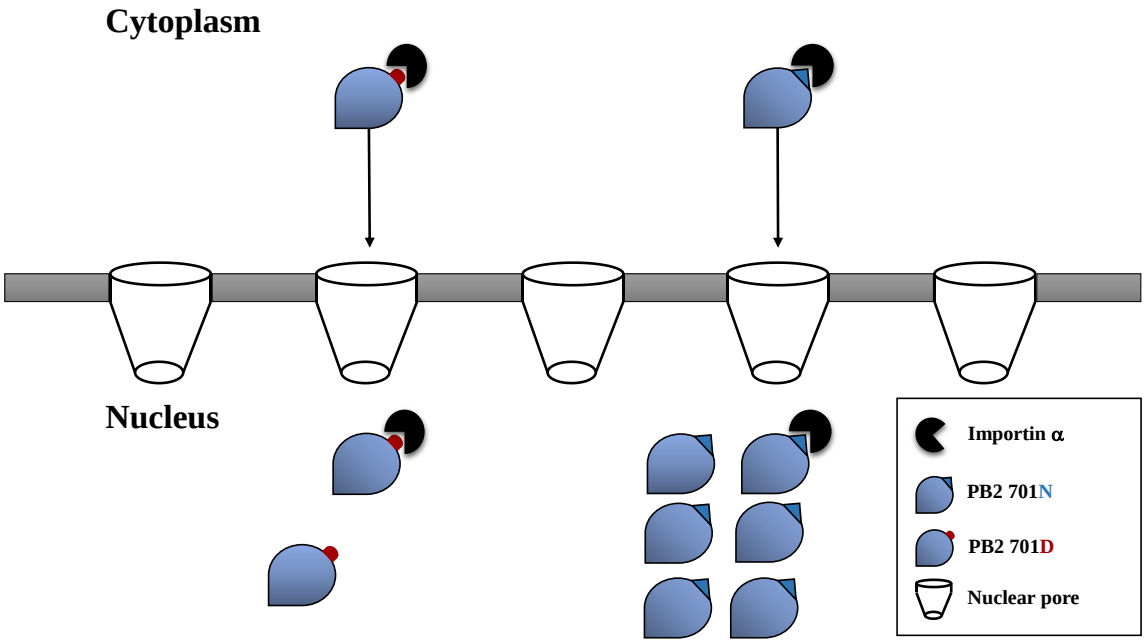

Figure 60: Import of PB2 701D or 701N into the nucleus of mammalian cells*. The nuclear import of newly synthesized PB2 protein is shown. The presence of the mutation D701N enables a better interaction with importin-α and an increased import of PB2 into the nucleus.*

Import analysis exhibit that mutation D701N is able to positively influence the nuclear entry of vRNP. Moreover, it is demonstrated that the effect of mutation D701N is not only limited to the import of newly synthesized PB2 protein but also promote the entry of incoming vRNP (**cf. Figure 5**, **step 4 and 6**). Mutation D701N is therefore directly active when PB2 is bound to the nucleocapsid. As already pointed out mutation S714R cooperates with D701N for the exposure of the NLS domain [36]. Nevertheless, the presented immunofluorescence results show that S714R does not promote an enhanced import of vRNP into the nucleus. Quantification of nuclear entry between viruses containing PB2 with mutation D701N or D701N-S714R would provide more informations on the role of mutation S714R.

The direct impact of D701N on vRNP import should be discussed. It could be argued that, from the structural point of view, the interaction between PB2, NP and PB1 could affect the exposure of the NLS in the C-terminal part of PB2. Reich et al have recently published the structure of the complete polymerase, including PA, PB1 and PB2. Their results suggest that the PB2 subunit is the most mobile part of the polymerase complex. PB1 and PA heterodimer are well interacting, and for a functional polymerase, PB2 might need a conformational flexibility. The authors observed a detached and flexible arm of the polymerase which is most likely the C-terminal part of PB2 [136]. Therefore it is conceivable, that the NLS domain of PB2 is exposed and flexible enough to interact with the importins (**Figure 61**).

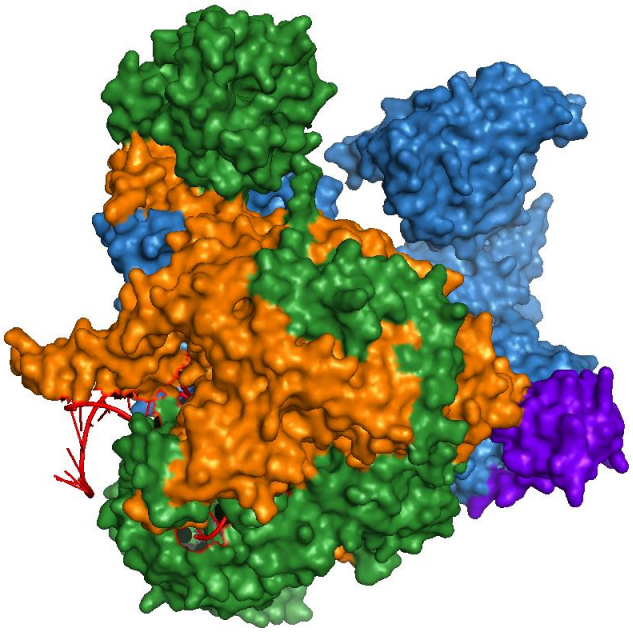

***Figure 61 : 3D structure of the polymerase complex**. Here is represented the interaction of the polymerase proteins. PB2 is coloured in blue and its NLS domain is represented in purple, PB1 in orange and PA in green. (Adapted from Reich et al, 2014)*

The NP protein, associated with the viral RNA, is essential for vRNP nuclear import. It was demonstrated that the unconventional NLS domain of NP was the dominant NLS in this process [35]. Therefore, the drastic effect on vRNP import of the NLS domain of PB2 has to be discussed. Wu et al demonstrated that blocking both NLS signals of NP (by mimetic peptide or antibodies) led to a decreased nuclear localisation of vRNP, but was not abolished [188]. Two hypothesis could explain this phenotype: (i) The NLS domains are not blocked all at once and enable a partial entry or (ii) the NLS domain of PB2 partially rescues the vRNP entry into the nucleus. Furthermore, O'Neil et al have observed the importance of NP for vRNA nuclear import in absence of the polymerase subunits, and therefore conceive that the polymerase complex may influence the nuclear import as well [125].

It would be of interest to discriminate the role of PB2 versus NP in vRNP transport. However, these two proteins use the same carriers for the import (importin-α/β) [81] and a recent study described that mutation in the unconventional NLS of NP affects vRNP formation and thus RNA synthesis [146]. The data presented here do not assume that PB2 will override the role of NP, but in contrast, cooperatively act to increase the nuclear import.

Taken together, the results discussed in chapter 9.2 throw light on two different mechanisms by which adaptive mutations E627K and D701N enhance virus replication in the mammalian host. Mutation E627K prevents RIG-I activation mediated by incoming vRNP and thus, promotes its escape from the innate immune response. Mutation D701N accelerates transport of vRNP into the nucleus where replication and transcription take place and by clearance of vRNP from the cytoplasm it further contributes to RIG-I activation.

10 REFERENCES

1. (1980) A revision of the system of nomenclature for influenza viruses: a WHO memorandum. Bull World Health Organ 58:585-591
2. Alexander DJ (2007) An overview of the epidemiology of avian influenza. Vaccine 25:5637-5644
3. Ank N, Paludan SR (2009) Type III IFNs: new layers of complexity in innate antiviral immunity. Biofactors 35:82-87
4. Arranz R, Coloma R, Chichon FJ, Conesa JJ, Carrascosa JL, Valpuesta JM, Ortin J, Martin-Benito J (2012) The structure of native influenza virion ribonucleoproteins. Science 338:1634-1637
5. Bae SH, Cheong HK, Lee JH, Cheong C, Kainosho M, Choi BS (2001) Structural features of an influenza virus promoter and their implications for viral RNA synthesis. Proc Natl Acad Sci U S A 98:10602-10607
6. Banks J, Speidel ES, Moore E, Plowright L, Piccirillo A, Capua I, Cordioli P, Fioretti A, Alexander DJ (2001) Changes in the haemagglutinin and the neuraminidase genes prior to the emergence of highly pathogenic H7N1 avian influenza viruses in Italy. Arch Virol 146:963-973
7. Barber MR, Aldridge JR, Jr., Webster RG, Magor KE (2010) Association of RIG-I with innate immunity of ducks to influenza. Proc Natl Acad Sci U S A 107:5913-5918
8. Barman S, Ali A, Hui EK, Adhikary L, Nayak DP (2001) Transport of viral proteins to the apical membranes and interaction of matrix protein with glycoproteins in the assembly of influenza viruses. Virus Res 77:61-69
9. Baron J (2012) Aktivierung von Influenza-A Viren des Subtyps H9N2 durch Matriptase und andere humane Serinproteasen. Biologie. Philipps University, Marburg, p 138
10. Baron J, Tarnow C, Mayoli-Nussle D, Schilling E, Meyer D, Hammami M, Schwalm F, Steinmetzer T, Guan Y, Garten W, Klenk HD, Bottcher-Friebertshauser E (2013) Matriptase, HAT, and TMPRSS2 activate the hemagglutinin of H9N2 influenza A viruses. J Virol 87:1811-1820
11. Baudin F, Bach C, Cusack S, Ruigrok RW (1994) Structure of influenza virus RNP. I. Influenza virus nucleoprotein melts secondary structure in panhandle RNA and exposes the bases to the solvent. Embo j 13:3158-3165
12. Baum A, Sachidanandam R, Garcia-Sastre A (2010) Preference of RIG-I for short viral RNA molecules in infected cells revealed by next-generation sequencing. Proc Natl Acad Sci U S A 107:16303-16308
13. Belgnaoui SM, Paz S, Hiscott J (2011) Orchestrating the interferon antiviral response through the mitochondrial antiviral signaling (MAVS) adapter. Curr Opin Immunol 23:564-572
14. Bienz K, Loffler H (1969) [Influenza virus morphology: structure of the influenza A2-("Hongkong")-virus]. Experientia 25:987-989
15. Biswas SK, Nayak DP (1994) Mutational analysis of the conserved motifs of influenza A virus polymerase basic protein 1. J Virol 68:1819-1826
16. Boivin S, Cusack S, Ruigrok RW, Hart DJ (2010) Influenza A virus polymerase: structural insights into replication and host adaptation mechanisms. J Biol Chem 285:28411-28417
17. Boivin S, Hart DJ (2011) Interaction of the influenza A virus polymerase PB2 C-terminal region with importin alpha isoforms provides insights into host adaptation and polymerase assembly. J Biol Chem 286:10439-10448
18. Bottcher E, Matrosovich T, Beyerle M, Klenk HD, Garten W, Matrosovich M (2006) Proteolytic activation of influenza viruses by serine proteases TMPRSS2 and HAT from human airway epithelium. J Virol 80:9896-9898
19. Bottcher E, Freuer C, Steinmetzer T, Klenk HD, Garten W (2009) MDCK cells that express proteases TMPRSS2 and HAT provide a cell system to propagate influenza viruses in the absence of trypsin and to study cleavage of HA and its inhibition. Vaccine 27:6324-6329
20. Braam J, Ulmanen I, Krug RM (1983) Molecular model of a eucaryotic transcription complex: functions and movements of influenza P proteins during capped RNA-primed transcription. Cell 34:609-618

21. Bui M, Whittaker G, Helenius A (1996) Effect of M1 protein and low pH on nuclear transport of influenza virus ribonucleoproteins. J Virol 70:8391-8401
22. Bui M, Wills EG, Helenius A, Whittaker GR (2000) Role of the influenza virus M1 protein in nuclear export of viral ribonucleoproteins. J Virol 74:1781-1786
23. Butt KM, Smith GJ, Chen H, Zhang LJ, Leung YH, Xu KM, Lim W, Webster RG, Yuen KY, Peiris JS, Guan Y (2005) Human infection with an avian H9N2 influenza A virus in Hong Kong in 2003. J Clin Microbiol 43:5760-5767
24. Chaipan C, Kobasa D, Bertram S, Glowacka I, Steffen I, Tsegaye TS, Takeda M, Bugge TH, Kim S, Park Y, Marzi A, Pohlmann S (2009) Proteolytic activation of the 1918 influenza virus hemagglutinin. J Virol 83:3200-3211
25. Chen GW, Chang SC, Mok CK, Lo YL, Kung YN, Huang JH, Shih YH, Wang JY, Chiang C, Chen CJ, Shih SR (2006) Genomic signatures of human versus avian influenza A viruses. Emerg Infect Dis 12:1353-1360
26. Chen H, Yuan H, Gao R, Zhang J, Wang D, Xiong Y, Fan G, Yang F, Li X, Zhou J, Zou S, Yang L, Chen T, Dong L, Bo H, Zhao X, Zhang Y, Lan Y, Bai T, Dong J, Li Q, Wang S, Li H, Gong T, Shi Y, Ni X, Li J, Fan J, Wu J, Zhou X, Hu M, Wan J, Yang W, Li D, Wu G, Feng Z, Gao GF, Wang Y, Jin Q, Liu M, Shu Y (2014) Clinical and epidemiological characteristics of a fatal case of avian influenza A H10N8 virus infection: a descriptive study. Lancet 383:714-721
27. Chen LM, Davis CT, Zhou H, Cox NJ, Donis RO (2008) Genetic compatibility and virulence of reassortants derived from contemporary avian H5N1 and human H3N2 influenza A viruses. PLoS Pathog 4:e1000072
28. Chen S, Cheng A, Wang M (2013) Innate sensing of viruses by pattern recognition receptors in birds. Vet Res 44:82
29. Chen W, Calvo PA, Malide D, Gibbs J, Schubert U, Bacik I, Basta S, O'Neill R, Schickli J, Palese P, Henklein P, Bennink JR, Yewdell JW (2001) A novel influenza A virus mitochondrial protein that induces cell death. Nat Med 7:1306-1312
30. Choi YK, Ozaki H, Webby RJ, Webster RG, Peiris JS, Poon L, Butt C, Leung YH, Guan Y (2004) Continuing evolution of H9N2 influenza viruses in Southeastern China. J Virol 78:8609-8614
31. Coloma R, Valpuesta JM, Arranz R, Carrascosa JL, Ortin J, Martin-Benito J (2009) The structure of a biologically active influenza virus ribonucleoprotein complex. PLoS Pathog 5:e1000491
32. Cong YL, Pu J, Liu QF, Wang S, Zhang GZ, Zhang XL, Fan WX, Brown EG, Liu JH (2007) Antigenic and genetic characterization of H9N2 swine influenza viruses in China. J Gen Virol 88:2035-2041
33. Cong YL, Wang CF, Yan CM, Peng JS, Jiang ZL, Liu JH (2008) Swine infection with H9N2 influenza viruses in China in 2004. Virus Genes 36:461-469
34. Cros JF, Palese P (2003) Trafficking of viral genomic RNA into and out of the nucleus: influenza, Thogoto and Borna disease viruses. Virus Res 95:3-12
35. Cros JF, Garcia-Sastre A, Palese P (2005) An unconventional NLS is critical for the nuclear import of the influenza A virus nucleoprotein and ribonucleoprotein. Traffic 6:205-213
36. Czudai-Matwich V, Otte A, Matrosovich M, Gabriel G, Klenk HD (2014) PB2 mutations D701N and S714R promote adaptation of an influenza H5N1 virus to a mammalian host. J Virol 88:8735-8742
37. Davidson S, Crotta S, McCabe TM, Wack A (2014) Pathogenic potential of interferon alphabeta in acute influenza infection. Nat Commun 5:3864
38. de la Luna S, Martin J, Portela A, Ortin J (1993) Influenza virus naked RNA can be expressed upon transfection into cells co-expressing the three subunits of the polymerase and the nucleoprotein from simian virus 40 recombinant viruses. J Gen Virol 74 (Pt 3):535-539
39. Deng T, Engelhardt OG, Thomas B, Akoulitchev AV, Brownlee GG, Fodor E (2006) Role of ran binding protein 5 in nuclear import and assembly of the influenza virus RNA polymerase complex. J Virol 80:11911-11919
40. Dias A, Bouvier D, Crepin T, McCarthy AA, Hart DJ, Baudin F, Cusack S, Ruigrok RW (2009) The cap-snatching endonuclease of influenza virus polymerase resides in the PA subunit. Nature 458:914-918

41. Doms RW, Helenius A, White J (1985) Membrane fusion activity of the influenza virus hemagglutinin. The low pH-induced conformational change. J Biol Chem 260:2973-2981
42. Dudek SE, Wixler L, Nordhoff C, Nordmann A, Anhlan D, Wixler V, Ludwig S (2011) The influenza virus PB1-F2 protein has interferon antagonistic activity. Biol Chem 392:1135-1144
43. Ehrhardt C, Seyer R, Hrincius ER, Eierhoff T, Wolff T, Ludwig S (2010) Interplay between influenza A virus and the innate immune signaling. Microbes Infect 12:81-87
44. Essere B, Yver M, Gavazzi C, Terrier O, Isel C, Fournier E, Giroux F, Textoris J, Julien T, Socratous C, Rosa-Calatrava M, Lina B, Marquet R, Moules V (2013) Critical role of segment-specific packaging signals in genetic reassortment of influenza A viruses. Proc Natl Acad Sci U S A 110:E3840-3848
45. Feng Y, Mao H, Xu C, Jiang J, Chen Y, Yan J, Gao J, Li Z, Xia S, Lu Y (2013) Origin and characteristics of internal genes affect infectivity of the novel avian-origin influenza A (H7N9) virus. PLoS One 8:e81136
46. Flick R, Neumann G, Hoffmann E, Neumeier E, Hobom G (1996) Promoter elements in the influenza vRNA terminal structure. Rna 2:1046-1057
47. Flick R, Hobom G (1999) Interaction of influenza virus polymerase with viral RNA in the 'corkscrew' conformation. J Gen Virol 80 (Pt 10):2565-2572
48. Fouchier RA, Schneeberger PM, Rozendaal FW, Broekman JM, Kemink SA, Munster V, Kuiken T, Rimmelzwaan GF, Schutten M, Van Doornum GJ, Koch G, Bosman A, Koopmans M, Osterhaus AD (2004) Avian influenza A virus (H7N7) associated with human conjunctivitis and a fatal case of acute respiratory distress syndrome. Proc Natl Acad Sci U S A 101:1356-1361
49. Fouchier RA, Munster V, Wallensten A, Bestebroer TM, Herfst S, Smith D, Rimmelzwaan GF, Olsen B, Osterhaus AD (2005) Characterization of a novel influenza A virus hemagglutinin subtype (H16) obtained from black-headed gulls. J Virol 79:2814-2822
50. Gabriel G, Dauber B, Wolff T, Planz O, Klenk HD, Stech J (2005) The viral polymerase mediates adaptation of an avian influenza virus to a mammalian host. Proc Natl Acad Sci U S A 102:18590-18595
51. Gabriel G, Abram M, Keiner B, Wagner R, Klenk HD, Stech J (2007) Differential polymerase activity in avian and mammalian cells determines host range of influenza virus. J Virol 81:9601-9604
52. Gabriel G, Herwig A, Klenk HD (2008) Interaction of polymerase subunit PB2 and NP with importin alpha1 is a determinant of host range of influenza A virus. PLoS Pathog 4:e11
53. Gabriel G, Fodor E (2014) Molecular Determinants of Pathogenicity in the Polymerase Complex. Curr Top Microbiol Immunol
54. Gack MU, Shin YC, Joo CH, Urano T, Liang C, Sun L, Takeuchi O, Akira S, Chen Z, Inoue S, Jung JU (2007) TRIM25 RING-finger E3 ubiquitin ligase is essential for RIG-I-mediated antiviral activity. Nature, England, pp 916-920
55. Gack MU, Albrecht RA, Urano T, Inn K-S, Huang IC, Carnero E, Farzan M, Inoue S, Jung JU, García-Sastre A (2009) Influenza A Virus NS1 Targets the Ubiquitin Ligase TRIM25 to Evade Recognition by the Host Viral RNA Sensor RIG-I. Cell Host & Microbe 5:439-449
56. Gao R, Cao B, Hu Y, Feng Z, Wang D, Hu W, Chen J, Jie Z, Qiu H, Xu K, Xu X, Lu H, Zhu W, Gao Z, Xiang N, Shen Y, He Z, Gu Y, Zhang Z, Yang Y, Zhao X, Zhou L, Li X, Zou S, Zhang Y, Yang L, Guo J, Dong J, Li Q, Dong L, Zhu Y, Bai T, Wang S, Hao P, Yang W, Han J, Yu H, Li D, Gao GF, Wu G, Wang Y, Yuan Z, Shu Y (2013) Human infection with a novel avian-origin influenza A (H7N9) virus. N Engl J Med 368:1888-1897
57. Garcia-Sastre A, Biron CA (2006) Type 1 interferons and the virus-host relationship: a lesson in detente. Science 312:879-882
58. Garten W, Klenk H-D (2008) Cleavage activation of the Influenza Virus hemagglutinin and its role in pathogenesis. In: Institute of Virology PU, Marburg, Germany (ed)
59. Gastaminza P, Perales B, Falcon AM, Ortin J (2003) Mutations in the N-terminal region of influenza virus PB2 protein affect virus RNA replication but not transcription. J Virol 77:5098-5108
60. Gerber M, Isel C, Moules V, Marquet R (2014) Selective packaging of the influenza A genome and consequences for genetic reassortment. Trends Microbiol 22:446-455

61. Gomez-Puertas P, Albo C, Perez-Pastrana E, Vivo A, Portela A (2000) Influenza virus matrix protein is the major driving force in virus budding. J Virol 74:11538-11547
62. Gonzalez S, Ortin J (1999) Distinct regions of influenza virus PB1 polymerase subunit recognize vRNA and cRNA templates. Embo j 18:3767-3775
63. Graef KM, Vreede FT, Lau YF, McCall AW, Carr SM, Subbarao K, Fodor E (2010) The PB2 subunit of the influenza virus RNA polymerase affects virulence by interacting with the mitochondrial antiviral signaling protein and inhibiting expression of beta interferon. J Virol 84:8433-8445
64. Guan Y, Shortridge KF, Krauss S, Webster RG (1999) Molecular characterization of H9N2 influenza viruses: were they the donors of the "internal" genes of H5N1 viruses in Hong Kong? Proc Natl Acad Sci U S A 96:9363-9367
65. Guilligay D, Tarendeau F, Resa-Infante P, Coloma R, Crepin T, Sehr P, Lewis J, Ruigrok RW, Ortin J, Hart DJ, Cusack S (2008) The structural basis for cap binding by influenza virus polymerase subunit PB2. Nat Struct Mol Biol 15:500-506
66. Haller O, Kochs G, Weber F (2007) Interferon, Mx, and viral countermeasures. Cytokine Growth Factor Rev 18:425-433
67. Haller O, Weber F (2007) Pathogenic viruses: smart manipulators of the interferon system. Curr Top Microbiol Immunol 316:315-334
68. Hatta M, Halfmann P, Wells K, Kawaoka Y (2002) Human influenza a viral genes responsible for the restriction of its replication in duck intestine. Virology 295:250-255
69. Hay AJ, Skehel JJ, McCauley J (1982) Characterization of influenza virus RNA complete transcripts. Virology 116:517-522
70. Hayden FG, Pavia AT (2006) Antiviral management of seasonal and pandemic influenza. J Infect Dis 194 Suppl 2:S119-126
71. Herfst S, Schrauwen EJ, Linster M, Chutinimitkul S, de Wit E, Munster VJ, Sorrell EM, Bestebroer TM, Burke DF, Smith DJ, Rimmelzwaan GF, Osterhaus AD, Fouchier RA (2012) Airborne transmission of influenza A/H5N1 virus between ferrets. Science 336:1534-1541
72. Hoffmann E, Neumann G, Kawaoka Y, Hobom G, Webster RG (2000) A DNA transfection system for generation of influenza A virus from eight plasmids. Proc Natl Acad Sci U S A 97:6108-6113
73. Hoffmann E, Stech J, Guan Y, Webster RG, Perez DR (2001) Universal primer set for the full-length amplification of all influenza A viruses. Arch Virol 146:2275-2289
74. Holsinger LJ, Lamb RA (1991) Influenza virus M2 integral membrane protein is a homotetramer stabilized by formation of disulfide bonds. Virology 183:32-43
75. Honda A, Ueda K, Nagata K, Ishihama A (1988) RNA polymerase of influenza virus: role of NP in RNA chain elongation. J Biochem 104:1021-1026
76. Horimoto T, Kawaoka Y (2005) Influenza: lessons from past pandemics, warnings from current incidents. Nat Rev Microbiol 3:591-600
77. Hossain MJ, Hickman D, Perez DR (2008) Evidence of expanded host range and mammalian-associated genetic changes in a duck H9N2 influenza virus following adaptation in quail and chickens. PLoS One 3:e3170
78. Huang RT, Wahn K, Klenk HD, Rott R (1980) Fusion between cell membrane and liposomes containing the glycoproteins of influenza virus. Virology 104:294-302
79. Huang TS, Palese P, Krystal M (1990) Determination of influenza virus proteins required for genome replication. J Virol 64:5669-5673
80. Hudjetz B, Gabriel G (2012) Human-like PB2 627K influenza virus polymerase activity is regulated by importin-alpha1 and -alpha7. PLoS Pathog 8:e1002488
81. Hutchinson EC, Fodor E (2012) Nuclear import of the influenza A virus transcriptional machinery. Vaccine 30:7353-7358
82. Iwai A, Shiozaki T, Kawai T, Akira S, Kawaoka Y, Takada A, Kida H, Miyazaki T (2010) Influenza A virus polymerase inhibits type I interferon induction by binding to interferon beta promoter stimulator 1. J Biol Chem 285:32064-32074
83. Jagger BW, Wise HM, Kash JC, Walters KA, Wills NM, Xiao YL, Dunfee RL, Schwartzman LM, Ozinsky A, Bell GL, Dalton RM, Lo A, Efstathiou S, Atkins JF, Firth AE, Taubenberger JK, Digard P (2012) An overlapping protein-coding region in influenza A virus segment 3 modulates the host response. Science 337:199-204

84. Karpala AJ, Stewart C, McKay J, Lowenthal JW, Bean AG (2011) Characterization of chicken Mda5 activity: regulation of IFN-beta in the absence of RIG-I functionality. J Immunol 186:5397-5405
85. Kawaoka Y, Krauss S, Webster RG (1989) Avian-to-human transmission of the PB1 gene of influenza A viruses in the 1957 and 1968 pandemics. J Virol 63:4603-4608
86. Kim CU, Lew W, Williams MA, Liu H, Zhang L, Swaminathan S, Bischofberger N, Chen MS, Mendel DB, Tai CY, Laver WG, Stevens RC (1997) Influenza neuraminidase inhibitors possessing a novel hydrophobic interaction in the enzyme active site: design, synthesis, and structural analysis of carbocyclic sialic acid analogues with potent anti-influenza activity. J Am Chem Soc 119:681-690
87. Klenk HD, Rott R, Orlich M, Blodorn J (1975) Activation of influenza A viruses by trypsin treatment. Virology 68:426-439
88. Klumpp K, Ruigrok RW, Baudin F (1997) Roles of the influenza virus polymerase and nucleoprotein in forming a functional RNP structure. Embo j 16:1248-1257
89. Koerner I, Kochs G, Kalinke U, Weiss S, Staeheli P (2007) Protective role of beta interferon in host defense against influenza A virus. J Virol 81:2025-2030
90. Kohlway A, Luo D, Rawling DC, Ding SC, Pyle AM (2013) Defining the functional determinants for RNA surveillance by RIG-I. EMBO Rep 14:772-779
91. Kolakofsky D, Kowalinski E, Cusack S (2012) A structure-based model of RIG-I activation. Rna 18:2118-2127
92. Kowalinski E, Lunardi T, McCarthy AA, Louber J, Brunel J, Grigorov B, Gerlier D, Cusack S (2011) Structural basis for the activation of innate immune pattern-recognition receptor RIG-I by viral RNA. Cell 147:423-435
93. Labadie K, Dos Santos Afonso E, Rameix-Welti MA, van der Werf S, Naffakh N (2007) Host-range determinants on the PB2 protein of influenza A viruses control the interaction between the viral polymerase and nucleoprotein in human cells. Virology 362:271-282
94. Lamb RA, Zebedee SL, Richardson CD (1985) Influenza virus M2 protein is an integral membrane protein expressed on the infected-cell surface. Cell 40:627-633
95. Levy DE, Marie IJ, Durbin JE (2011) Induction and function of type I and III interferon in response to viral infection. Curr Opin Virol 1:476-486
96. Li C, Hatta M, Watanabe S, Neumann G, Kawaoka Y (2008) Compatibility among polymerase subunit proteins is a restricting factor in reassortment between equine H7N7 and human H3N2 influenza viruses. J Virol 82:11880-11888
97. Li KS, Xu KM, Peiris JS, Poon LL, Yu KZ, Yuen KY, Shortridge KF, Webster RG, Guan Y (2003) Characterization of H9 subtype influenza viruses from the ducks of southern China: a candidate for the next influenza pandemic in humans? J Virol 77:6988-6994
98. Li W, Chen H, Sutton T, Obadan A, Perez DR (2014) Interactions between the influenza A virus RNA polymerase components and retinoic acid-inducible gene I. J Virol 88:10432-10447
99. Li X, Qi W, He J, Ning Z, Hu Y, Tian J, Jiao P, Xu C, Chen J, Richt J, Ma W, Liao M (2012) Molecular basis of efficient replication and pathogenicity of H9N2 avian influenza viruses in mice. PLoS One 7:e40118
100. Lin YP, Shaw M, Gregory V, Cameron K, Lim W, Klimov A, Subbarao K, Guan Y, Krauss S, Shortridge K, Webster R, Cox N, Hay A (2000) Avian-to-human transmission of H9N2 subtype influenza A viruses: relationship between H9N2 and H5N1 human isolates. Proc Natl Acad Sci U S A 97:9654-9658
101. Loo YM, Fornek J, Crochet N, Bajwa G, Perwitasari O, Martinez-Sobrido L, Akira S, Gill MA, Garcia-Sastre A, Katze MG, Gale M, Jr. (2008) Distinct RIG-I and MDA5 signaling by RNA viruses in innate immunity. J Virol 82:335-345
102. Lu Y, Wambach M, Katze MG, Krug RM (1995) Binding of the influenza virus NS1 protein to double-stranded RNA inhibits the activation of the protein kinase that phosphorylates the elF-2 translation initiation factor. Virology 214:222-228
103. Manz B, Brunotte L, Reuther P, Schwemmle M (2012) Adaptive mutations in NEP compensate for defective H5N1 RNA replication in cultured human cells. Nat Commun 3:802
104. Martin K, Helenius A (1991) Transport of incoming influenza virus nucleocapsids into the nucleus. J Virol 65:232-244

105. Massin P, van der Werf S, Naffakh N (2001) Residue 627 of PB2 is a determinant of cold sensitivity in RNA replication of avian influenza viruses. J Virol 75:5398-5404
106. Matrosovich MN, Matrosovich TY, Gray T, Roberts NA, Klenk HD (2004) Human and avian influenza viruses target different cell types in cultures of human airway epithelium. Proc Natl Acad Sci U S A 101:4620-4624
107. McCullers JA (2014) The co-pathogenesis of influenza viruses with bacteria in the lung. Nat Rev Microbiol 12:252-262
108. McKimm-Breschkin JL (2013) Influenza neuraminidase inhibitors: antiviral action and mechanisms of resistance. Influenza Other Respir Viruses 7 Suppl 1:25-36
109. Mehle A, Doudna JA (2008) An inhibitory activity in human cells restricts the function of an avian-like influenza virus polymerase. Cell Host Microbe 4:111-122
110. Mehle A, Doudna JA (2009) Adaptive strategies of the influenza virus polymerase for replication in humans. Proc Natl Acad Sci U S A 106:21312-21316
111. Meroni G, Diez-Roux G (2005) TRIM/RBCC, a novel class of 'single protein RING finger' E3 ubiquitin ligases. Bioessays 27:1147-1157
112. Meurs EF, Watanabe Y, Kadereit S, Barber GN, Katze MG, Chong K, Williams BR, Hovanessian AG (1992) Constitutive expression of human double-stranded RNA-activated p68 kinase in murine cells mediates phosphorylation of eukaryotic initiation factor 2 and partial resistance to encephalomyocarditis virus growth. J Virol 66:5805-5814
113. Mok CK, Yen HL, Yu MY, Yuen KM, Sia SF, Chan MC, Qin G, Tu WW, Peiris JS (2011) Amino acid residues 253 and 591 of the PB2 protein of avian influenza virus A H9N2 contribute to mammalian pathogenesis. J Virol 85:9641-9645
114. Moncorge O, Mura M, Barclay WS (2010) Evidence for avian and human host cell factors that affect the activity of influenza virus polymerase. J Virol 84:9978-9986
115. Munster VJ, Veen J, Olsen B, Vogel R, Osterhaus AD, Fouchier RA (2006) Towards improved influenza A virus surveillance in migrating birds. Vaccine 24:6729-6733
116. Munster VJ, Baas C, Lexmond P, Waldenstrom J, Wallensten A, Fransson T, Rimmelzwaan GF, Beyer WE, Schutten M, Olsen B, Osterhaus AD, Fouchier RA (2007) Spatial, temporal, and species variation in prevalence of influenza A viruses in wild migratory birds. PLoS Pathog 3:e61
117. Muramoto Y, Noda T, Kawakami E, Akkina R, Kawaoka Y (2013) Identification of novel influenza A virus proteins translated from PA mRNA. J Virol 87:2455-2462
118. Naffakh N, Massin P, Escriou N, Crescenzo-Chaigne B, van der Werf S (2000) Genetic analysis of the compatibility between polymerase proteins from human and avian strains of influenza A viruses. J Gen Virol 81:1283-1291
119. Naffakh N, Tomoiu A, Rameix-Welti MA, van der Werf S (2008) Host restriction of avian influenza viruses at the level of the ribonucleoproteins. Annu Rev Microbiol 62:403-424
120. Nayak DP, Hui EK, Barman S (2004) Assembly and budding of influenza virus. Virus Res 106:147-165
121. Nemeroff ME, Barabino SM, Li Y, Keller W, Krug RM (1998) Influenza virus NS1 protein interacts with the cellular 30 kDa subunit of CPSF and inhibits 3'end formation of cellular pre-mRNAs. Mol Cell 1:991-1000
122. Neumann G, Noda T, Kawaoka Y (2009) Emergence and pandemic potential of swine-origin H1N1 influenza virus. Nature 459:931-939
123. Newcomb LL, Kuo RL, Ye Q, Jiang Y, Tao YJ, Krug RM (2009) Interaction of the influenza a virus nucleocapsid protein with the viral RNA polymerase potentiates unprimed viral RNA replication. J Virol 83:29-36
124. Ng AK, Chan WH, Choi ST, Lam MK, Lau KF, Chan PK, Au SW, Fodor E, Shaw PC (2012) Influenza polymerase activity correlates with the strength of interaction between nucleoprotein and PB2 through the host-specific residue K/E627. PLoS One 7:e36415
125. O'Neill RE, Jaskunas R, Blobel G, Palese P, Moroianu J (1995) Nuclear import of influenza virus RNA can be mediated by viral nucleoprotein and transport factors required for protein import. J Biol Chem 270:22701-22704
126. Ortega J, Martin-Benito J, Zurcher T, Valpuesta JM, Carrascosa JL, Ortin J (2000) Ultrastructural and functional analyses of recombinant influenza virus ribonucleoproteins suggest dimerization of nucleoprotein during virus amplification. J Virol 74:156-163

127. Otte A, Gabriel G (2011) 2009 pandemic H1N1 influenza A virus strains display differential pathogenicity in C57BL/6J but not BALB/c mice. Virulence 2:563-566
128. Paterson D, te Velthuis AJ, Vreede FT, Fodor E (2014) Host restriction of influenza virus polymerase activity by PB2 627E is diminished on short viral templates in a nucleoprotein-independent manner. J Virol 88:339-344
129. Peiris JS, Guan Y, Markwell D, Ghose P, Webster RG, Shortridge KF (2001) Cocirculation of avian H9N2 and contemporary "human" H3N2 influenza A viruses in pigs in southeastern China: potential for genetic reassortment? J Virol 75:9679-9686
130. Peiris M, Yuen KY, Leung CW, Chan KH, Ip PL, Lai RW, Orr WK, Shortridge KF (1999) Human infection with influenza H9N2. Lancet, England, pp 916-917
131. Pflug A, Guilligay D, Reich S, Cusack S (2014) Structure of influenza A polymerase bound to the viral RNA promoter. Nature
132. Pinto LH, Holsinger LJ, Lamb RA (1992) Influenza virus M2 protein has ion channel activity. Cell 69:517-528
133. Poon LL, Pritlove DC, Fodor E, Brownlee GG (1999) Direct evidence that the poly(A) tail of influenza A virus mRNA is synthesized by reiterative copying of a U track in the virion RNA template. J Virol 73:3473-3476
134. Qi W, Zhou X, Shi W, Huang L, Xia W, Liu D, Li H, Chen S, Lei F, Cao L, Wu J, He F, Song W, Li Q, Liao M, Liu M (2014) Genesis of the novel human-infecting influenza A(H10N8) virus and potential genetic diversity of the virus in poultry, China. Euro Surveill 19
135. Rameix-Welti MA, Tomoiu A, Dos Santos Afonso E, van der Werf S, Naffakh N (2009) Avian Influenza A virus polymerase association with nucleoprotein, but not polymerase assembly, is impaired in human cells during the course of infection. J Virol 83:1320-1331
136. Reich S, Guilligay D, Pflug A, Malet H, Berger I, Crepin T, Hart D, Lunardi T, Nanao M, Ruigrok RW, Cusack S (2014) Structural insight into cap-snatching and RNA synthesis by influenza polymerase. Nature
137. Reid AH, Fanning TG, Hultin JV, Taubenberger JK (1999) Origin and evolution of the 1918 "Spanish" influenza virus hemagglutinin gene. Proc Natl Acad Sci U S A 96:1651-1656
138. Reis AL, McCauley JW (2013) The influenza virus protein PB1-F2 interacts with IKKbeta and modulates NF-kappaB signalling. PLoS One 8:e63852
139. Resa-Infante P, Gabriel G (2013) The nuclear import machinery is a determinant of influenza virus host adaptation. Bioessays 35:23-27
140. Robertson JS, Schubert M, Lazzarini RA (1981) Polyadenylation sites for influenza virus mRNA. J Virol 38:157-163
141. Rott R (1985) [Influenza virus infections in man and animal]. Berl Munch Tierarztl Wochenschr 98:340-344
142. Sadler AJ, Williams BR (2008) Interferon-inducible antiviral effectors. Nat Rev Immunol 8:559-568
143. Saito T, Hirai R, Loo YM, Owen D, Johnson CL, Sinha SC, Akira S, Fujita T, Gale M, Jr. (2007) Regulation of innate antiviral defenses through a shared repressor domain in RIG-I and LGP2. Proc Natl Acad Sci U S A 104:582-587
144. Salomon R, Franks J, Govorkova EA, Ilyushina NA, Yen HL, Hulse-Post DJ, Humberd J, Trichet M, Rehg JE, Webby RJ, Webster RG, Hoffmann E (2006) The polymerase complex genes contribute to the high virulence of the human H5N1 influenza virus isolate A/Vietnam/1203/04. J Exp Med 203:689-697
145. Samson M, Pizzorno A, Abed Y, Boivin G (2013) Influenza virus resistance to neuraminidase inhibitors. Antiviral Res 98:174-185
146. Sanchez A, Guerrero-Juarez CF, Ramirez J, Newcomb LL (2014) Nuclear localized Influenza nucleoprotein N-terminal deletion mutant is deficient in functional vRNP formation. Virol J 11:155
147. Schlee M, Roth A, Hornung V, Hagmann CA, Wimmenauer V, Barchet W, Coch C, Janke M, Mihailovic A, Wardle G, Juranek S, Kato H, Kawai T, Poeck H, Fitzgerald KA, Takeuchi O, Akira S, Tuschl T, Latz E, Ludwig J, Hartmann G (2009) Recognition of 5′ Triphosphate by RIG-I Helicase Requires Short Blunt Double-Stranded RNA as Contained in Panhandle of Negative-Strand Virus. Immunity 31:25-34

148. Schrauwen EJA, Fouchier RAM (2014) Host adaptation and transmission of influenza A viruses in mammals. Emerg Microbes Infect 3:e9
149. Selman M, Dankar SK, Forbes NE, Jia J-J, Brown EG (2012) Adaptive mutation in influenza A virus non-structural gene is linked to host switching and induces a novel protein by alternative splicing. Emerg Microbes Infect 1:e42
150. Sharma K, Tripathi S, Ranjan P, Kumar P, Garten R, Deyde V, Katz JM, Cox NJ, Lal RB, Sambhara S, Lal SK (2011) Influenza A virus nucleoprotein exploits Hsp40 to inhibit PKR activation. PLoS One 6:e20215
151. Siren J, Imaizumi T, Sarkar D, Pietila T, Noah DL, Lin R, Hiscott J, Krug RM, Fisher PB, Julkunen I, Matikainen S (2006) Retinoic acid inducible gene-I and mda-5 are involved in influenza A virus-induced expression of antiviral cytokines. Microbes Infect 8:2013-2020
152. Skehel JJ, Bayley PM, Brown EB, Martin SR, Waterfield MD, White JM, Wilson IA, Wiley DC (1982) Changes in the conformation of influenza virus hemagglutinin at the pH optimum of virus-mediated membrane fusion. Proc Natl Acad Sci U S A 79:968-972
153. Skehel JJ, Wiley DC (2000) Receptor binding and membrane fusion in virus entry: the influenza hemagglutinin. Annu Rev Biochem 69:531-569
154. Smith GJ, Vijaykrishna D, Bahl J, Lycett SJ, Worobey M, Pybus OG, Ma SK, Cheung CL, Raghwani J, Bhatt S, Peiris JS, Guan Y, Rambaut A (2009) Origins and evolutionary genomics of the 2009 swine-origin H1N1 influenza A epidemic. Nature 459:1122-1125
155. Song W, Wang P, Mok BW, Lau SY, Huang X, Wu WL, Zheng M, Wen X, Yang S, Chen Y, Li L, Yuen KY, Chen H (2014) The K526R substitution in viral protein PB2 enhances the effects of E627K on influenza virus replication. Nat Commun 5:5509
156. Stasakova J, Ferko B, Kittel C, Sereinig S, Romanova J, Katinger H, Egorov A (2005) Influenza A mutant viruses with altered NS1 protein function provoke caspase-1 activation in primary human macrophages, resulting in fast apoptosis and release of high levels of interleukins 1beta and 18. J Gen Virol 86:185-195
157. Steel J, Lowen AC, Mubareka S, Palese P (2009) Transmission of influenza virus in a mammalian host is increased by PB2 amino acids 627K or 627E/701N. PLoS Pathog 5:e1000252
158. Stieneke-Grober A, Vey M, Angliker H, Shaw E, Thomas G, Roberts C, Klenk HD, Garten W (1992) Influenza virus hemagglutinin with multibasic cleavage site is activated by furin, a subtilisin-like endoprotease. Embo j 11:2407-2414
159. Subbarao EK, London W, Murphy BR (1993) A single amino acid in the PB2 gene of influenza A virus is a determinant of host range. J Virol 67:1761-1764
160. Subbarao K, Klimov A, Katz J, Regnery H, Lim W, Hall H, Perdue M, Swayne D, Bender C, Huang J, Hemphill M, Rowe T, Shaw M, Xu X, Fukuda K, Cox N (1998) Characterization of an avian influenza A (H5N1) virus isolated from a child with a fatal respiratory illness. Science 279:393-396
161. Takeuchi O, Akira S (2009) Innate immunity to virus infection. Immunol Rev 227:75-86
162. Tarendeau F, Boudet J, Guilligay D, Mas PJ, Bougault CM, Boulo S, Baudin F, Ruigrok RW, Daigle N, Ellenberg J, Cusack S, Simorre JP, Hart DJ (2007) Structure and nuclear import function of the C-terminal domain of influenza virus polymerase PB2 subunit. Nat Struct Mol Biol 14:229-233
163. Tashiro M, Ciborowski P, Klenk HD, Pulverer G, Rott R (1987) Role of Staphylococcus protease in the development of influenza pneumonia. Nature 325:536-537
164. Taubenberger JK, Reid AH, Krafft AE, Bijwaard KE, Fanning TG (1997) Initial genetic characterization of the 1918 "Spanish" influenza virus. Science 275:1793-1796
165. Taubenberger JK, Morens DM (2008) The pathology of influenza virus infections. Annu Rev Pathol 3:499-522
166. Tong S, Zhu X, Li Y, Shi M, Zhang J, Bourgeois M, Yang H, Chen X, Recuenco S, Gomez J, Chen LM, Johnson A, Tao Y, Dreyfus C, Yu W, McBride R, Carney PJ, Gilbert AT, Chang J, Guo Z, Davis CT, Paulson JC, Stevens J, Rupprecht CE, Holmes EC, Wilson IA, Donis RO (2013) New world bats harbor diverse influenza A viruses. PLoS Pathog 9:e1003657
167. Varga ZT, Ramos I, Hai R, Schmolke M, Garcia-Sastre A, Fernandez-Sesma A, Palese P (2011) The influenza virus protein PB1-F2 inhibits the induction of type I interferon at the level of the MAVS adaptor protein. PLoS Pathog 7:e1002067

168. Vasin AV, Temkina OA, Egorov VV, Klotchenko SA, Plotnikova MA, Kiselev OI (2014) Molecular mechanisms enhancing the proteome of influenza A viruses: an overview of recently discovered proteins. Virus Res 185:53-63
169. von Itzstein M, Wu WY, Kok GB, Pegg MS, Dyason JC, Jin B, Van Phan T, Smythe ML, White HF, Oliver SW, et al. (1993) Rational design of potent sialidase-based inhibitors of influenza virus replication. Nature 363:418-423
170. Vreede FT, Jung TE, Brownlee GG (2004) Model suggesting that replication of influenza virus is regulated by stabilization of replicative intermediates. J Virol 78:9568-9572
171. Wahlgren J (2011) Influenza A viruses: an ecology review. Infect Ecol Epidemiol 1
172. Wan H, Perez DR (2006) Quail carry sialic acid receptors compatible with binding of avian and human influenza viruses. Virology 346:278-286
173. Wan H, Perez DR (2007) Amino acid 226 in the hemagglutinin of H9N2 influenza viruses determines cell tropism and replication in human airway epithelial cells. J Virol 81:5181-5191
174. Wang J, Sun Y, Xu Q, Tan Y, Pu J, Yang H, Brown EG, Liu J (2012) Mouse-adapted H9N2 influenza A virus PB2 protein M147L and E627K mutations are critical for high virulence. PLoS One 7:e40752
175. Ward AC, Castelli LA, Lucantoni AC, White JF, Azad AA, Macreadie IG (1995) Expression and analysis of the NS2 protein of influenza A virus. Arch Virol 140:2067-2073
176. Weber F, Haller O, Kochs G (1997) Conserved vRNA end sequences of Thogoto-orthomyxovirus suggest a new panhandle structure. Arch Virol 142:1029-1033
177. Weber F, Haller O (2007) Viral suppression of the interferon system. Biochimie 89:836-842
178. Weber M, Weber F (2014) Segmented negative-strand RNA viruses and RIG-I: divide (your genome) and rule. Curr Opin Microbiol 20:96-102
179. Weber M, Weber F (2014) RIG-I-like receptors and negative-strand RNA viruses: RLRly bird catches some worms. Cytokine Growth Factor Rev
180. Weber M, Weber F (2014) Monitoring activation of the antiviral pattern recognition receptors RIG-I and PKR by limited protease digestion and native PAGE. J Vis Exp:e51415
181. Weber M, Sediri H, Felgenhauer U, Binzen I, Bänfer S, Jacob R, Brunotte L, Garcia-Sastre A, Schmid-Burgk J, Schmidt T, Hornung V, Kochs G, Schwemmle M, Klenk H-D, Weber F (in press) Influenza virus adaptation PB2-627K modulates nucleocapsid inhibition by the pathogen sensor RIG-I. Cell Host Microbe
182. Webster RG, Bean WJ, Gorman OT, Chambers TM, Kawaoka Y (1992) Evolution and ecology of influenza A viruses. Microbiol Rev 56:152-179
183. Wharton SA, Belshe RB, Skehel JJ, Hay AJ (1994) Role of virion M2 protein in influenza virus uncoating: specific reduction in the rate of membrane fusion between virus and liposomes by amantadine. J Gen Virol 75 (Pt 4):945-948
184. Wise HM, Hutchinson EC, Jagger BW, Stuart AD, Kang ZH, Robb N, Schwartzman LM, Kash JC, Fodor E, Firth AE, Gog JR, Taubenberger JK, Digard P (2012) Identification of a novel splice variant form of the influenza A virus M2 ion channel with an antigenically distinct ectodomain. PLoS Pathog 8:e1002998
185. Wisskirchen C, Ludersdorfer TH, Muller DA, Moritz E, Pavlovic J (2011) The cellular RNA helicase UAP56 is required for prevention of double-stranded RNA formation during influenza A virus infection. J Virol 85:8646-8655
186. Wong KK, Bull RA, Rockman S, Scott G, Stelzer-Braid S, Rawlinson W (2011) Correlation of polymerase replication fidelity with genetic evolution of influenza A/Fujian/411/02(H3N2) viruses. J Med Virol 83:510-516
187. Wu R, Zhang H, Yang K, Liang W, Xiong Z, Liu Z, Yang X, Shao H, Zheng X, Chen M, Xu D (2009) Multiple amino acid substitutions are involved in the adaptation of H9N2 avian influenza virus to mice. Vet Microbiol 138:85-91
188. Wu WW, Sun YH, Pante N (2007) Nuclear import of influenza A viral ribonucleoprotein complexes is mediated by two nuclear localization sequences on viral nucleoprotein. Virol J 4:49
189. Wunderlich K, Juozapaitis M, Ranadheera C, Kessler U, Martin A, Eisel J, Beutling U, Frank R, Schwemmle M (2011) Identification of high-affinity PB1-derived peptides with enhanced affinity to the PA protein of influenza A virus polymerase. Antimicrob Agents Chemother 55:696-702

190. Xu C, Hu WB, Xu K, He YX, Wang TY, Chen Z, Li TX, Liu JH, Buchy P, Sun B (2012) Amino acids 473V and 598P of PB1 from an avian-origin influenza A virus contribute to polymerase activity, especially in mammalian cells. J Gen Virol 93:531-540
191. Xu KM, Li KS, Smith GJ, Li JW, Tai H, Zhang JX, Webster RG, Peiris JS, Chen H, Guan Y (2007) Evolution and molecular epidemiology of H9N2 influenza A viruses from quail in southern China, 2000 to 2005. J Virol 81:2635-2645
192. Yamada S, Hatta M, Staker BL, Watanabe S, Imai M, Shinya K, Sakai-Tagawa Y, Ito M, Ozawa M, Watanabe T, Sakabe S, Li C, Kim JH, Myler PJ, Phan I, Raymond A, Smith E, Stacy R, Nidom CA, Lank SM, Wiseman RW, Bimber BN, O'Connor DH, Neumann G, Stewart LJ, Kawaoka Y (2010) Biological and structural characterization of a host-adapting amino acid in influenza virus. PLoS Pathog 6:e1001034
193. Yasuda J, Nakada S, Kato A, Toyoda T, Ishihama A (1993) Molecular assembly of influenza virus: association of the NS2 protein with virion matrix. Virology 196:249-255
194. Zhang H, Li X, Guo J, Li L, Chang C, Li Y, Bian C, Xu K, Chen H, Sun B (2014) The PB2 E627K mutation contributes to the high polymerase activity and enhanced replication of H7N9 influenza virus. J Gen Virol 95:779-786

11 LIST OF FIGURES AND TABLES

12 APPENDICES

12.1 Amino Acid Abreviation

Amino Acid	3-letter code	1-letter code
Alanine	Ala	A
Arginine	Arg	R
Asparagine	Asn	N
Aspartic acid	Asp	D
Cysteine	Cys	C
Glutamic acid	Glu	E
Glutamine	Gln	Q
Glycine	Gly	G
Histidine	His	H
Isoleucine	Ile	I
Leucine	Leu	L
Lysine	Lys	K
Methionine	Met	M
Phenylalanine	Phe	F
Proline	Pro	P
Serine	Ser	S
Threonine	Thr	T
Tryptophan	Try	W
Tyrosine	Tyr	Y
Valine	Val	V

12.2 Amino acid sequence of PB2 subunit

A/Quail/Shantou/2061/2000 and A/Quail/Shantou/782/2000

MERIKELRDLMSQSRTREILTKTTVDHMAIIKKYTSGRQEKNPALRMKWMMAMKYPITADKRIMEMIP
ERNEQGQTLWSKTNDAGSDRVMVSPLAVTWWNRNGPTASTVHYPKVYKTYFEKVERLKHGTFGPVH
FRNQVKIRRRVDMNPGHADLSAKEAQEVIMEVVFPNEVGARILTSESQLTITKEKREELKNCNIAPLMV
AYMLERELVRKTRFLPVAGGTSSVYIEVLHLTQGTCWEQMYTPGGEVRNDDVDQSLIIAARNIVRRAT
VSADPLASLLEMCHSTQIGGVRMVDILKQNPTEEQAVDICKAAMGLKISSSFSFGGFTFKRTKGSSVKRE
EEVLTGNLQTLKIKVHEGYEEFTMVGRRATAILRKATRRMIQLIVSGRDEQSIAEAIIVAMVFSQEDCMI
KAVRGDLNFVNRANQRLNPMHQLLRHFQKNAKVLFQNWGIEPIDNVMGMIGILPDMTPSTEMSLRGV
RVSKMGVDEYSSTERVVVSIDRFLRVRDQQGNVLLSPEEVSETQGMEKLTITYSSSMMWEINGPESVLV
NTYQWIIRNWETVKIQWSQEPTMLYNKMEFEPFQSLVPKAARSQYSGFVRTLFQQMRDVLGTFDTVQII
KLLPFAAAPPEQSRMQFSSLTVNVRGSGMRILVRGNSPAFNYNKTTKRLTILGKDAGALTEDPDEGTAG
VESAVLRGFLILGKEDKRYGPALSINELSNLTKGEKANVLIGQGDVVLVMKRKRDSSILTDSQTATKRIR
MAIN*

A/Seal/Massachusetts/1/1980

MERIKELRDLMSQSRTREILTKTTVDHMAIIKKYTSGRQEKNPALRMKWMMAMKYPITADKRIMEMIP
ERNEQGQTLWSKTNDAGSDRVMVSPLAVTWWNRNGPTTSTVHYPKVYKTYFEKVERMKHGTFGPVH
FRNQVKIRRRVDINPGHADLSAKEAQDVIMEVVFPNEVGARILTSESQLTITKEKKEKLQDCKIAPLMVA
YMLERELVRKTRFLPVAGGTSSVYIEVLHLTQGTCWEQMYTPGGEVRNDDIDQSLIIAARNIVRRATVS
ADPLASLLEMCHSTQIGGIRMVDILRQNPTEEQAVDICKAAMGLRISSSFSFGGFTFKRTSGSSVKREEEV
LTGNLQTLKIRVHEGYEEFTMVGRRATAILRKATRRLIQLIVSGRDEQSIAEAIIVAMVFSQEDCMIKAV
RGDLNFVNRANQRLNPMHQLLRHFQKDAKVLFQNWGIEPIDNVMGMIGILPDMTPSTEMSLRGIRVSK
MGVDEYSSTERVVVSIDRFLRVRDQRGNVLLSPEEVSETQGTEKLTITYSSSMMWEINGPESVLINTYQ
WIIRNWETVKIQWSQDPTMLYNKMEFEPFQSLVPKAARGQYSGFVRTLFQQMRDVLGTFDTVQIIKLLP
FAAAPPEQSRMQFSSLTVNVRGSGMRILIRGNSPVFNYNKATKRLTVLGKDAGALTEDPDEGTAGVES
AVLRGFLILGKEDKRYGPALSINELSNLAKGEKANVLIGQGDVVLVMKRKRDSSILTDSQTATKRIRMA
IN*

A/Hamburg/05/2009

MERIKELRDLMSQSRTREILTKTTVDHMAIIKKYTSGRQEKNPALRMKWMMAMRYPITADKRIMDMIP
ERNEQGQTLWSKTNDAGSDRVMVSPLAVTWWNRNGPTTSTVHYPKVYKTYFEKVERLKHGTFGPVH
FRNQVKIRRRVDTNPGHADLSAKEAQDVIMEVVFPNEVGARILTSESQLAITKEKKEELQDCKIAPLMV
AYMLERELVRKTRFLPVAGGTGSVYIEVLHLTQGTCWEQMYTPGGEVRNDDVDQSLIIAARNIVRRAA
VSADPLASLLEMCHSTQIGGVRMVDILRQNPTEEQAVDICKAAIGLRISSSFSFGGFTFKRTSGSSVKKEE
EVLTGNLQTLKIRVHEGYEEFTMVGRRATAILRKATRRLIQLIVSGRDEQSIAEAIIVAMVFSQEDCMIK
AVRGDLNFVNRANQRLNPMHQLLRHFQKDAKVLFQNWGIESIDNVMGMIGILPDMTPSTEMSLRGIRV
SKMGVDEYSSTERVVVSIDRFLRVRDQRGNVLLSPEEVSETQGTERLTITYSSSMMWEINGPESVLVNT
YQWIIRNWEIVKIQWSQDPTMLYNKMEFEPFQSLVPKATRSRYSGFVRTLFQQMRDVLGTFDTVQIIKL
LPFAAAPPEQSRMQFSSLTVNVRGSGLRILVRGNSPVFNYNKATKRLTVLGKDAGALTEDPDEGTSGVE
SAVLRGFLILGKEDKRYGPALSINELSNLAKGEKANVLIGQGDVVLVMKRKRDSSILTDSQTATKRIRM
AIN*

A/Anhui/1/2013

MERIKELRDLMSQSRTREILTKTTVDHMAIIKKYTSGRQEKNPALRMKWMMAMKYPITADKRIMEMIP
ERNEQGQTLWSKTNDAGSDRVMVSPLAVTWWNRNGPTTSTVHYPKVYKTYFEKVERLKHGTFGPVH
FRNQVKIRRRVDINPGHADLSAKEAQDVIMEVVFPNEVGARILTSESQLTITKEKKKELQDCKIAPLMVA
YMLERELVRKTRFLPVAGGTSSVYIEVLHLTQGTCWEQMYTPGGEVRNDDVDQSLIIAARNIVRRATVS
ADPLASLLEMCHSTQIGGVRMVDILRQNPTEEQAVDICKAAMGLRISSSFSFGGFTFKRTSGSSVKREEE
VLTGNLQTLKIRVHEGYEEFTMVGRRATAILRKATRRLIQLIVSGKDEQSIAEAIIVAMVFSQEDCMIKA
VRGDLNFVNRANQRLNPMHQLLRHFQKDAKVLFQNWGIEPIDNVMGMIGILPDMTPSTEMSLRGVRV
SKMGVDEYSSTERVVVSIDRFLRVRDQRGNVLLSPEEVSETQGTEKLTITYSSSMMWEINGPESVLVNT
YQWIIRNWENVKIQWSQDPTMLYNKMEFEPFQSLVPKAARGQYSGFVRVLFQQMRDVLGTFDTVQIIK
LLPFAAAPPKQSRMQFSSLTVNVRGSGMRIVVRGNSPVFNYNKATKRLTVLGKDAGALMEDPDEGTA
GVESAVLRGFLILGKEDKRYGPALSINELSNLAKGEKANVLIGQGDVVLVMKRKRDSSILTDSQTATKR
IRMAIN*

12.3 Veröffentlichungen

12.3.1 Publikationen

Influenza virus adaptation PB2-627K modulates nucleocapsid inhibition by the pathogen sensor RIG-I.
Michaela Weber, **Hanna Sediri**, Ulrike Felgenhauer, Ina Binzen, Sebastian Bänfer, Ralf Jacob, Linda Brunotte, Adolfo García-Sastre, Jonathan L. Schmid-Burgk, Tobias Schmidt, Veit Hornung, Georg Kochs, Martin Schwemmle, Hans-Dieter Klenk, and Friedemann Weber, Cell Host Microbes *(in press)*

TMPRSS2 is a host cell factor that is essential for pneumotropism and pathogenicity of H7N9 and H1N1 influenza A virus in mice.
Tarnow, Carolin; Engels, Geraldine; Arendt, Annika; Schwalm, Folker; **Sediri, Hanna**; Garten, Wolfgang; Klenk, Hans-Dieter; Gabriel, Gülsah; Böttcher-Friebertshäuser, Eva. J Virol, May 2014.

Polymerase mutations in PB2 subunit promoting adaptation of avian influenza virus of subtype H9N2 to mammals
Hanna Sediri, Swantje Thiele, Folker Schwalm, Gülsah Gabriel, Hans-Dieter Klenk (under preparation)

12.3.2 Vorträge

Polymerase mutations promoting adaptation of avian influenza virus of subtype H9N2, H7N9 and pH1N1.
April 2014-FluPharm meeting, Hamburg, Deutschland

Polymerase mutations promoting adaptation of avian influenza virus of subtype H9N2 and H7N9 to mammals.
März 2014 - 24th Annual Meeting of German Society for Virology, Alpbach, Österreich

The role of the influenza virus polymerase in host adaptation.
Oktober 2013- SFB 593 Meeting, Kleinwalsertal, Deutschland.

Effects of adaptive PB2 mutations on Replication and Transcription.
April 2013- FluPharm meeting, Wien, Österreich

12.3.3 Poster

Polymerase mutations promoting adaptation of avian influenza virus of subtype H9N2 to mammals.
Hanna Sediri, Folker Schwalm, Hans-Dieter Klenk *September 2012- International meeting of Influenza, Münster, Deutschland.*

Polymerase mutations promoting adaptation of avian influenza virus of subtype H9N2 to mammals.
Hanna Sediri, Folker Schwalm, Hans-Dieter Klenk *März 2012 - 22nd Annual Meeting of German Society for Virology, Essen, Deutschland.*

12.4 Verzeichnis der akademischen Lehrer

Meine akademischer Lehrer waren Boudaly, Joliot, Badel, Regnier, Silar, Dupret, Rodrigues-Lima, Pasquali, Viguier, Van Der Werf, Janel, Bazin, Laurenti, Alcaïde-Loridan, Blondel, Hazan, Thoulouze, Vartanian, Tordo, Ceccaldi, Gessain, Niedergang, Margottin-Goguet, Nisole, Klenk

12.5 Acknowledgments

I would like to thank Prof. Dr. Hans-Dieter Klenk, for the opportunity to do my PhD thesis under his supervision and for the help he provided over these 4 years, through intensive discussion and support. I would also like to thank Prof. Dr. Gulsah Gabriel and Dr. Swantje Thiele for the mice collaboration. We went through a lot, but we finally did it.

I would like to thank particularly Michaela Gerlach and Prof. Dr. Friedemann Weber for the fantastic collaboration which resulted in a great paper.

I would like to thank all the members of the lab who were presents over these 4 years of PhD: Aybicke, Folker, Catharina, Eva, for the great time, discussions and advices without forgetting, Joanna who showed and taught me a lot when I arrived (especially the Joanna's language), Carolin that I was always "looking for", my dear twin labmate Annika with who I shared a lot more than just a birthday, Cornelius for your cute mistakes and Lisa for being such a good "minime". Thank you girls for all your help, and for teaching me German manners and thank you for the fantastic fondue and crêpes evening.

I would also like to thank for their scientific and human support, all the "sheep company" including Markus (even far in the US), Julia (for all the fire and rock you could give me), Thomas (for the mayonnaise song), Jan (for your attentive ear and your unconditional help), Alex (for being a friend always truthful), Michi (for being such a sunshine to me), Steph (pour tous les bons moments qu'on a vécu en 4 ans et le soutien que tu m'as apporté) and Andreas (for being who you are). Without you, Germany would never have been the same to me!

I would also like to thank all the members of the institute who helped me to improve my German skills with small talks and kindness.

I would finally like to thank my family. Merci à mes parents toujours là pour me remonter le moral (et on sait combien d'appels il y a eu) ou les bretelles, merci à Tawfik et Khadi pour toutes les discussions dominicales, merci à Monir pour le soutien de sa chèvre, et mes grands-parents. Je n'oublie évidemment pas mes deux sœurs chéries, Olpha et Doura, qui n'ont pas toujours compris ce que je faisais, mais m'ont soutenu à leur façon.

I would like to finish with one of the sentence we kept saying in the lab:

At the end, everything is going to be fine. If it's not fine, it's not the end !